

Phonon damping in a 2D superfluid: insufficiency of Fermi's golden rule at low temperature

Yvan Castin, Alan Serafin, Alice Sinatra

Laboratoire Kastler Brossel, ENS-Université PSL, CNRS, Université Sorbonne and Collège de France, 24 rue Lhomond, 75231 Paris, France

Abstract

It is generally accepted that the phonon gas of a superfluid always enters a weak coupling regime at sufficiently low temperatures, whatever the strength of the interactions between the underlying particles (constitutive of the superfluid). Thus, in this limit, we should always be able to calculate the damping rate of thermal phonons by applying Fermi's golden rule to the Hamiltonian H_3 of cubic phonon-phonon coupling taken from quantum hydrodynamics, at least in the case of a convex acoustic branch and in the collisionless regime (where the eigenfrequency of the considered phonons remains much greater than the gas thermalization rate). Using the many-body Green's function method, we predict that, unexpectedly, this is not true in two dimensions, contrary to the three-dimensional case. We confirm this prediction with classical phonon-field simulations and a non-perturbative theory in H_3 , where the fourth order is regularized by hand, giving a complex energy to the virtual phonons of the four-phonon collisional processes. For a weakly interacting fluid and a phonon mode in the long-wavelength limit, we predict a damping rate about three times lower than that of the golden rule.

Keywords: Bose gas ; two-dimensional superfluid ; cold atom gas ; Beliaev-Landau phonon damping; many-body Green's functions; quantum hydrodynamics

Contents

| | | |
|----------|--|-----------|
| 1 | Presentation of the problem and general reasoning | 2 |
| 2 | Numerical experiment in the classical field model | 7 |
| 2.1 | Quantum hydrodynamics Hamiltonian | 7 |
| 2.2 | Classical field model | 8 |
| 2.3 | Numerical results | 10 |
| 3 | Study at leading order in phonon-phonon coupling | 11 |
| 3.1 | Calculation of the self-energy | 12 |
| 3.2 | Analytical studies: one-parameter universality | 14 |
| 3.3 | Comparison with classical field simulations | 16 |
| 4 | Study at fourth order in H_3 | 17 |
| 4.1 | Calculation with the diagrammatic formalism of reference [7] | 17 |
| 4.2 | Calculation using Landau approach | 22 |
| 4.3 | Failure of order four in the limit $\epsilon = k_B T / mc^2 \rightarrow 0$ | 26 |

E-mail: yvan.castin@lkb.ens.fr (Yvan Castin), a.serafin@protonmail.com (Alan Serafin), alice.sinatra@lkb.ens.fr (Alice Sinatra)

| | | |
|-------------------|---|-----------|
| 5 | Nonperturbative theories in H_3 | 29 |
| 5.1 | Atomic physics-type regularization | 29 |
| 5.2 | Condensed matter regularization | 30 |
| 5.3 | Regularized theory in the weakly interacting limit | 32 |
| 6 | Conclusion | 34 |
| Appendix A | Analytic continuation of $\tilde{\Sigma}_{\tilde{q}}^{(2,2)}(\tilde{\zeta})$ to the lower half-plane and validity conditions of the golden rule | 34 |
| Appendix B | First deviation of the signal from the golden-rule exponential for the theory at second order in H_3 | 36 |
| Appendix C | Double Matsubara sums in the theory at fourth order in H_3 | 37 |
| Appendix D | A linear divergence of $\tilde{\Sigma}_{\tilde{q}}^{(4,2)}(\tilde{\zeta})$ away from the origin | 38 |
| Appendix E | The long-time behavior of the signal in the $(\rho\xi^2)^{-1} \rightarrow 0$ limit of non-perturbative theories | 40 |

1. Presentation of the problem and general reasoning

In dimension $d \geq 2$, we consider a spatially homogeneous system of particles with short-range interactions, entirely superfluid in its ground state and prepared at a non-zero but arbitrarily low temperature, which allows us to restrict its study to leading order in temperature by means of an effective low-energy theory. Irrespective of the quantum statistics (bosonic or fermionic) of the particles and the strength of their interactions (in gas or liquid phase), this system has an acoustic excitation branch, i.e. with a linear departure in wave number (with no band gap), whose quanta are the phonons.

The coupling between low-wavenumber phonons (of energy $< \eta k_B T$, where temperature $T \rightarrow 0$ then cutoff $\eta \rightarrow +\infty$ at the end of the calculations) is deduced from the quantum hydrodynamics of Landau and Khalatnikov [1], the effective Hamiltonian taking the form ¹

$$H = H_2 + H_3 + H_4 \quad (1)$$

where term H_n is of degree n in terms of $\hat{b}_{\mathbf{k}}^\dagger$ and $\hat{b}_{\mathbf{k}}$, bosonic creation and annihilation operators of a phonon of wave vector \mathbf{k} in a quantization box $[0, L]^d$ with periodic boundary conditions. The term H_2 represents an ideal gas of phonons of dispersion relation $\varepsilon_{\mathbf{k}}$,

$$H_2 = \sum_{\mathbf{k} \neq 0} \varepsilon_{\mathbf{k}} \hat{b}_{\mathbf{k}}^\dagger \hat{b}_{\mathbf{k}} \quad (2)$$

The precise form of the coupling terms H_3 and H_4 in equation (1) is of little importance at this stage and will be given in section 2. The coupling between phonons makes the system acoustically non-linear and causes the damping of sound waves, the subject of the present work.

We limit our study of damping here (i) to modes of wave vector \mathbf{q} in the collisionless regime $\varepsilon_{\mathbf{q}} \gg \hbar \Gamma_{\text{th}}$ where Γ_{th} is the thermalization rate of the phonon gas or, what amounts to the same thing, the damping rate of thermal phonons of energy $\varepsilon_{\mathbf{k}} \simeq k_B T$, and (ii) to the case of an acoustic branch with a convex start in wavenumber, which can be limited to its cubic approximation at low temperature:

$$\varepsilon_{\mathbf{k}} = \hbar c k \left[1 + \frac{\gamma}{8} \left(\frac{\hbar k}{mc} \right)^2 \right] \quad \text{with } \gamma > 0 \quad (3)$$

1. The inclusion of higher-order terms H_5, H_6 , etc., would be meaningless without gradient corrections to the energy functional of quantum hydrodynamics [2], corrections which also bring the curvature term (here put by hand) into equation (3).

where m is the mass of a particle, c is the speed of sound at zero temperature and γ is a dimensionless curvature parameter.^{2,3} These assumptions allow us to describe damping in terms of elementary phonon-coupling processes⁴ and, as is generally accepted, to deduce the damping rate from Fermi's golden rule applied to the H_3 term of the Hamiltonian.⁵ Indeed, it is expected that at sufficiently low temperatures, the phonon gas will always enter the weak coupling regime, even if the constituent particles of the system are strongly interacting (as in liquid helium 4, for example [6]). We will show in this section, by simple reasoning, that this is true in dimension $d = 3$ but not in dimension $d = 2$. Phonon damping in the two-dimensional case will therefore be the subject of further study (beyond the golden rule) in subsequent sections.

Our simple reasoning is based on many-body Green's function method [7]. To fix ideas and the Green's function to be considered, we assume that the gas, initially at thermal equilibrium for the Hamiltonian H (density operator $\hat{\sigma}(0) = \hat{\sigma}_{\text{th}} \propto \exp(-H/k_B T)$), is excited by the sudden creation of a coherent state of phonons in mode \mathbf{q} :

$$\hat{\sigma}(0^+) = \hat{U}_{\text{exc}} \hat{\sigma}_{\text{th}} \hat{U}_{\text{exc}}^\dagger \quad \text{with} \quad \hat{U}_{\text{exc}} = e^{\alpha \hat{b}_{\mathbf{q}}^\dagger - \alpha^* \hat{b}_{\mathbf{q}}} \quad (4)$$

Experimentally, this excitation procedure can be carried out by a short-duration Bragg laser pulse [8, 9, 10, 11, 12]. The amplitude $\langle \hat{b}_{\mathbf{q}}(t) \rangle$ of the coherent state is then measured over time, for example through the gas density (more precisely, its Fourier components of wave vectors $\pm \mathbf{q}$). In the limit of very low initial excitation, we enter the linear response regime and can formally expand the unitary excitation operator \hat{U}_{exc} to order one in α in equation (4) to obtain

$$\langle \hat{b}_{\mathbf{q}}(t) \rangle \stackrel{t \geq 0}{\underset{\alpha \rightarrow 0}{\equiv}} \alpha \langle [\hat{b}_{\mathbf{q}}(t), \hat{b}_{\mathbf{q}}^\dagger(0)] \rangle_{\text{th}} + O(\alpha^2) \quad (5)$$

where $\hat{b}_{\mathbf{q}}(t)$ is written in Heisenberg representation for the evolution unperturbed by \hat{U}_{exc} , $\hat{b}_{\mathbf{q}}(t) = e^{iHt/\hbar} \hat{b}_{\mathbf{q}}(0) e^{-iHt/\hbar}$, the mean of the left-hand side is taken in the perturbed state $\hat{\sigma}(0^+)$ and that of the right-hand side in the initial unperturbed thermal state $\hat{\sigma}_{\text{th}}$, and we have used the fact that $\langle \hat{b}_{\mathbf{q}}(0) \hat{b}_{\mathbf{q}}(t) \rangle_{\text{th}} = \langle \hat{b}_{\mathbf{q}}(t) \hat{b}_{\mathbf{q}}(0) \rangle_{\text{th}} = 0$ by non-conservation of the total momentum. Using section 31 of reference [7], we relate our signal to the two-point Green's function \mathcal{G} of the phonon field and the associated self-energy Σ (noted Σ^* in [7]):⁶

$$s(t) \equiv e^{i\varepsilon_{\mathbf{q}} t/\hbar} \langle [\hat{b}_{\mathbf{q}}(t), \hat{b}_{\mathbf{q}}^\dagger(0)] \rangle_{\text{th}} \stackrel{t \geq 0}{\equiv} \int_{C_+} \frac{dz}{2i\pi} e^{-i(z - \varepsilon_{\mathbf{q}})t/\hbar} \mathcal{G}(\mathbf{q}, z) \quad \text{with} \quad \mathcal{G}(\mathbf{q}, z) = \frac{1}{z - \varepsilon_{\mathbf{q}} - \Sigma(\mathbf{q}, z)} \quad (6)$$

where the integration path C_+ runs in the upper half of the complex plane parallel to the real axis from $+\infty$ to $-\infty$ and where we have, for convenience, removed the free evolution due to the Hamiltonian H_2 . In the following, it will be advantageous to take as the new complex energy variable in Σ the deviation from the free-evolution energy, any confusion being avoided by indexing the wave vector dependence:

$$\Sigma(\mathbf{q}, z) = \Sigma_{\mathbf{q}}(\zeta) \quad \text{with} \quad \zeta \equiv z - \varepsilon_{\mathbf{q}} \quad \text{hence} \quad \mathcal{G}(\mathbf{q}, z) = \frac{1}{\zeta - \Sigma_{\mathbf{q}}(\zeta)} \quad (7)$$

2. As in quantum electrodynamics, the parameters appearing in the Hamiltonian are in fact the bare values, different from the actual values measured in an experiment, the passage from one to the other being made by a procedure known as "renormalisation". Equation (2) should therefore refer to a bare dispersion relation $\varepsilon_{\mathbf{k}}^{(0)}$ and equation (3) to a bare speed of sound $c^{(0)}$ and a bare curvature parameter $\gamma^{(0)}$. We do not do so here to lighten the notations, and because this renormalization does not intervene in dimension $d = 2$ at the leading order in temperature.

3. The choice $\gamma > 0$ excludes superfluids of paired spin 1/2 fermions in the limit, known as BCS, of a weakly attractive interaction between particles [3].

4. In the opposite regime $\varepsilon_{\mathbf{q}} \ll \hbar\Gamma_{\text{th}}$, the system has time to relax to a juxtaposition of local thermodynamic equilibrium states during an oscillation period of the sound wave of wavevector \mathbf{q} and damping at non-zero temperature is described through transport or viscosity coefficients, obtained by solving kinetic equations and which enter into partial differential equations on densities, velocities, volume entropy, etc, of a two-fluid model [4].

5. In the case $\gamma < 0$ of an acoustic branch with a concave start, the three-phonon processes induced by H_3 to order one do not conserve momentum-energy, and an extended formulation of the golden rule (taking into account the four-phonon processes induced by H_3 to order two and by H_4 to order one) must be used to obtain a non-zero damping rate, see references [1, 5] and our section 4.2.

6. Recall that, originally, \mathcal{G} and Σ are functions of (\mathbf{r}, t) and (\mathbf{r}', t') , where \mathbf{r}, \mathbf{r}' are two position vectors and t, t' are two times. By spatial homogeneity and stationarity of the thermal state, they are reduced to functions of $(\mathbf{r} - \mathbf{r}', t - t')$, whose space-time Fourier transforms are functions of (\mathbf{k}, ω) ; the analytic continuation of the latter to complex frequencies z/\hbar leads to functions $\mathcal{G}(\mathbf{k}, z)$ and $\Sigma(\mathbf{k}, z)$ of equation (6).

From this exact formalism, we can recover the exponential damping of Fermi's golden rule $|s(t)|^2 \simeq \exp(-\Gamma_q t)$ in two steps. (i) First, the pole approximation [13] is performed, neglecting the energy dependence of Σ :

$$\Sigma_{\mathbf{q}}(\zeta) \approx \Sigma_{\mathbf{q}}(i0^+) \quad \text{so that} \quad s(t) \simeq s_{\text{pole}}(t) = \exp[-i\Sigma_{\mathbf{q}}(i0^+)t/\hbar] \quad (8)$$

(ii) As the pole approximation is generally legitimate only in a weak coupling limit between phonons, it suffices to calculate $\Sigma_{\mathbf{q}}$ at the leading order in the coupling, i.e. at second order in H_3 , but also at first order in H_4 if we need to know $\text{Re} \Sigma_{\mathbf{q}}$. The central question of this section is whether simply taking a low-temperature limit with proper rescaling of the wave number of the mode under consideration,⁷

$$\epsilon \equiv k_B T / mc^2 \rightarrow 0 \quad \text{with} \quad \bar{q} \equiv \hbar c q / k_B T \quad \text{fixed} \quad (9)$$

is enough to bring the phonon gas into the weak coupling regime and justify the two steps. We'll see that the answer depends on the dimensionality of the system.

Step (i). To justify the pole approximation, we rely on the scaling laws describing the behavior of the self-energy at low temperature:

$$\Sigma_{\mathbf{q}}(\zeta) = k_B T \epsilon^\nu \tilde{\Sigma}_{\bar{q}}(\zeta / (k_B T \epsilon^\sigma)) \quad (10)$$

After outputting the energy scale $k_B T$, two exponents ν and σ remain, the first characterizing the order of magnitude of function $\Sigma_{\mathbf{q}}(\zeta)$, the second its energy width around $\zeta = 0$. It is understood that the new function $\tilde{\Sigma}_{\bar{q}}$ has a finite, non-zero limit when $\epsilon \rightarrow 0$. After inserting form (10) into the signal expression (6), we perform the following scaling on the conjugate variables ζ and t ,

$$\zeta \equiv k_B T \epsilon^\nu \tilde{\zeta} \quad ; \quad t \equiv \tilde{t} \hbar / (k_B T \epsilon^\nu) \quad (11)$$

to obtain the reduced expression

$$s(t) = \int_{C_+} \frac{d\tilde{\zeta}}{2i\pi} \frac{e^{-i\tilde{\zeta}\tilde{t}}}{\tilde{\zeta} - \tilde{\Sigma}_{\bar{q}}(\epsilon^{\nu-\sigma}\tilde{\zeta})} \quad (12)$$

in which ϵ still has to tend towards zero at a fixed \tilde{t} . We then see that, if $\nu > \sigma$, the argument of function $\tilde{\Sigma}_{\bar{q}}$ tends towards zero by positive imaginary-part values when $\epsilon \rightarrow 0$, which means it can be replaced by $i0^+$: we find the pole approximation (8), which is exact in this limit.

Step (ii). To find out whether it's sufficient to calculate the self-energy to the leading order in phonon coupling, let's keep only the cubic coupling H_3 for simplicity (we can check that the quartic coupling H_4 doesn't change anything qualitatively), omit the non-resonant processes it contains (terms in $\hat{b}^\dagger \hat{b}^\dagger \hat{b}^\dagger$ and $\hat{b} \hat{b} \hat{b}$) of sub-dominant contribution in the $\epsilon \rightarrow 0$ limit, and estimate the order of magnitude of its contribution of order $2n$ to $\Sigma_{\mathbf{q}}(i0^+)$ as follows:⁸

$$\Sigma_{\mathbf{q}}^{(2n)}(i0^+) \approx \int \left(\prod_{i=1}^n d^d k_i \right) \langle |\mathcal{H}_3| \rangle \frac{1}{\Delta E_1} \langle |\mathcal{H}_3| \rangle \dots \langle |\mathcal{H}_3| \rangle \frac{1}{\Delta E_{2n-1}} \langle |\mathcal{H}_3| \rangle \quad (13)$$

Let's briefly justify form (13) (the reader is referred to sections 3 and 4 for a detailed treatment of cases $n = 1$ and $n = 2$). Order $2n$ involves $2n$ actions of H_3 so $2n$ matrix elements $\langle |\mathcal{H}_3| \rangle$, each of which introduces a new independent phonon wave vector \mathbf{k}_i (Beliaev terms $\hat{b}^\dagger \hat{b}^\dagger \hat{b}$ in H_3) or makes one disappear (Landau terms $\hat{b}^\dagger \hat{b} \hat{b}$); the other phonon wave vectors that appear are deduced from \mathbf{k}_i and \mathbf{q} by conservation of momentum. Since the $2n$ actions of H_3 must conserve the number of phonons as a whole, there must be as many Beliaev processes as Landau processes, leading to exactly n independent wave vectors on which to sum. In the thermodynamic limit, we express H_3 in terms of the volumic Hamiltonian such that $H_3 = \mathcal{H}_3 / L^{d/2}$ and replace the sum over the \mathbf{k}_i by an integral. Finally, between each

7. It should be pointed out that the strength of the interactions between the constituent particles of the fluid does not vary in the limit (9), so that the speed of sound c remains constant. On the other hand, limit (9) automatically brings mode \mathbf{q} into the collisionless regime $\epsilon_{\mathbf{q}} \gg \hbar \Gamma_{\text{th}}$ because the rate Γ_{th} of gas thermalization, which can be estimated by the damping rate of phonons of wave number $\approx k_B T / \hbar c$, tends to zero faster than linearly in temperature, as we shall see.

8. As H_3 changes the parity of the phonon number, the odd-order contributions $2n + 1$ are zero.

matrix element of H_3 appears an energy denominator representing the free propagation of Hamiltonian H_2 and giving the energy difference between the initial state with a phonon \mathbf{q} and an intermediate state. Each ΔE_j ($1 \leq j \leq 2n - 1$) can be expressed as the algebraic sum (i.e. with a plus or minus sign) of j elementary energy defects $\varepsilon_{\mathbf{k}} + \varepsilon_{\mathbf{k}'} - \varepsilon_{\mathbf{k}''}$ corresponding to a $\mathbf{k} + \mathbf{k}' \leftrightarrow \mathbf{k}''$ Beliaev-Landau process. In the low-temperature limit $\epsilon \rightarrow 0$, the integral (13) is in general dominated by “small-angle” processes, where *all* intermediate phonons (those with wave vectors \mathbf{k}_i and others) are almost collinear to and in the same direction as \mathbf{q} [1, 5]; more precisely, we find that the angles θ_i between vectors \mathbf{q} and \mathbf{k}_i must be $O(\gamma^{1/2}\epsilon)$ for ΔE_j to reach their minimum energy scale $k_B T \epsilon^2$ and for the integrand to be amplified by the “small-denominator” effect, which leads to the expansion of the elementary energy defect

$$\varepsilon_{\mathbf{k}} + \varepsilon_{\mathbf{k}'} - \varepsilon_{\mathbf{k}''=\mathbf{k}+\mathbf{k}'} \underset{\epsilon \rightarrow 0}{\sim} k_B T \gamma \epsilon^2 \left[\frac{\bar{k}\bar{k}'}{\bar{k} + \bar{k}'} \frac{(\theta - \theta')^2}{2\gamma\epsilon^2} - \frac{3}{8} \bar{k}\bar{k}'(\bar{k} + \bar{k}') \right] \quad (14)$$

where γ is the curvature parameter in the dispersion relation (3), angles $\theta = \widehat{(\mathbf{q}, \mathbf{k})}$ and $\theta' = \widehat{(\mathbf{q}, \mathbf{k}')}$ are introduced, and the scaling of k to \bar{k} by its typical value $k_B T / \hbar c$ is based on equation (9). The ΔE_j are thus effectively of order $k_B T \epsilon^2$ and each $d^d k_i$ integration element in (13) written in polar or spherical coordinates brings out a factor $(k_B T / \hbar c)^d (\gamma^{1/2} \epsilon)^{d-1}$. It remains to give the estimate of the matrix elements of \mathcal{H}_3 , which is easily derived from their expression (31) to come (the coupling constant Λ is given by equation (28)):

$$\langle |\mathcal{H}_3| \rangle \approx (k\xi k' \xi k'' \xi)^{1/2} (1 + \Lambda) \frac{mc^2}{\rho^{1/2}} \approx \epsilon^{3/2} (1 + \Lambda) \frac{mc^2 \xi^{d/2}}{(\rho \xi^d)^{1/2}} \quad (15)$$

where we have introduced the density ρ of the fluid and the so-called relaxation or correlation length of the superfluid,

$$\xi = \frac{\hbar}{mc} \quad (16)$$

We thus end up with the estimate

$$\boxed{\Sigma_{\mathbf{q}}^{(2n)}(i0^+) \underset{\epsilon \rightarrow 0}{\approx} k_B T \gamma \epsilon^2 \left[\frac{\epsilon^{2d-4} (1 + \Lambda)^2}{\gamma^{(5-d)/2} \rho \xi^d} \right]^n \quad (n > 0, d \geq 2)} \quad (17)$$

which designates the quantity in square brackets as the small parameter of the perturbative expansion of $\Sigma_{\mathbf{q}}$ in the coupling. The degree in ϵ of the leading non-zero order, corresponding to the choice $n = 1$ in equation (17), gives the value of the exponent ν in equation (10):

$$\nu = 2d - 2 \quad (18)$$

The value of the second exponent σ is obtained by generalizing estimate (13) to the case $\zeta \neq 0$, which amounts to adding ζ to the energy of the initial state and therefore to each energy denominator, $\Delta E_j \rightarrow \Delta E_j + \zeta$. As we've seen, $\Delta E_j \approx k_B T \epsilon^2$; this is also the width of the self-energy around $z = \epsilon_{\mathbf{q}}$ (around $\zeta = 0$), so that

$$\sigma = 2 \quad (19)$$

irrespective of dimensionality.

Three-dimensional case. In dimension $d = 3$, where $\nu = 4 > \sigma = 2$ and where $2d - 4 = 2 > 0$ in the square brackets of equation (17), steps (i) and (ii) are justified and the damping of mode \mathbf{q} is described exactly by Fermi's golden rule in the limit (9). We then find the low-temperature behavior of the imaginary part of $\Sigma_{\mathbf{q}}(i0^+)$,

$$\begin{aligned} \text{Im} \Sigma_{\mathbf{q}}^{d=3}(i0^+) \underset{\epsilon \rightarrow 0}{\overset{\bar{q} \text{ fixed}}{\sim}} & - \frac{9k_B T \epsilon^4 (1 + \Lambda)^2}{32\pi\rho\xi^3} \left[\int_0^{\bar{q}} d\bar{k} \bar{k}^2 (\bar{q} - \bar{k})^2 (\bar{n}_{\bar{k}}^{\text{lin}} + 1/2) + \int_0^{+\infty} d\bar{k} \bar{k}^2 (\bar{k} + \bar{q})^2 (\bar{n}_{\bar{k}}^{\text{lin}} - \bar{n}_{\bar{k}+\bar{q}}^{\text{lin}}) \right] \\ & = - \frac{9k_B T \epsilon^4 (1 + \Lambda)^2}{32\pi\rho\xi^3} \left\{ \frac{\bar{q}^5}{60} + 48[g_5(1) - g_5(e^{-\bar{q}})] - 24\bar{q}g_4(e^{-\bar{q}}) + 4\bar{q}^2[g_3(1) - g_3(e^{-\bar{q}})] \right\} \quad (20) \end{aligned}$$

corresponding exactly to the Γ_q damping rate given in reference [5] (multiplied by the usual $-\hbar/2$ factor). In equation (20), Bose functions $g_\alpha(z) = \sum_{n=1}^{+\infty} z^n/n^\alpha$ have been introduced and it has been possible to replace the dispersion relation $\varepsilon_{\mathbf{k}}$ by its linear approximation $\hbar c k$ in the occupation numbers, which is indicated by the exponent “lin”:

$$\bar{n}_k^{\text{lin}} = \frac{1}{\exp \bar{k} - 1} \quad (21)$$

It is satisfying to note that the prefactor in (20) is indeed that predicted by (17) for $n = 1$ (and $d = 3$); in particular, it is independent of the curvature parameter γ . Green’s function formalism also gives access to the real part, which was out of reach of reference [5] and represents the thermal energy shift of phonon \mathbf{q} ,⁹

$$\text{Re } \Sigma_{\mathbf{q}, \text{th}}^{d=3}(i0^+) \underset{\epsilon \rightarrow 0}{\overset{\bar{q} \text{ fixed}}{\sim}} \frac{k_B T \epsilon^4 (1 + \Lambda)^2}{2\pi^2 \rho \xi^3} \left\{ \bar{q} \zeta(4) \left[-27 \ln \frac{e(3\gamma)^{1/2} \epsilon}{4} + \frac{2 + 18\Lambda + 3\Lambda_*/2}{(1 + \Lambda)^2} \right] + \frac{9}{8} \int_0^{+\infty} d\bar{k} \bar{k}^2 \bar{n}_k^{\text{lin}} \left[(\bar{k} - \bar{q})^2 \ln |\bar{k} - \bar{q}| - (\bar{k} + \bar{q})^2 \ln(\bar{k} + \bar{q}) \right] \right\} \quad (22)$$

where ζ is the Riemann zeta function, such that $\zeta(s) = g_s(1)$, and $\zeta(4) = \pi^4/90$. For the real part, we obtain a more complicated form than that of (17) because (a) the angles between \mathbf{q} and \mathbf{k} of order $\theta \approx \epsilon^0$ contribute at the same level as the small angles $\theta \approx \epsilon$,¹⁰ and (b) the quartic Hamiltonian H_4 also contributes, which forces us to introduce the second coupling constant Λ_* of equation (28). In particular, we notice a logarithmic correction to the $k_B T \epsilon^4$ law. In the $\bar{q} \rightarrow 0$ limit, expression (22) becomes $\sim \hbar q \delta c_{\text{th}}$, where coefficient δc_{th} is the thermal correction to the speed of collisionless sound in the fluid. The value of δc_{th} derived from Andreev and Khalatnikov’s kinetic theory [15], see equation (45) in reference [14], is in good agreement with ours,¹¹ but that deduced from the leading order of effective field theory, see equation (33) in reference [14], is in disagreement.

Two-dimensional case. In dimension $d = 2$, where $\nu = \sigma = 2$ and where $2d - 4 = 0$, we fail to justify step (i) and step (ii) at low temperature! In particular, the bracketed expression in equation (17) does not depend on ϵ and only becomes a small parameter in the $\rho \xi^2 \gg 1$ limit where the underlying superfluid itself (and not just the phonon gas) enters the weakly interacting regime. So, in $d = 2$, taking the $\epsilon \rightarrow 0$ limit makes neither the pole approximation nor the $\Sigma_{\mathbf{q}}(\zeta)$ second-order calculation in phonon coupling accurate. To obtain the correct expression of the signal in this limit, we need to calculate $\tilde{\Sigma}_{\bar{q}}(\zeta)$ for all values of ζ and at all orders in H_3 . However, let’s take as a reference value the low-temperature behavior of $\Sigma_{\mathbf{q}}(i0^+)$ at the leading order in the coupling ($n = 1$):

$$\Sigma_{\mathbf{q}}^{(2)}(i0^+) \underset{\epsilon \rightarrow 0}{\overset{\bar{q} \text{ fixed}}{\sim}} -i \frac{9k_B T \epsilon^2 (1 + \Lambda)^2}{8\pi (3\gamma)^{1/2} \rho \xi^2} \left[\int_0^{\bar{q}} d\bar{k} \bar{k} (\bar{q} - \bar{k}) (\bar{n}_k^{\text{lin}} + 1/2) + \int_0^{+\infty} d\bar{k} \bar{k} (\bar{k} + \bar{q}) (\bar{n}_k^{\text{lin}} - \bar{n}_{k+\bar{q}}^{\text{lin}}) \right] = \boxed{-i \frac{9k_B T \epsilon^2 (1 + \Lambda)^2}{8\pi (3\gamma)^{1/2} \rho \xi^2} \left[\frac{\bar{q}^3}{12} + 2\zeta(2)\bar{q} \right]} \equiv -i \frac{\hbar \Gamma_q}{2} \quad (23)$$

9. We omit in (22) the so-called quantum component, independent of occupation numbers, which is at the leading order in ϵ the sum of two contributions, (i) an ill-defined contribution, linear combination of monomials q, q^3 and q^5 with coefficients divergently dependent on the ultraviolet cutoff η of equation (26), which must therefore be reabsorbed in $\varepsilon_{\mathbf{q}}$, i.e. in a redefinition of the dispersion relation (see also footnote 2), and (ii) a universal contribution predicted quantitatively by quantum hydrodynamics, $\text{Re } \Sigma_{\mathbf{q}, \text{quant univ}}^{d=3}(i0^+) = [3(1 + \Lambda)^2 / (160\pi^2)] (\hbar^2 q^5 / m\rho) \ln(\hbar q / mc)$. Such a contribution in $q^5 \ln q$ was qualitatively expected in reference [2]. It appears in equation (35) of reference [14], with the correct numerical coefficient but with an extra factor c .

10. Indeed, in the angular integration, in $d = 3$, $\sin \theta d\theta / (\Delta E / k_B T)$ is $\approx \epsilon^0$ at large angles and $\approx \epsilon^2 / \epsilon^2 = \epsilon^0$ at small angles, where ΔE is an energy denominator. This phenomenon does not occur for the imaginary part, given the energy-conserving Dirac distribution $\delta(\Delta E)$ and the fact that ΔE only vanishes at small angles for low-temperature thermal phonons. In practice, to obtain (22), we split the angular integral into two intervals, $\theta \in [0, \alpha]$ and $\theta \in [\alpha, \pi]$, where $\alpha \ll 1$ is fixed. In the first interval, the curvature term in the dispersion relation is kept in the denominator of the integrand, but the numerator is replaced by its leading order in θ (i.e. $\sin \theta \approx \theta$). In the second interval, we use the linear dispersion relation, but keep all the dependence in θ of the trigonometric functions. All calculations done, the lower and upper parts of the integral include a divergence in $\ln \alpha$ which disappears exactly in their sum.

11. Perfect agreement is reached if, in equation (45) of [14], we replace $\ln 27$ by $25/6 - 2C + \ln(3/2) + 2\zeta'(4)/\zeta(4) = \ln(26.852 \dots)$ where $C = 0.577 \dots$ is Euler’s constant. This small deviation results from an approximation made by Andreev and Khalatnikov in the calculation of an integral, that of equation (13) in [15].

with $\zeta(2) = \pi^2/6$. At sufficiently low temperatures, $\Sigma_{\mathbf{q}}^{(2)}(i0^+)$ becomes pure imaginary and reduces to $-i\hbar\Gamma_q/2$ where Γ_q is the damping rate of the golden rule at the leading order in ϵ (the quartic Hamiltonian H_4 does not show a real part here as it is subleading in ϵ , see section 3). Equation (23) is, as far as we know, original. In limits $\bar{q} \rightarrow 0$ and $\bar{q} \rightarrow +\infty$, it reproduces equations (30) and (22) of reference [16] (times $-i\hbar$ given the conventions of [16]), which deals with the two-dimensional gas of weakly interacting bosons for which $\gamma = 1$ (as in the Bogoliubov spectrum) and $\Lambda = 0$ (as in the zero-temperature mean-field equation of state $\mu = \rho g$ used in [16]). In the following, in dimension $d = 2$, we go beyond Fermi's golden rule with classical field numerical simulations in section 2 and with the Green's function method to higher and higher orders in H_3 in later sections: to order two in section 3, to order four in section 4 and non-perturbatively in section 5; to our surprise, we are forced to do so by the failure of estimate (17) for $n \geq 2$. In fact, by an explicit calculation of the fourth order contribution in H_3 in section 4, we establish a troubling result that disproves (17) in dimension $d = 2$: $\Sigma_{\mathbf{q}}^{(4)}(i0^+)$ does not tend to zero as $k_B T \epsilon^2$ at low temperature $\epsilon \rightarrow 0$, but as $k_B T \epsilon^0$, see equation (96). This effectively makes the perturbative expansion in powers of H_3 unusable in this limit, since the fourth order becomes much larger than the second order for a fixed interaction strength $(\rho \xi^2)^{-1}$ in the superfluid. To obtain an operational description of the damping, section 5, contrary to equation (17), takes the limit $\epsilon \rightarrow 0$ with fixed $\tilde{\zeta} \neq 0$ in $\tilde{\Sigma}_{\bar{q}}^{(4)}(\tilde{\zeta})$, regularizes the result (divergent at $\tilde{\zeta} = 0$) nonperturbatively by assigning finite lifetimes to the intermediate phonons of the four-phonon collisional processes, and calculates the integral over $\tilde{\zeta}$ in equation (12), finally obtaining a damping rate scaling as $k_B T \epsilon^2$ as expected. We conclude in section 6.

2. Numerical experiment in the classical field model

Experimental studies of sound in two-dimensional superfluid ultracold atomic gases have so far concentrated on the hydrodynamic [17, 18] regime or, in the collisionless regime, on the $\epsilon = k_B T / mc^2 \geq 1$ [19, 20, 21] temperature interval. To verify that in dimension $d = 2$, the low-temperature limit (9) is not sufficient to render accurate the exponential decay predicted by Fermi's golden rule, we therefore carry out in this section a numerical study of phonon damping, at all orders in coupling H_3 , in the classical field model. We first recall the quantum hydrodynamics Hamiltonian of Landau and Khalatnikov. We then explain how to numerically integrate its classical field version and introduce a correlation function that is more convenient to calculate than signal (6), but almost equivalent. We then analyze the results obtained for different interaction strengths.

2.1. Quantum hydrodynamics Hamiltonian

Quantum hydrodynamics is an effective low-energy theory that provides accurate predictions to leading order in temperature, even for a strongly interacting fluid [1]. The fluid is decomposed into small, but still mesoscopic elements of size b ($b \gg \xi = \hbar/mc$). Each element, with center \mathbf{r} , is (i) sufficiently large that it has a large number of particles ($\rho b^d \gg 1$), allowing it to be assigned a phase operator $\hat{\phi}(\mathbf{r})$ canonically conjugated to its particle number operator $\hat{\rho}(\mathbf{r})b^d$, $[\hat{\rho}(\mathbf{r})b^d, \hat{\phi}(\mathbf{r}')] = i\delta_{\mathbf{r},\mathbf{r}'}$, and (ii) small enough to be considered both as homogeneous ($b \ll \lambda_{\text{th}}$ where $\lambda_{\text{th}} = 2\pi\hbar c/k_B T$ is the de Broglie wavelength of a thermal phonon in the fluid) and in its ground state ($k_B T \ll \epsilon_{\text{exc}}^{\text{min}}$ where $\epsilon_{\text{exc}}^{\text{min}} = \hbar c(2\pi/b)$ is the minimum phonon excitation energy in the small element).¹² The Hamiltonian is then the sum of the kinetic energies of the center of mass and the internal energy of each small element:

$$H_{\text{hydro}} = \sum_{\mathbf{r}} \frac{1}{2} m \hat{\mathbf{v}}(\mathbf{r}) \cdot \hat{\rho}(\mathbf{r}) b^d \hat{\mathbf{v}}(\mathbf{r}) + b^d e_0(\hat{\rho}(\mathbf{r})) \quad (24)$$

where $\hat{\mathbf{v}} = (\hbar/m)\mathbf{grad} \hat{\phi}$ is the fluid velocity field and $e_0(\rho)$ is the bulk energy density in the ground state at density ρ . At low temperatures, the density field $\hat{\rho}(\mathbf{r})$ fluctuates little and the phase field $\hat{\phi}(\mathbf{r})$ varies slowly; we separate them

12. The ultraviolet cutoff to come corresponds more or less to the choice $\pi/b \approx \eta k_B T / \hbar c$. Even so, b remains well below the coherence length of the fluid at sufficiently low temperatures. This is obvious in $d = 3$ because of the presence of condensate. It is also true in $d = 2$ where the first-order coherence function $g_1(\mathbf{r})$ decreases at large distances as $\exp[mk_B T \ln(\xi/r)/(2\pi\hbar^2\rho_s)]$ where $\rho_s \approx \rho$ is the superfluid density [22, 23, 24]. This makes the assumption $\hat{\mathbf{v}} = (\hbar/m)\mathbf{grad} \hat{\phi}$ used in reference [1] and in equation (24) plausible.

into their Fourier components of zero wave vector $\hat{\rho}_0 = \hat{N}/L^d \simeq \rho$ and $\hat{\phi}_0$, and into spatial fluctuations $\delta\hat{\rho}(\mathbf{r})$ and $\delta\hat{\phi}(\mathbf{r})$ admitting modal expansions [25]

$$\delta\hat{\rho}(\mathbf{r}) = \frac{1}{L^{d/2}} \sum_{\mathbf{k} \neq \mathbf{0}} \left(\frac{\hbar\rho k}{2mc} \right)^{1/2} (\hat{b}_{\mathbf{k}} + \hat{b}_{-\mathbf{k}}^\dagger) e^{i\mathbf{k}\cdot\mathbf{r}} \quad ; \quad \delta\hat{\phi}(\mathbf{r}) = \frac{-i}{L^{d/2}} \sum_{\mathbf{k} \neq \mathbf{0}} \left(\frac{mc}{2\hbar\rho k} \right)^{1/2} (\hat{b}_{\mathbf{k}} - \hat{b}_{-\mathbf{k}}^\dagger) e^{i\mathbf{k}\cdot\mathbf{r}} \quad (25)$$

where $\hat{b}_{\mathbf{k}}^\dagger$ and $\hat{b}_{\mathbf{k}}$ are the creation and annihilation operators of a phonon of wave vector \mathbf{k} in the quantization box $[0, L]^d$, c is the speed of sound at zero temperature, given by $mc^2 = \rho(d\mu/d\rho)$ with $\mu = de_0/d\rho$ the chemical potential of the fluid in the ground state. As in any effective theory, we need to put an ultraviolet cutoff in the space of wave vectors, which we take here to be isotropic

$$\hbar ck < \eta k_B T \quad (26)$$

and to which the sums (25) are restricted; we'll let the temperature tend towards zero as in (9) and then $\eta \rightarrow +\infty$ (in the quantum case) without encountering divergences if all goes well. It remains to expand H_{hydro} into powers of $\delta\hat{\rho}$ and $\mathbf{grad} \delta\hat{\phi}$. Zero order provides a constant of no interest. Order one is zero by construction. Order two, diagonalized by the transformation (25), gives back the Hamiltonian H_2 of equation (2) with a linear dispersion relation, the curvature in equation (3) having to be put in by hand, see references [1, 5] and our footnote 1. The third and fourth orders, giving the coupling between phonons in equation (1), are written in representation \mathbf{r} :

$$H_3 = b^d \sum_{\mathbf{r}} \frac{1}{2} m \hat{\mathbf{v}}(\mathbf{r}) \cdot \delta\hat{\rho}(\mathbf{r}) \hat{\mathbf{v}}(\mathbf{r}) + \frac{1}{6} \frac{d^2\mu}{d\rho^2} \delta\hat{\rho}(\mathbf{r})^3 \quad ; \quad H_4 = b^d \sum_{\mathbf{r}} \frac{1}{24} \frac{d^3\mu}{d\rho^3} \delta\hat{\rho}(\mathbf{r})^4 \quad (27)$$

knowing that $\mathbf{grad} \hat{\phi} = \mathbf{grad} \delta\hat{\phi}$. They involve the dimensionless coupling constants

$$\Lambda = \rho \frac{d^2\mu}{d\rho^2} / (3 \frac{d\mu}{d\rho}) = \rho^2 \frac{d^2\mu}{d\rho^2} / (3mc^2) \quad \text{and} \quad \Lambda_* = \rho^3 \frac{d^3\mu}{d\rho^3} / (mc^2) \quad (28)$$

To reveal the physical processes contained in H_3 and already mentioned in section 1, we insert in (27) the modal expansions (25) and collect together the terms of the same type, Beliaev, Landau and non-resonant respectively:

$$H_3 = H_3^{(+)} + H_3^{(-)} + H_3^{(\text{non res.})} \quad (29)$$

with

$$H_3^{(-)} = (H_3^{(+)})^\dagger = \frac{1}{2L^{d/2}} \sum_{\mathbf{k}, \mathbf{k}'} \mathcal{A}(\mathbf{k}, \mathbf{k}'; \mathbf{k} + \mathbf{k}') \hat{b}_{\mathbf{k} + \mathbf{k}'}^\dagger \hat{b}_{\mathbf{k}} \hat{b}_{\mathbf{k}'} \quad ; \quad H_3^{(\text{non res.})} = \frac{1}{6L^{d/2}} \sum_{\mathbf{k}, \mathbf{k}'} \mathcal{A}(\mathbf{k}, \mathbf{k}'; -(\mathbf{k} + \mathbf{k}')) (\hat{b}_{\mathbf{k}} \hat{b}_{\mathbf{k}'} \hat{b}_{-(\mathbf{k} + \mathbf{k}')} + \text{h.c.}) \quad (30)$$

and the coupling amplitude¹³

$$\mathcal{A}(\mathbf{k}, \mathbf{k}'; \mathbf{k}'') = mc^2 \left(\frac{\hbar^3 k k' k''}{8\rho m^3 c^3} \right)^{1/2} \left(3\Lambda + \frac{\mathbf{k} \cdot \mathbf{k}'}{kk'} + \frac{\mathbf{k} \cdot \mathbf{k}''}{kk''} + \frac{\mathbf{k}' \cdot \mathbf{k}''}{k'k''} \right) \quad (31)$$

Of course, all wave vectors $\mathbf{k}, \mathbf{k}', \pm(\mathbf{k} + \mathbf{k}')$ appearing in the Hamiltonian are non-zero and subject to condition (26). Writing H_4 in representation \hat{b} and \hat{b}^\dagger is of little interest here, and we dispense with it.

2.2. Classical field model

The model is built by replacing operators $\hat{b}_{\mathbf{k}}$ and $\hat{b}_{\mathbf{k}}^\dagger$ in section 2.1 with complex amplitudes $b_{\mathbf{k}}$ and $b_{\mathbf{k}}^*$. This only makes sense for highly populated phonon modes, which imposes a choice of cutoff $\eta \lesssim 1$ in equation (26); in the simulations, we'll take $\eta = 1$. At thermal equilibrium, mode occupation numbers are no longer given by Bose's law, but by equipartition $\bar{n}_{\mathbf{k}}^{\text{clas}} = k_B T / \varepsilon_{\mathbf{k}}$.

13. By choice of notation, our amplitude \mathcal{A} differs by a factor of two from that of reference [5] (more precisely by a factor $2mc^2/\rho^{1/2}$).

Let's restrict our numerical study to the experimentally relevant case of a gas of spinless bosons in the quasi-2D regime, where the chemical potential μ in the xOy plane is less than, but not very small compared to $\hbar\omega_\perp$, the quantum of excitation of the motion along Oz ; in this case, the equation of state takes the simple form $\mu = \rho g$ with $g = (8\pi)^{1/2}\hbar^2 a_{3D}/(ma_\perp)$, where a_{3D} is the 3D scattering length and $a_\perp = (\hbar/m\omega_\perp)^{1/2}$ the size of the harmonic oscillator along Oz [26, 27], so that $\Lambda = \Lambda_* = 0$ in equation (28) and $H_4 \equiv 0$ in equation (27).¹⁴

The numerical simulation method is described in detail in reference [34]. To sample the initial state, $b_{\mathbf{k}}$ are drawn according to the (Gaussian) thermal distribution for the H_2 Hamiltonian, then the resulting field is evolved with the full Hamiltonian H to reach true thermal equilibrium by ergodicity. The time evolution on each dt step is split into the evolution due to H_2 during $dt/2$, the evolution due to H_3 alone during dt and then again the evolution due to H_2 during $dt/2$. The evolution due to H_2 is calculated exactly in \mathbf{k} space, while the evolution due to H_3 is calculated in \mathbf{r} ¹⁵ space by the fourth-order Runge-Kutta method [35], remembering to filter the field in \mathbf{k} space as in equation (26) after each action of H_3 in \mathbf{r} space to eliminate the cut-off-violating processes that H_3 has induced.¹⁶ The dt step must be small enough for the total energy on a single realization to be conserved to better than one percent of the typical $\langle |H_3| \rangle$ interaction energy, where $\langle \dots \rangle$ is the average over a large number of realizations, itself a very small fraction of the total energy.

It would be numerically inefficient to determine phonon damping by simulating a Bragg excitation (4), as this would require a large number of independent simulations for each new value of wave vector \mathbf{q} , while ensuring that amplitude α is small enough to be in the linear response regime.¹⁷ We prefer to use the following correlation function, allowing all possible values of \mathbf{q} to be processed in parallel by simple averaging over the same set of independent realizations:¹⁸

$$s_*(t) \equiv \frac{e^{i\varepsilon_{\mathbf{q}}t/\hbar} \langle \hat{b}_{\mathbf{q}}(t) \hat{b}_{\mathbf{q}}^\dagger(0) \rangle_{\text{th}}}{\langle \hat{b}_{\mathbf{q}}(0) \hat{b}_{\mathbf{q}}^\dagger(0) \rangle_{\text{th}}} \underset{t>0}{\simeq} \lim_{\delta \rightarrow 0^+} \int_{-\infty}^{+\infty} \frac{d\varepsilon}{-2i\pi} e^{-i(\varepsilon - \varepsilon_{\mathbf{q}})t/\hbar} \frac{\mathcal{G}(\mathbf{q}, \varepsilon + i\delta) + [\mathcal{G}(\mathbf{q}, \varepsilon + i\delta) - \mathcal{G}(\mathbf{q}, \varepsilon - i\delta)]}{1 + 1/[\exp(\varepsilon/k_B T) - 1]} \quad (32)$$

In practice, this signal is very close to that of equation (6), which in simulations allows us to identify it with $s(t)$, as we'll do in the figure caption:

$$s_*(t) \simeq s(t) \quad (33)$$

Indeed, even for the strongest interaction considered in our simulations, we have, for any value of energy ε , the property $|\text{Im}\Sigma(\mathbf{q}, \varepsilon + i0^+)| \ll \varepsilon_{\mathbf{q}}$, so that the difference between the bracketed Green's functions $\mathcal{G}(\mathbf{q}, \varepsilon \pm i\delta)$ in equation (32), which can only result from a non-zero imaginary part of the self-energy in the limit $\delta \rightarrow 0^+$, is very small except in the width of "Lorentzian" $\mathcal{G}(\mathbf{q}, \varepsilon + i0^+)$ where $|\varepsilon - \varepsilon_{\mathbf{q}}| \lesssim |\text{Im}\Sigma(\mathbf{q}, \varepsilon + i0^+)| \ll \varepsilon_{\mathbf{q}}, k_B T$. It is therefore an excellent approximation to replace ε by $\varepsilon_{\mathbf{q}}$ in Bose's law in the numerator of the integrand in (32). By analyticity in the lower complex half-plane, the term proportional to $\mathcal{G}(\mathbf{q}, z - i\delta) \exp(-izt/\hbar)$ then gives a zero contribution to the integrand for $t > 0$ (this can be seen by closing the integration path with a semicircle at infinity and using Cauchy's

14. The Popov equation of state of a strictly two-dimensional Bose gas in the weakly interacting regime corresponds to a chemical potential-dependent pseudo-coupling constant, $g(\mu) = 4\pi\hbar^2/[m \ln(\varepsilon_0/\mu)]$ where $\varepsilon_0 = 4\hbar^2/[ma_{2D}^2 \exp(2C + 1)]$, a_{2D} is the 2D scattering length and $C = 0.577\dots$ is the Euler constant [28, 29]. In its range of validity [30], it leads to non-zero but small values of Λ and Λ_* , for example $\Lambda = mg(\mu)/(12\pi\hbar^2)/[1 - mg(\mu)/(4\pi\hbar^2)]^2 \simeq mg(\mu)/(12\pi\hbar^2) \ll 1$. The quasi- and strictly 2D regimes are connected by noting that $g = g(\mu = 0.105965\dots \hbar\omega_\perp)$ in view of the expression of a_{2D} in terms of a_{3D} and a_\perp given in references [31, 32, 33].

15. Since the equations of motion deriving from H_3 are local in \mathbf{r} space (or quasi-local since they involve spatial gradients), the complexity on a step dt is of degree one in the number of points \mathcal{N} on the numerical grid; in \mathbf{k} space, they are strongly non-local (each amplitude $b_{\mathbf{k}}$ is roughly coupled to all the others) resulting in catastrophic complexity $\propto \mathcal{N}^2$.

16. The change from \mathbf{r} to \mathbf{k} is performed by a fast Fourier transform, in which the wave vectors span the set $\mathcal{D} \cap (2\pi/L)\mathbb{Z}^d$ with $\mathcal{D} = [-k_{\text{max}}, k_{\text{max}}]^d$ (each Cartesian component k_α of \mathbf{k} has a meaning modulo $2k_{\text{max}}$, so that \mathcal{D} can be regarded as the first Brillouin zone of the spatial lattice $(\pi/k_{\text{max}})\mathbb{Z}^d$, which is precisely that spanned by \mathbf{r} in the simulations with restriction to $[0, L]^d$). The naive choice $k_{\text{max}} = \eta k_B T/\hbar c$ associated with the cutoff (26) is not suitable: the processes of H_3 bringing phonons out of the corresponding first Brillouin zone are then folded back into this zone (Umklapp processes) and can no longer be filtered. At the very least, $k_{\text{max}} = 2\eta k_B T/\hbar c$ must be used: filtering forces us to double the number of points per dimension.

17. The classical field version $\langle \partial b_{\mathbf{q}}(t)/\partial b_{\mathbf{q}}(0) \rangle_{\text{th}}$ of the correlation function $\langle [\hat{b}_{\mathbf{q}}(t), \hat{b}_{\mathbf{q}}^\dagger(0)] \rangle_{\text{th}}$, which involves a numerical derivative in the particular mode \mathbf{q} , faces the same problems.

18. The obtention of the right-hand side of equation (32) is done by means of the exact relation (31.24) of reference [7] but is here approximated as we replaced $\langle \hat{b}_{\mathbf{q}}(0) \hat{b}_{\mathbf{q}}^\dagger(0) \rangle_{\text{th}}$ in the denominator by $1 + \bar{n}_{\mathbf{q}}$, where $\bar{n}_{\mathbf{q}}$ is the Bose law at energy $\varepsilon_{\mathbf{q}}$; this is however an excellent approximation for our simulations.

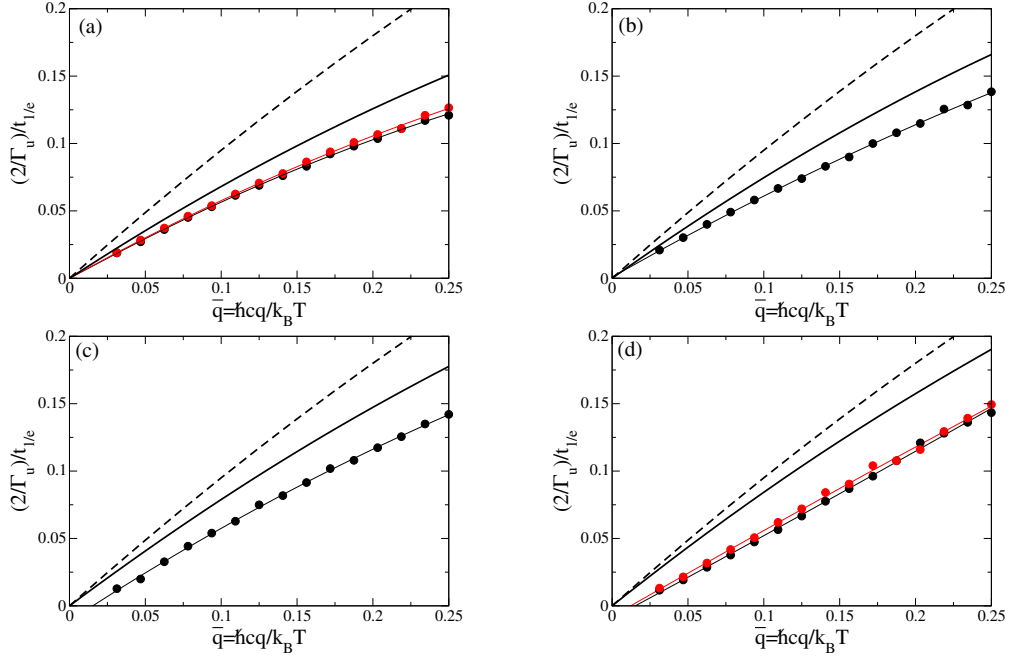


Figure 1: Inverse of the decay time at $1/e$ of the modulus of signal $s(t)$ (6) as a function of the wavenumber q of the modes along Ox , $\mathbf{q} = \pm q \mathbf{e}_x$, for different (increasingly weaker) interaction strengths in the two-dimensional superfluid of bosons: (a) $(\rho \xi^2)^{-1} = 0.64$, (b) $(\rho \xi^2)^{-1} = 0.46$, (c) $(\rho \xi^2)^{-1} = 0.28$, (d) $(\rho \xi^2)^{-1} = 0.1$. Discs (superimposed on a thin-line quadratic fit): numerical experiment with $\epsilon = 1/2$ (black) or $\epsilon = 1/3$ (red). Black dashed line: Fermi's golden rule (34) for the classical phononic field in the $\epsilon \rightarrow 0$ limit. Black solid line: many-body Green's function method with the $\Sigma_{\bar{q}}^{(2,2)}(\zeta)$ (40) self-energy (leading order in H_3 and ϵ). The other parameters have the following fixed values: $\gamma = 1$, $\Lambda = \Lambda_* = 0$, $\eta = 1$. In the simulations, the system size is large enough for the thermodynamic limit to be reached (a quantization box width of $L = 128\pi\hbar c/k_B T$ is sufficient). In the theory, the self-energies are replaced by their classical field versions to enable comparison with numerics. The rate Γ_u used as a unit is that of equation (34).

theorem) and we end up with (33). The same conclusion applies to the classical field model, where the two exponential functions in (32) are linearized.

2.3. Numerical results

In Figure 1, we plot the inverse of the decay time at $1/e$ of the signal as a function of the reduced wavenumber $\bar{q} = \hbar c q / k_B T$ of the mode under consideration, for four values of the interaction strength $1/(\rho \xi^2)$ and for one or two values of $\epsilon = k_B T / mc^2$, see the disks. The unit of time is $2\Gamma_u^{-1}$, where the constant Γ_u appears as a prefactor in the damping rate of Fermi's golden rule at the leading order in ϵ , here for the classical field:¹⁹

$$\Gamma_q^{\text{clas}} = \Gamma_u \bar{q} (\eta - \bar{q}/2) \quad \text{with} \quad \Gamma_u = \frac{9k_B T \epsilon^2 (1 + \Lambda)^2}{4\pi\hbar (3\gamma)^{1/2} \rho \xi^2} \quad (34)$$

As can be seen in panels (a) and (d) of Figure 1, the results normalized in this way do not depend significantly on ϵ at \bar{q} fixed and the $\epsilon \rightarrow 0$ limit appears to be reached; in the simulations, the inverse of the decay time at $1/e$ therefore varies indeed as $k_B T \epsilon^2$ at low temperature, as predicted by the golden rule and more generally by estimate (17) at all orders in H_3 . On the other hand, the \bar{q} dependence of the damping time is very poorly described by the golden rule, dashed line in Figure 1: as predicted by the general reasoning of section 1, the $\epsilon \rightarrow 0$ limit is therefore not sufficient in 2D to bring the phonon gas into a weak coupling regime. What section 1 didn't say, however, is that the golden

19. In expression (23) for the quantum field, we replace \bar{n}_k^{lin} by $1/\bar{k}$, neglect the term $1/2$ in front of \bar{n}_k^{lin} in the first integral and put the cutoff $\bar{k} < \eta - \bar{q}$ in the second.

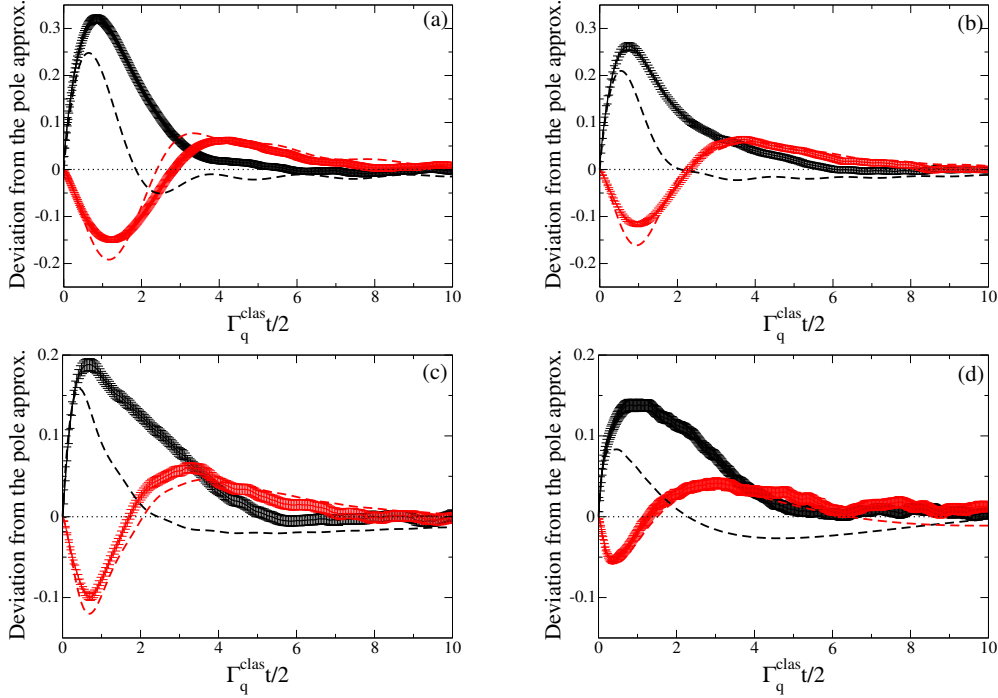


Figure 2: Deviation $s(t) - s_{\text{pole}}(t)$ of signal (6) from pole approximation (8) as a function of time, for the mode of reduced wavenumber $\bar{q} = 1/4$ along Ox and for the same interaction strengths as in Figure 1: (a) $(\rho\xi^2)^{-1} = 0.64$, (b) $(\rho\xi^2)^{-1} = 0.46$, (c) $(\rho\xi^2)^{-1} = 0.28$, (d) $(\rho\xi^2)^{-1} = 0.1$. Curves with error bars: results of the numerical experiment; dashed line: many-body Green's function theory with the $\bar{\Sigma}_{\bar{q}}^{(2,2)}(\zeta)$ (40) self-energy (leading order in H_3 and ϵ) in its classical field version. The real part of the deviation is shown in black, the imaginary part in red. We took $\epsilon = 1/2$ in the numerical experiment and for the calculation of $s_{\text{pole}}(t)$ (carried out to second order in H_3 and to all orders in ϵ) but we checked that we obtain the same results (within the error bars) for $\epsilon = 1/3$. The other parameters are fixed at $\gamma = 1$, $\Lambda = \Lambda_s = 0$, $\eta = 1$. In the simulations, the sizes are chosen to ensure that the thermodynamic limit is reached (width $L = 128\pi\hbar c/k_B T$ for (a), (b) and (c); double width for (d)). Time is scaled by the half-rate of the golden rule in the classical field (34).

rule remains insufficient even if the underlying superfluid enters the weakly interacting regime $(\rho\xi^2)^{-1} \rightarrow 0$, see panel (d) where a perturbative calculation at the leading order in H_3 should a priori be legitimate; the behavior at weak \bar{q} predicted by (34) is in fact particularly bad there.

To make the inadequacy of the golden rule even more glaring, we plot in Figure 2, as a function of time, the deviation of the numerical signal from the pole approximation (8) limited to second order at H_3 but taken to all orders in ϵ [see equation (39)] and transformed for the classical field (if we were at the leading order in ϵ , it would simply be the deviation from the exponential $\exp(-\Gamma_q^{\text{clas}} t/2)$ of the golden rule), for the same interaction strengths as before but for a fixed value of the reduced wave number, $\bar{q} = 1/4$, large enough to make it easy to reach the thermodynamic limit in simulations.²⁰ Here too, the $\epsilon \rightarrow 0$ limit is reached in simulations (when time t is scaled as in (11) with $\nu = 2d - 2 = 2$, which is done here by expressing it in units of $2/\Gamma_q^{\text{clas}}$), the expected deviation from the golden rule is indeed present and persists even in the weakly interacting limit $(\rho\xi^2)^{-1} \rightarrow 0$, at least on the real part.²¹

3. Study at leading order in phonon-phonon coupling

The classical field simulations of section 2 established the inadequacy of Fermi's golden rule in describing phonon damping in dimension $d = 2$; we have not shown this here, but in addition to disagreement on the decay time at $1/e$,

20. The smaller \bar{q} is, the lower the damping rate of the mode and the greater the granularity of the energy levels of the phonon gas in the quantization box, and the more we need to increase the size of the system to reach the thermodynamic limit.

21. If we move from panel (c) to panel (d) in Figure 2, the interaction strength is divided by ≈ 3 , the imaginary part is divided by ≈ 2 in maximum absolute value so may well tend towards zero, while the real part only decreases by a factor of ≈ 1.3 .

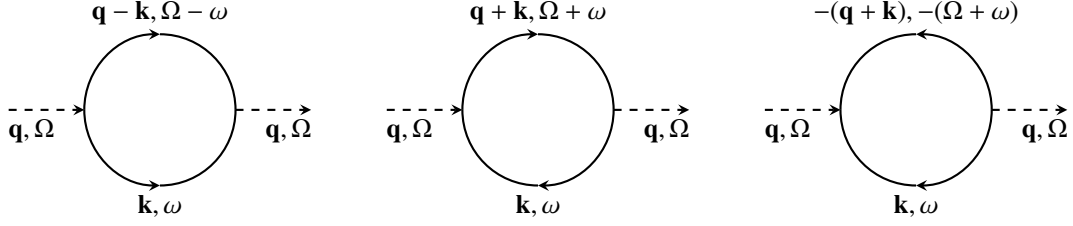


Figure 3: The self-energy $\Sigma(\mathbf{q}, z)$ is given at order two in H_3 by one-loop diagrams, corresponding to Beliaev, Landau and non-resonant processes (from left to right in the figure). Variables Ω and ω are the Matsubara energies associated with the incoming \mathbf{q} and internal \mathbf{k} wave vectors. Inner lines (of any orientation and to be summed) are solid, outer lines (whose orientation is fixed by the choice of Green's function) are dashed.

they reveal, in logarithmic scale, a non-exponential decay of the signal $s(t)$ [34]. In this section, we incriminate the approximation made in step (i) of section 1, and renounce it by retaining all the energy dependence of the self-energy in the integral expression (6) of $s(t)$, continuing however to calculate $\Sigma_{\mathbf{q}}(\zeta)$ at leading order in the phonon-phonon coupling and in ϵ (as in step (ii) of section 1). After a diagrammatic calculation of $\Sigma^{(2)}$, we obtain some analytical predictions put into a universal form and compare them with simulations.

3.1. Calculation of the self-energy

In the Hamiltonian H of equation (1), the cubic coupling H_3 seems to dominate over the quartic coupling H_4 , since it appears at order $\delta\hat{\rho}^3$ rather than $\delta\hat{\rho}^4$ in the expansion of the hydrodynamic Hamiltonian, see section 2.1. However, as H_3 does not conserve the phonon number, it must be treated at least at second order of perturbation theory in the calculation of $\Sigma_{\mathbf{q}}(\zeta)$, whereas H_4 gives a non-zero first order contribution, which is at first sight as large as that of H_3 .²² The full calculation is required.

At first order in perturbation theory, there's no need to use Feynman diagrams, as the contribution to $\Sigma_{\mathbf{q}}(\zeta)$ is independent of the ζ variable and can be obtained by the following simple procedure, justifiable by the quantum master equation method of reference [36]. We write the perturbation operator, here H_4 , in representation \hat{b}, \hat{b}^\dagger and in normal order, with the help of bosonic commutation relations (all \hat{b}^\dagger put on the left, all \hat{b} put on the right). Terms that do not preserve phonon number do not contribute. The terms $\hat{b}^\dagger \hat{b}$, being quadratic, are absorbed into a redefinition of the bare $\epsilon_{\mathbf{k}}$ eigenenergies of the modes (as was expected from footnote 2). Finally, we isolate in the remaining "true" quartic coupling terms the contributions $\hat{b}_{\mathbf{q}}^\dagger \hat{b}_{\mathbf{k}}^\dagger \hat{b}_{\mathbf{k}} \hat{b}_{\mathbf{q}}$, whose thermal averaging over the modes $\mathbf{k} \neq \mathbf{q}$ gives the \mathbf{q} -mode energy shift. All this is summarized by the compact expression

$$\Sigma_{\mathbf{q}}^{(H_4)}(\zeta) = \int \frac{d^d k}{(2\pi)^d} \langle \mathbf{q}, \mathbf{k} | \mathcal{H}_4^{\text{true}} | \mathbf{q}, \mathbf{k} \rangle \bar{n}_{\mathbf{k}} = \frac{\hbar^2 q \Lambda_*}{4m\rho} \int \frac{d^d k}{(2\pi)^d} k \bar{n}_{\mathbf{k}} \underset{\epsilon \rightarrow 0}{\approx} \frac{\bar{q} k_B T \epsilon^{d+1}}{\rho \xi^d} \quad (35)$$

where \mathcal{H}_4 is the volumic Hamiltonian such that $H_4 = \mathcal{H}_4/L^d$, the coupling constant Λ_* is that of equation (28), we have deduced the matrix element in the two-phonon state from expression (27) of H_4 and expression (25) of $\delta\hat{\rho}(\mathbf{r})$ and we have obtained the scaling behavior in the limit (9) in the right-hand side of equation (35) as in section 1. As we see from the contribution (17) of H_3 written for $n = 1$, the contribution of H_4 in dimension $d = 2$ (but not in dimension three) is subleading and can therefore be neglected when $\epsilon \rightarrow 0$. This is what we'll do from now on.

At second order in H_3 , it's best to use the method in reference [7].²³ This method provides a diagrammatic expansion of the self-energy $\Sigma(\mathbf{q}, z)$ for particular values of the complex energy variable, $z = \Omega \in 2i\pi k_B T \mathbb{Z}$, where Ω is called Matsubara energy,²⁴ which is then completed by an analytic continuation to $\mathbb{C} \setminus \mathbb{R}$ [7]. Here, as in Figure 3,

22. The contribution of H_3 to $\Sigma_{\mathbf{q}}(i0^+)$ involves the ratio $\langle |\mathcal{H}_3| \rangle^2 / \Delta E \approx \delta\hat{\rho}^{2 \times 3 - 2}$, that of H_4 involves the matrix element $\langle |\mathcal{H}_4| \rangle \approx \delta\hat{\rho}^4$, where we use the notations of equation (13) and the fact that the denominator ΔE , made up of energy differences of the quadratic Hamiltonian H_2 , is $\approx \delta\hat{\rho}^2$.

23. Since our phonon states already have the bosonic symmetry, we can dispense with the direct interaction and exchange lines introduced in [7].

24. As a slight departure from the usual notation [7], our Matsubara variables Ω, ω , etc., are not real frequencies but pure imaginary energies, i.e. we incorporate an additional factor $i\hbar$.

each diagram must have two vertices (we're at second order), where three phonon lines meet (H_3 is cubic in \hat{b}, \hat{b}^\dagger). The only possible topology is one-loop and, since two loops deduced from each other by rotation of angle π around their axis must be considered as identical, the four possible orientations of the two internal lines lead to only three distinct diagrams, represented in the order Beliaev, Landau and non-resonant in Figure 3 (using the typology of equation (29)). Given the conservation of Matsubara energy and momentum at each vertex (the sum of incoming quantities must equal that of outgoing quantities), there remains a single independent Matsubara energy ω and wave vector \mathbf{k} , on which to sum. Feynman's rules of section 25 of reference [7] then lead for our phonon gas of zero chemical potential to

$$\Sigma^{(2)}(\mathbf{q}, \Omega) = -k_B T \sum_{\omega \in 2i\pi k_B T \mathbb{Z}} \int \frac{d^d k}{(2\pi)^d} \left\{ \frac{(1/2)|\langle \mathbf{k}, \mathbf{q} - \mathbf{k} | \mathcal{H}_3 | \mathbf{q} \rangle|^2}{(\omega - \varepsilon_{\mathbf{k}})(\Omega - \omega - \varepsilon_{\mathbf{q}-\mathbf{k}})} + \frac{|\langle \mathbf{k} + \mathbf{q} | \mathcal{H}_3 | \mathbf{k}, \mathbf{q} \rangle|^2}{(\omega - \varepsilon_{\mathbf{k}})(\Omega + \omega - \varepsilon_{\mathbf{k}+\mathbf{q}})} + \frac{(1/2)|\langle 0 | \mathcal{H}_3 | \mathbf{q}, \mathbf{k}, -(\mathbf{k} + \mathbf{q}) \rangle|^2}{(\omega - \varepsilon_{\mathbf{k}})(-\Omega - \omega - \varepsilon_{-(\mathbf{k}+\mathbf{q})})} \right\} \quad (36)$$

in the thermodynamic limit with $\mathcal{H}_3 = H_3 L^{d/2}$, $|0\rangle$ the phonon vacuum and, for each contribution, a \mathbf{k} integration domain ensuring that the wavevectors $\mathbf{k}, \mathbf{q} - \mathbf{k}$, etc., satisfy the cutoff (26). Also included are symmetry factors $1/2$ when the two branches of the loop have the same orientation and are therefore physically identical. Matsubara sums are calculated by means of the general expression²⁵

$$\sum_{n \in \mathbb{Z}} \frac{1}{(2i\pi n - \bar{\varepsilon}_1)(2i\pi n - \bar{\varepsilon}_2)} = -\frac{\bar{n}_{\varepsilon_1} - \bar{n}_{\varepsilon_2}}{\bar{\varepsilon}_1 - \bar{\varepsilon}_2} \quad (37)$$

where the real or even complex energies ε_j are two by two distinct, and we set $\bar{\varepsilon} = \varepsilon/k_B T$ and $\bar{n}_\varepsilon = 1/(\exp \bar{\varepsilon} - 1)$. We then use the fact that $\Omega/k_B T \in 2i\pi \mathbb{Z}$ to make this variable disappear from Bose's law, and the relation $\bar{n}_{-\varepsilon} = -(1 + \bar{n}_\varepsilon)$ to bring us back to true occupation numbers (at positive energy). So, for example:

$$\bar{n}_{\Omega - \varepsilon_{\mathbf{q}-\mathbf{k}}} = \bar{n}_{-\varepsilon_{\mathbf{q}-\mathbf{k}}} = -(1 + \bar{n}_{\mathbf{q}-\mathbf{k}}) \quad (38)$$

The integrand becomes a rational function of the discrete variable Ω , and its analytic continuation to $\mathbb{C} \setminus \mathbb{R}$ is achieved by the simple substitution $\Omega \rightarrow z$. We get

$$\Sigma_{\mathbf{q}}^{(2)}(\zeta) = \int \frac{d^d k}{(2\pi)^d} \left\{ \frac{(1/2)|\langle \mathbf{k}, \mathbf{q} - \mathbf{k} | \mathcal{H}_3 | \mathbf{q} \rangle|^2}{\zeta + \varepsilon_{\mathbf{q}} - (\varepsilon_{\mathbf{k}} + \varepsilon_{\mathbf{q}-\mathbf{k}})} (\bar{n}_{\mathbf{k}} + \bar{n}_{\mathbf{q}-\mathbf{k}} + 1) + \frac{|\langle \mathbf{k} + \mathbf{q} | \mathcal{H}_3 | \mathbf{k}, \mathbf{q} \rangle|^2}{\zeta + \varepsilon_{\mathbf{q}} + \varepsilon_{\mathbf{k}} - \varepsilon_{\mathbf{q}+\mathbf{k}}} (\bar{n}_{\mathbf{k}} - \bar{n}_{\mathbf{q}+\mathbf{k}}) - \frac{(1/2)|\langle 0 | \mathcal{H}_3 | \mathbf{q}, \mathbf{k}, -(\mathbf{k} + \mathbf{q}) \rangle|^2}{\zeta + \varepsilon_{\mathbf{q}} + \varepsilon_{-(\mathbf{k}+\mathbf{q})} + \varepsilon_{\mathbf{k}}} (\bar{n}_{\mathbf{k}} + \bar{n}_{-(\mathbf{q}+\mathbf{k})} + 1) \right\} \quad (39)$$

It remains to take the limit $\epsilon \rightarrow 0$ at \bar{q} and $\tilde{\zeta}$ fixed as in equations (9,10,11) with, remember, exponents $\nu = \sigma = 2$ in dimension $d = 2$. Through the "small-denominator" effect described in section 1, each contribution to the integral (39) is dominated by configurations where the three wave vectors in the energy denominator are quasi-collinear and of the same direction (within an angle $O(\epsilon)$). In the first contribution, it suffices to use expansion (14) with $\mathbf{k}' = \mathbf{q} - \mathbf{k}$ (having \mathbf{k} and \mathbf{k}' quasicollinear and of the same direction then implies $k < q$); in the second, we use (14) with $\mathbf{k}' = \mathbf{q}$ which imposes nothing on k ; in the third, we are dealing with a sum with positive coefficients of three phonon energies, which can never be $O(k_B T \epsilon^2)$ (it is always $\approx k_B T \epsilon^0$), so that the corresponding contribution is subleading and negligible at low temperatures.²⁶ Respecting the order of the contributions in (39), and restricting ourselves to the strict upper half of the complex plane as in expression (6) of the signal, we get:²⁷

$$\tilde{\Sigma}_{\bar{q}}^{(2,2)}(\tilde{\zeta}) \stackrel{\text{Im } \tilde{\zeta} > 0}{=} \frac{9(1 + \Lambda)^2 (2\bar{q})^{1/2}}{64i\pi\rho\xi^2} \left\{ \int_0^{\bar{q}} d\bar{k} \frac{[\bar{k}(\bar{q} - \bar{k})]^{3/2} (1 + \bar{n}_k^{\text{lin}} + \bar{n}_{q-k}^{\text{lin}})}{[(3\gamma/8)\bar{q}\bar{k}(\bar{q} - \bar{k}) + \tilde{\zeta}]^{1/2}} + 2 \int_0^{\eta - \bar{q}} d\bar{k} \frac{[\bar{k}(\bar{q} + \bar{k})]^{3/2} (\bar{n}_k^{\text{lin}} - \bar{n}_{k+q}^{\text{lin}})}{[(3\gamma/8)\bar{q}\bar{k}(\bar{k} + \bar{q}) - \tilde{\zeta}]^{1/2}} \right\} \quad (40)$$

25. This is easily demonstrated by partial fraction decomposition of the summand with respect to variable n and using the identity $\lim_{N \rightarrow +\infty} \sum_{n=-N}^N 1/(2i\pi n - \bar{\varepsilon}) = -(\bar{n}_\varepsilon + 1/2) \forall \varepsilon \in \mathbb{C} \setminus 2i\pi \mathbb{Z}$ resulting from the properties of the digamma function $\psi(z)$ such as the reflection formula.

26. After these expansions, the angular integral is Lorentzian and can therefore be performed very well using Cauchy's formula, by closing the integration path with an infinite semicircle in the complex plane, after performing the change of variable $\theta = \epsilon \bar{\theta}$ on the angle θ between \mathbf{q} and \mathbf{k} and sending the integration bounds $\pm\pi/\epsilon$ over $\bar{\theta}$ to infinity. In the first contribution, the limiting behavior $\theta' \sim -k\theta/(q-k)$ of the angle θ' between \mathbf{q} and \mathbf{k}' was used beforehand.

27. The value of $\tilde{\Sigma}_{\bar{q}}^{(2,2)}(\tilde{\zeta})$ in the strict lower half of the complex plane can be deduced from the general relation valid for all orders in phonon coupling, $\Sigma_{\mathbf{q}}(\zeta)^* = \Sigma_{\mathbf{q}}(\zeta^*)$.

where the occupation numbers marked by the superscript “lin” are those (21) of the phonon modes for the linearized dispersion relation. In the left-hand side of (40), the second integer 2 in the exponent reminds us that $\Sigma^{(2)}$ is calculated to second order in ϵ ; the tildes on Σ and ζ remind us that a factor $k_B T \epsilon^2$ has been taken out of these quantities as in (10,11). Finally, despite the ever-present threat of quantum field fluctuations, we can take the limit of an infinite η cutoff without triggering ultraviolet divergence, so without having to renormalize any quantities whatsoever. Then, if we make $\check{\zeta}$ tend towards zero by positive imaginary parts in (40), we find equation (23).

3.2. Analytical studies: one-parameter universality

Remarkably, it is possible, by a simple change of variable, to ensure that in the leading-order theory in ϵ and in the coupling treated in this section 3, there remains only one parameter u containing all physical parameters such as the interaction strength $1/\rho\xi^2$, the curvature parameter γ and the coupling constant Λ , i.e. ²⁸

$$u = \frac{\pi\rho\xi^2\gamma^{3/2}}{\sqrt{3}(1+\Lambda)^2} \quad (41)$$

In fact, the new definitions marked with a Czech accent,

$$\check{t} = \frac{3\gamma\bar{q}}{8u}\check{\tau} = \frac{3\gamma\epsilon^2 cqt}{8u} \quad ; \quad \check{\zeta} = \frac{8u}{3\gamma\bar{q}}\check{\zeta} = \frac{8u\zeta}{3\gamma\epsilon^2 \hbar c q} \quad (42)$$

lead to a new self-energy and a new signal expression, clearly involving only u and the reduced variables \bar{q} and \check{t} :

$$\check{\Sigma}_{\bar{q}}^{(2,2)}(\check{\zeta}) = \frac{8u}{3\gamma\bar{q}}\check{\Sigma}_{\bar{q}}^{(2,2)}(\check{\zeta}) \stackrel{\text{Im}\check{\zeta}>0}{=} \frac{1}{i} \int_0^{\bar{q}} \frac{d\bar{k}}{2\bar{q}} \frac{[\bar{k}(\bar{q}-\bar{k})]^{3/2}(1+\bar{n}_k^{\text{lin}}+\bar{n}_{q-k}^{\text{lin}})}{[\bar{k}(\bar{q}-\bar{k})+\check{\zeta}/u]^{1/2}} + \frac{1}{i} \int_0^{+\infty} \frac{d\bar{k}}{\bar{q}} \frac{[\bar{k}(\bar{q}+\bar{k})]^{3/2}(\bar{n}_k^{\text{lin}}-\bar{n}_{q+k}^{\text{lin}})}{[\bar{k}(\bar{q}+\bar{k})-\check{\zeta}/u]^{1/2}} \quad (43)$$

and

$$s^{(2,2)}(t) = \int_{C_+} \frac{d\check{\zeta}}{2i\pi} e^{-i\check{\zeta}t} \check{\mathcal{G}}_{\bar{q}}^{(2,2)}(\check{\zeta}) \quad \text{with} \quad \check{\mathcal{G}}_{\bar{q}}^{(2,2)}(\check{\zeta}) = \frac{1}{\check{\zeta} - \check{\Sigma}_{\bar{q}}^{(2,2)}(\check{\zeta})} \quad (44)$$

In this case, we speak of one-parameter universality.

Let's carry out the analytic continuation of function (43) from the upper to the lower half-plane through its branch cut on the real axis. ²⁹ This will enable us, as in reference [13], to separate the signal into the contribution of a contour around a displaced branch cut (power-law decreasing contribution at long times) and the contribution of a pole in the analytically continued Green's function (exponentially decreasing contribution in time), see our Figure 4b, which improves physical understanding. First, we need to identify the branch points (immutable singularities) of $\check{\Sigma}_{\bar{q}}^{(2,2)}(\check{\zeta})$ on the real axis. Since the values of $\check{\zeta}$ that make the square root argument in the denominator vanish, span the interval $[-u\bar{q}^2/4, 0]$ when \bar{k} spans $[0, \bar{q}]$ in the first contribution to (43), and span $[0, +\infty[$ when \bar{k} spans \mathbb{R}^+ in the second, we might expect to have two branch points, $\check{\zeta} = -u\bar{q}^2/4$ and $\check{\zeta} = 0$. ³⁰ In reality, by subtle compensation between the two contributions, only $\check{\zeta} = -u\bar{q}^2/4$ remains; the branch cut $[-u\bar{q}^2/4, +\infty[$ starts from this point, as shown in Figure 4a. ³¹ The branch cut can then be rotated by an angle $\phi \in]-\pi, -\pi/2[$ to bring it into the third quadrant, by analytic

28. For the same to apply in the classical field model, we would also have to incorporate the cut-off parameter η into u , i.e. introduce the quantity $u_{\text{clas}} = \eta u$. This is unnecessary here, as we have taken $\eta = 1$ in the simulations. As a curiosity, let's point out, for the classical field and in the limit $\bar{q} \ll 1$, that the signal $s^{(2,2)}(t)$ defined below ceases to start at value 1 in $t = 0$ (as it should physically) if $u_{\text{clas}} < 1$, which we link mathematically to the appearance of a pole of the Green's function on the real axis. Consequently, it would be interesting to know whether all two-dimensional physical systems (even in very strong interaction, provided it's short-range) lead to $u > 1$.

29. There's a mathematical subtlety here that the reader will forgive us for. Implicitly, from expression (43) for $\check{\Sigma}_{\bar{q}}^{(2,2)}(\check{\zeta})$, valid only for $\text{Im}\check{\zeta} > 0$, we define a function in all $\mathbb{C} \setminus \mathbb{R}$ by applying (43) as it is for $\text{Im}\check{\zeta} < 0$; the branch cut $[-u\bar{q}^2/4, +\infty[$ mentioned in the text and shown in Figure 4a corresponds to this function rather than to the true self-energy $\check{\Sigma}_{\bar{q}}^{(2,2)}(\check{\zeta})$, whose branch cut is \mathbb{R} in its entirety and which would therefore be less convenient to analytically continue from the upper half-plane to the lower half-plane, for the same final result (we see that it's \mathbb{R} in its entirety (i) by considering the energy denominator $\zeta + \Delta E$ in the Landau contribution of equation (39) and checking that ΔE spans \mathbb{R} when θ/ϵ and \bar{k} span \mathbb{R}^+ in (14) with $\mathbf{k}' = \mathbf{q}$, or (ii) by using the relation $iz^{1/2} = -\text{signe}(\text{Im}z)(-z)^{1/2}$, $\forall z \in \mathbb{C} \setminus \mathbb{R}$, to make the factor i disappear in (43) and obtain a physically correct expression over all $\mathbb{C} \setminus \mathbb{R}$ satisfying $\Sigma_{\mathbf{q}}(\zeta)^* = \Sigma_{\mathbf{q}}(\zeta^*)$, whose branch cut is then shown to be \mathbb{R}).

30. For example, $\check{\zeta} \mapsto \int_a^b dx/(\check{\zeta}-x)^{1/2} = 2(\check{\zeta}-b)^{1/2} - 2(\check{\zeta}-a)^{1/2}$ has the real numbers a and b as branch points.

31. If we return to variable $\check{\zeta}$, the branch point is at $-3\gamma\bar{q}^3/32$.

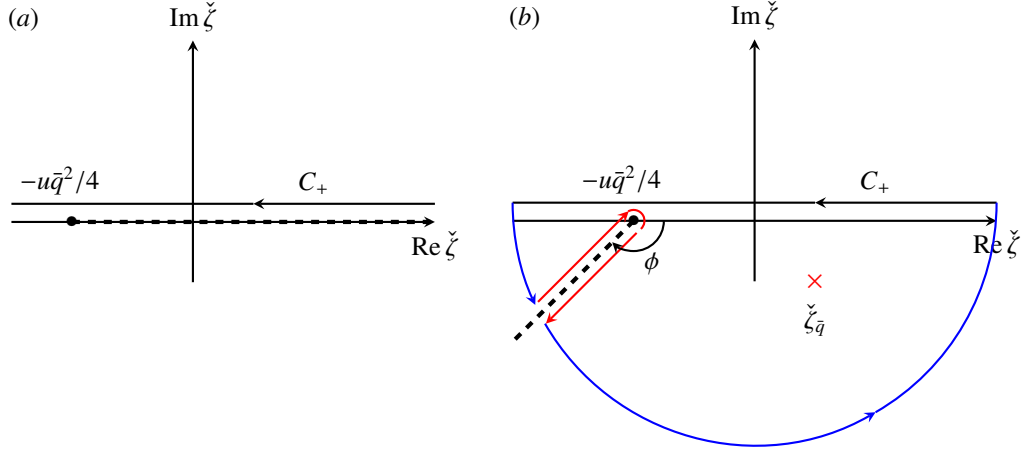


Figure 4: (a) Singularities of Green's function $\check{\mathcal{G}}_{\bar{q}}^{(2,2)}(\check{\zeta})$ in the complex plane and (b) integration path followed in calculating signal (44) to obtain the first deviation (47) from the pole approximation. The change of variable (42) $\check{\zeta} = 8(z - \varepsilon_{\bar{q}})u / (3\gamma\hbar c q \varepsilon^2)$ was performed to reveal a one-parameter universality u (41). Black horizontal line: original integration path in (44). Black disk: $\check{\zeta} \mapsto \check{\mathcal{G}}_{\bar{q}}^{(2,2)}(\check{\zeta})$ branch point. Dashed half-line: original branch cut of $\check{\zeta} \mapsto \check{\mathcal{G}}_{\bar{q}}^{(2,2)}(\check{\zeta})$ in (a), and rotated by an angle $\phi \in]-\pi, -\pi/2[$ in (b) by analytic continuation of $\check{\zeta} \mapsto \check{\mathcal{G}}_{\bar{q}}^{(2,2)}(\check{\zeta})$ from the upper to the lower half-plane, resulting in the $\check{\zeta}_{\bar{q}}$ pole (red cross). In (b), to apply Cauchy's theorem, we close C_+ with two portions of a circle at infinity (in blue) and a contour (in red) which bypasses the displaced branch cut.

continuation of $\check{\Sigma}_{\bar{q}}^{(2,2)}(\check{\zeta})$ from the upper half-plane to the lower half-plane, the new branch cut being the half-line $-u\bar{q}^2/4 + \exp(i\phi)\mathbb{R}^+$, see Figure 4b. As shown in Appendix A and agreeing that $z^{3/2} = z\sqrt{z}$, the function continued in this way is written:

$$\check{\Sigma}_{\bar{q}\downarrow}^{(2,2)}(\check{\zeta}) = \frac{e^{3i\phi/2}}{i} \int_0^{+\infty} \frac{d\bar{k}}{\bar{q}} \frac{(\bar{k}^2 - e^{-i\phi}\bar{q}^2/4)^{3/2}}{[\bar{k}^2 - e^{-i\phi}(\bar{q}^2/4 + \check{\zeta}/u)]^{1/2}} \left[\frac{1}{\exp(e^{i\phi/2}\bar{k} - \bar{q}/2) - 1} - \frac{1}{\exp(e^{i\phi/2}\bar{k} + \bar{q}/2) - 1} \right] \quad (45)$$

In particular, it is analytic on a neighborhood of $\check{\zeta} = 0$ (see Appendix A, which also gives its value and that of its derivative at this point). On the other hand, the corresponding Green's function $\check{\mathcal{G}}_{\bar{q}\downarrow}^{(2,2)}(\check{\zeta})$ has a pole $\check{\zeta}_{\bar{q}}$ in the fourth quadrant, as we have verified numerically.³²

Rather than numerically evaluating the contour and pole contributions to the signal, let's now extract analytically from form (45) the “very substance” of the theory at order two in H_3 , noting for example that it is illusory to calculate the position of the $\check{\zeta}_{\bar{q}}$ pole at all orders in $1/u$ since the self-energy is calculated here only at order one in $1/u$. On the other hand, limiting ourselves to order zero in $1/u$, which would mean taking the $u \rightarrow +\infty$ limit at \bar{q} fixed, would be too poor, as the signal would then be reduced to the exponential of Fermi's golden rule. As can be seen from (43), the new self-energy depends on u only through the ratio $\check{\zeta}/u$; so it tends towards its value at $i0^+$ when u tends to $+\infty$ under the integral sign ($\check{\zeta}$ and $\check{\gamma}$ being fixed in (44)). A more interesting result is obtained by taking the limit $u \rightarrow +\infty$ for

$$Q = u^{1/2}\bar{q} \quad \text{and} \quad \check{\gamma} \quad \text{fixed} \quad (46)$$

so that the branch point in Figure 4 remains fixed instead of being rejected at infinity (which would effectively make the contour contribution disappear). We then find a correction of order $u^{-1/2}$ to Fermi's golden rule signal; as $u^{-1} \ll u^{-1/2}$ one would expect that we can keep this correction without having to calculate the self-energy at the next order (order four) in H_3 , even if we'll see in section 5 that this is not the case. Let's report the technical details in Appendix B and

32. If angle ϕ is too close to $-\pi/2$ (which we'll avoid in the following) and if \bar{q} is quite small, a second pole of imaginary part < 0 , of uncertain physical interpretation, may appear to the left of the displaced branch cut.

give the result directly in quantum theory:

$$s^{(2,2)}(t) \stackrel{Q \text{ and } \check{t} \text{ fixed}}{u \rightarrow +\infty} e^{-\pi^2 \check{t}/3} + \frac{S(\check{t})}{u^{1/2}} + O(1/u) \quad \text{with} \quad S(\check{t}) = S_{\text{contour}}(\check{t}) + S_{\text{pole}}(\check{t}) \quad (47)$$

The first contribution is the real-valued exponential of the golden rule in limit $\bar{q} \rightarrow 0$. The second is divided into the contour and pole contributions established in [Appendix B](#):

$$S_{\text{contour}}(\check{t}) = -\frac{e^{iQ^2 \check{t}/4}}{\pi} \int_0^{e^{i(\phi+\pi)(+\infty)}} dz \frac{e^{i\check{t}z} \int_0^{\pi/2} d\alpha \left(z \sin^2 \alpha + \frac{Q^2}{4} \right)^{1/2}}{\left(\frac{Q^2}{4} + z - i\frac{\pi^2}{3} \right)^2} \quad ; \quad S_{\text{pole}}(\check{t}) = e^{-\pi^2 \check{t}/3} (\delta\check{Z} - i\delta\check{\zeta}_{\bar{q}} \check{t}) \quad (48)$$

where angle ϕ is freely chosen in $]-\pi, -\pi/2[$ (result (48) does not depend on it). In a power expansion of $u^{-1/2}$, $\delta\check{\zeta}_{\bar{q}}$ is the first deviation of the pole from the pole approximation $-i\pi^2/3$ (multiplied by $u^{1/2}$) and $\delta\check{Z}$ is the first deviation from one of the residue of $\check{\mathcal{G}}_{\bar{q}\downarrow}^{(2,2)}(\check{\zeta})$ (also multiplied by $u^{1/2}$):³³

$$\delta\check{\zeta}_{\bar{q}} = \int_0^{+\infty} dK \left[1 - \frac{(K^2 + Q^2/4)^{1/2}}{(K^2 - i\frac{\pi^2}{3} + \frac{Q^2}{4})^{1/2}} \right] \quad ; \quad \delta\check{Z} = \frac{1}{2} \int_0^{+\infty} dK \frac{(K^2 + Q^2/4)^{1/2}}{(K^2 - i\frac{\pi^2}{3} + \frac{Q^2}{4})^{3/2}} \quad (49)$$

In [Figure 5](#), we show function $S(\check{t})$ of equation (47) for $Q = 1$, together with predictions drawn numerically from $\check{\Sigma}_{\bar{q}}^{(2,2)}(\check{\zeta})$ for finite values of u . It can be seen that $u = 20$ has already reached the asymptotic regime, so the same is expected for the parameters of the classical field simulations in [Fig. 2d](#), which correspond to $u \simeq 18.14$ and $Q \simeq 1.06$. So function $S(\check{t})$ is not just a mathematical curiosity, and its predictions are not without practical interest. Let's keep two of them, due to the contour: the behavior at short times is square-root, which accounts for the rapid rise of the signal in [Figure 5](#), and the behavior at long times is sinusoidal damped as the inverse of time, its continuous connection to that at short times explaining the sign changes on this figure,^{34 35}

$$S(\check{t}) \underset{\check{t} \rightarrow 0^+}{\sim} 2e^{-i\pi/4} (\check{t}/\pi)^{1/2} \quad ; \quad S(\check{t}) \underset{\check{t} \rightarrow +\infty}{\sim} \frac{-iQ/4}{\left(\frac{Q^2}{4} - i\frac{\pi^2}{3} \right)^2} \frac{e^{iQ^2 \check{t}/4}}{\check{t}} \quad (50)$$

3.3. Comparison with classical field simulations

In order to compare with the simulations of section 2, we transpose the quantum treatments of sections 3.1 and 3.2 to the classical field: in equation (40), we must keep the cutoff parameter η finite (it is one in the simulations), neglect the term 1 in front of the occupation numbers \bar{n}_k^{lin} and replace these by the classical equipartition law $1/\bar{k}$. As a test, note that the corresponding value of $\Sigma_{\mathbf{q}}^{(2,2)}(i0^+)$ is then written as $-i\hbar\Gamma_{\mathbf{q}}^{\text{clas}}/2$, where $\Gamma_{\mathbf{q}}^{\text{clas}}$ is the damping rate (34), as it should be. In what follows, we of course retain the full dependence of $\check{\Sigma}_{\mathbf{q}}^{(2,2)}(\check{\zeta})$ on $\check{\zeta}$ when calculating signal $s^{(2,2)}(t)$ by Green's function.

The corresponding predictions for the decay time at 1/e are shown in thick black solid lines on each panel of [Figure 1](#). They are in all cases closer to the simulations than the golden rule, but paradoxically the improvement

33. As signal (6) starts exactly at one, $S(0) = 0$ so the contour contribution for $\check{t} = 0$ must exactly cancel out that of the pole residue's deviation from one. Verification is non-trivial. The main idea is to reduce $S_{\text{contour}}(0)$ to a simple integral by inverting the integration on z and α in (48) (a primitive function of $(z+a)^{1/2}/(z+b)^2$ is known, where a and b are two constants). Moreover, we note that $\text{Re } \delta\check{Z} > 0$ for all Q : the first correction in $u^{-1/2}$ makes the residue \check{Z} of modulus > 1 and therefore the pole $\check{\zeta}_{\bar{q}}$ of spectral weight > 1 .

34. If $\check{t} \rightarrow +\infty$, the integral giving $S_{\text{contour}}(\check{t})$ is dominated by values of z close to zero and z can be replaced by 0 in the integrand, everywhere except in $\exp(i\check{t}z)$. If $\check{t} \rightarrow 0^+$, the integral giving $\exp(iQ^2 \check{t}/4)S_{\text{contour}}(\check{t}) - S_{\text{contour}}(0)$ is dominated by values of z close to infinity, so reduces to the Fresnel integral $(-1/\pi) \int_0^{+\infty} dz [\exp(i\check{t}z) - 1]/z^{3/2}$ whose value is known (we've taken $\phi + \pi = 0^+$ for simplicity).

35. A more explicit expression of the signal can be obtained in the limit $Q \rightarrow 0$: $S(\check{t}) = \left(\frac{\check{t}}{\pi} \right)^{1/2} e^{-i\pi/4} - \frac{\sqrt{3}}{2\pi} e^{-i\pi/4} \left(\frac{2\pi\check{t}}{3} - 1 \right) \text{erfi}(\sqrt{\pi^2 \check{t}/3}) e^{-\pi^2 \check{t}/3}$, where erfi is the imaginary error function, which has the same behavior at short times as in (50) but the new behavior at long times $S(\check{t}) \underset{\check{t} \rightarrow +\infty}{\sim} -\frac{e^{-i\pi/4}}{2\pi^{1/2}} \left(\frac{3}{\pi^2} \right)^2 \frac{1}{\check{t}^{3/2}}$. Since function erfi is, despite its name, real-valued on the real axis, we find that $\text{Re } S(\check{t}) = -\text{Im } S(\check{t})$ in this limit, a property of which a trace remains in [Figure 5](#).

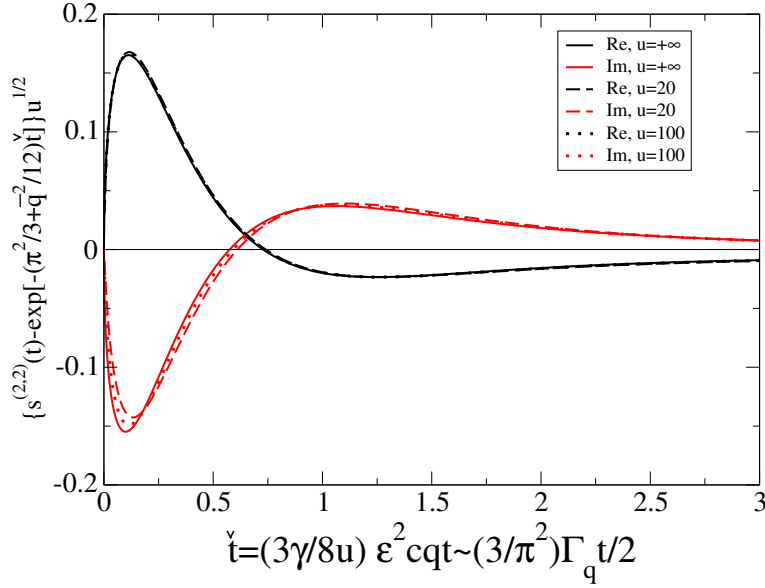


Figure 5: In quantum theory and for a self-energy calculated at order two in H_3 and at order two in $\epsilon = k_B T/mc^2$, deviation of signal (6) from Fermi's golden rule exponential $\exp(-\Gamma_q t/2)$ multiplied by $u^{1/2}$ (the universal parameter u is given by (41), the rate Γ_q by (23)) and plotted as a function of reduced time (42) for real and imaginary parts, for increasing values of u (the underlying two-dimensional superfluid is more and more weakly interacting) but for a scaled wave number as in (46) kept constant, $Q = 1$. Curves for finite values of u : obtained by numerical integration of expression (44). Curves for $u = +\infty$: taken from analytical prediction (47) (they simply correspond to $\text{Re } S(\tilde{\zeta})$ and $\text{Im } S(\tilde{\zeta})$).

is clearest in the strong interaction regime (a) and becomes very modest in the weakly interacting regime (d). This deterioration was, however, to be expected from the reasoning preceding equation (46): if $\rho\xi^2$ increases at a fixed \tilde{q} , the second-order Green's function calculation in H_3 must reduce to the golden rule, thus deviating from the simulations.

Analysis of Figure 2 showing the time dependence of the signal gives us a further clue as to what happens when we reduce the interaction strength, $(\rho\xi^2)^{-1} \rightarrow 0$. The predictions derived from $\tilde{\Sigma}_{\tilde{q}}^{(2,2)}(\tilde{\zeta})$ are this time shown as dashed lines (those from the golden rule would be identically zero). They come remarkably close to the simulations for the imaginary part of the deviation $s(t) - s_{\text{pole}}(t)$ (the red dashed line almost merges with the numerical results in panel (d)), but they show a persistent, and even increasing in relative values, disagreement on the real part, which explains the previous failure on the decay time at $1/e$.

The anomaly exhibited by the real part in Figure 2d is striking if we recall the analytical predictions of Figure 5 (even if they are for the quantum field): the real part and the imaginary part, for the corresponding values of u and Q ($u \simeq 18.14$ and $Q \simeq 1.06$, remember), should be more or less symmetrical to each other with respect to the abscissa axis (see also footnote 35), which is far from being the case in the simulations. In conclusion, the calculation of the signal with the self-energy $\tilde{\Sigma}_{\tilde{q}}^{(2,2)}(\tilde{\zeta})$, by fault of the real part, fails to account for the first deviation from the golden rule in the limit $u \rightarrow +\infty$ where it had every chance of excelling.

4. Study at fourth order in H_3

To understand the persistent discrepancy in the real part of the signal between the numerical simulations in section 2 and the theoretical study at second-order in H_3 in section 3, even when the two-dimensional superfluid enters the weakly interacting limit $(\rho\xi^2)^{-1} \rightarrow 0$, we calculate the self-energy at fourth order in H_3 , either with the usual diagrammatic formalism in section 4.1, or by a Landau-style reasoning in section 4.2, which provides an interesting physical insight and leads to a more compact expression. In section 4.3, however, we show that the fourth-order result is useless in the low-temperature limit $\epsilon = k_B T/mc^2 \rightarrow 0$ of interest here.

4.1. Calculation with the diagrammatic formalism of reference [7]

The two topologies. We directly omit the quartic Hamiltonian H_4 in equation (1) and the non-resonant terms $H_3^{(\text{non res.})}$ in the cubic Hamiltonian (29), as their contributions to $\Sigma^{(4)}$ are subleading in the limit $\epsilon \rightarrow 0$ (this is obvious for $H_3^{(\text{non res.})}$, which does not benefit from the “small-denominator” effect, and this will be justified for H_4 in section 4.2). The coupling Hamiltonian therefore reduces to the terms $H_3^{(+/-)}$ given in equation (30). In the corresponding fourth-order Feynman diagrams, each of the four vertices is the meeting point of three phonon lines, leading to two

possible topologies, (i) inner-loop and (ii) bridge, as shown in Figure 6. In the first topology, we lift the degeneracy by arbitrarily putting the inner loop in the upper branch, and remember (as in section 3) that swapping the two inner-loop lines leads to the same diagram; after orientation of internal lines, this leaves eight distinct diagrams. In the second topology, the degeneracy is lifted by orientating the bridge line downwards; six distinct diagrams remain. In reality, in the terminology of Figure 6, the contributions of diagrams B_3 and B_4 to $\Sigma^{(4)}$ double, as do those of P_2 and P_3 and those of P_4 and P_6 .³⁶ Only eleven truly independent diagrams remain.

Calculating a generic inner-loop diagram. It's convenient to number the internal lines from $j = 1$ to 5 as on the left-hand side of Figure 7. Each line has an orientation $s_j \in \{-1; 1\}$ (left to right if $s_j = 1$, right to left if $s_j = -1$), a wave vector \mathbf{k}_j and a Matsubara energy $\omega_j \in 2i\pi k_B T\mathbb{Z}$. In Figure 6, we have chosen to always have $s_3 \geq s_4$ in order to avoid the double counting of diagrams mentioned above. As independent quadrivectors, we've chosen those in lines 2 and 3, which we've renamed as follows:

$$(\mathbf{k}_2, \omega_2) = (\mathbf{k}, \omega) \quad ; \quad (\mathbf{k}_3, \omega_3) = (\mathbf{k}', \omega') \quad (51)$$

The others can be deduced by energy-momentum conservation at each vertex. For example, the sum of the wave vectors arriving at a given vertex is equal to the sum of the wave vectors departing from it, giving:

$$\mathbf{k}_1 = s_1(\mathbf{q} - s_2\mathbf{k}) \quad ; \quad \mathbf{k}_4 = s_4(s_2\mathbf{k} - s_3\mathbf{k}') \quad ; \quad \mathbf{k}_5 = s_2s_5\mathbf{k} \quad (52)$$

The same relations apply to Matsubara energies. Given the rules set out in section 25 of reference [7], the contribution to the self-energy of the generic inner-loop diagram B_i is:

$$\Sigma_{B_i}^{(4)}(\mathbf{q}, z) = \frac{(-k_B T)^2}{1 + \delta_{s_3, s_4}} \int \frac{d^d k}{(2\pi)^d} \int \frac{d^d k'}{(2\pi)^d} \mathcal{A}(\mathbf{k}_1, \mathbf{k}_2; \mathbf{q}) \mathcal{A}(\mathbf{k}_3, \mathbf{k}_4; \mathbf{k}_2) \mathcal{A}(\mathbf{k}_3, \mathbf{k}_4; \mathbf{k}_5) \mathcal{A}(\mathbf{k}_1, \mathbf{k}_5; \mathbf{q}) \sum_{\omega, \omega' \in 2i\pi k_B T\mathbb{Z}} \frac{1}{\prod_{j=1}^5 (\omega_j - \varepsilon_{\mathbf{k}_j})} \quad (53)$$

where we temporarily have $z = \Omega \in 2i\pi k_B T\mathbb{Z}$ (see section 3.1). To write the transition amplitudes at each vertex, we used the invariance of function \mathcal{A} of equation (31) by permutation of its three arguments and hence the fact that matrix elements $\langle \mathbf{k}_2, \mathbf{k}_3 | \mathcal{H}_3 | \mathbf{k}_1 \rangle$, $\langle \mathbf{k}_1, \mathbf{k}_3 | \mathcal{H}_3 | \mathbf{k}_2 \rangle$ and $\langle \mathbf{k}_1, \mathbf{k}_2 | \mathcal{H}_3 | \mathbf{k}_3 \rangle$ are all equal to $\mathcal{A}(\mathbf{k}_2, \mathbf{k}_3; \mathbf{k}_1)$. The denominator of the symmetry factor in front of the integrals is 2 if the two lines of the inner loop have the same orientation (to compensate for the double counting of configurations differing only by the exchange of quadrivectors (\mathbf{k}_3, ω_3) and (\mathbf{k}_4, ω_4) and in this case physically identical); otherwise, these two lines are distinguishable and the symmetry factor is 1. The Matsubara double sum is calculated explicitly in Appendix C, which also shows that its expression simplifies in the limit of small angles $O(\epsilon) \rightarrow 0$ between the wave vectors, where we can restrict to $s_2 = s_5$ (otherwise, the diagram's contribution is subleading in ϵ , see equation (56) below):

$$\sum_{\omega, \omega' \in 2i\pi k_B T\mathbb{Z}} \frac{(k_B T)^2}{\prod_{j=1}^5 (\omega_j - \varepsilon_{\mathbf{k}_j})} \underset{\epsilon \rightarrow 0}{\overset{\text{diag. } B}{\sim}} -s_1 s_4 \frac{(\bar{n}_{\varepsilon_3} - \bar{n}_{-s_3 s_4 \varepsilon_4})(\bar{n}_{-s_1 \varepsilon_1} - \bar{n}_{s_2 \varepsilon_2})}{(\zeta - \zeta_1)^2 (\zeta - \zeta_2)} \quad (54)$$

with variable $\zeta = z - \varepsilon_{\mathbf{q}}$ and ζ_j all of order $k_B T \epsilon^2$,

$$\zeta_1 \equiv s_1 \varepsilon_{\mathbf{k}_1} + s_2 \varepsilon_{\mathbf{k}_2} - \varepsilon_{\mathbf{q}} \quad ; \quad \zeta_2 \equiv s_1 \varepsilon_{\mathbf{k}_1} + s_3 \varepsilon_{\mathbf{k}_3} + s_4 \varepsilon_{\mathbf{k}_4} - \varepsilon_{\mathbf{q}} \quad (55)$$

The dependence in ζ of form (54) on the right-hand side is easy to interpret physically since $\zeta_1 + \varepsilon_{\mathbf{q}}$ and $\zeta_2 + \varepsilon_{\mathbf{q}}$ are the energies of the intermediate states marked by the vertical lines on the left-hand side of Figure 7: in fact, they are the sums of the energies of the internal lines j intersected by each vertical line counted algebraically, i.e. weighted by the orientations s_j (if $s_j = -1$, the phonon on line j is going backward in time and its energy must be counted negatively). This validates estimate (13) by reproducing its energy denominators.

³⁶ There is indeed a non-trivial symmetry connecting certain diagrams. To see this, let's apply a vertical axis rotation of angle π to each diagram, then change the orientation of all lines (internal and external); this does not change the value of the diagram's contribution to $\Sigma^{(4)}$. Most diagrams are mapped on themselves in this way, with the exception of pairs $\{B_3, B_4\}$, $\{P_2, P_3\}$ and $\{P_4, P_6\}$, whose two partners are simply exchanged (remember, in the case of bridge diagrams, that a horizontal axis rotation of angle π , which restores the original orientation of the vertical line, does not change the value of the diagram). This means that $\Sigma_{B_3}^{(4)}(\mathbf{q}, z) = \Sigma_{B_4}^{(4)}(\mathbf{q}, z)$, $\Sigma_{P_2}^{(4)}(\mathbf{q}, z) = \Sigma_{P_3}^{(4)}(\mathbf{q}, z)$ and $\Sigma_{P_4}^{(4)}(\mathbf{q}, z) = \Sigma_{P_6}^{(4)}(\mathbf{q}, z)$ as announced.

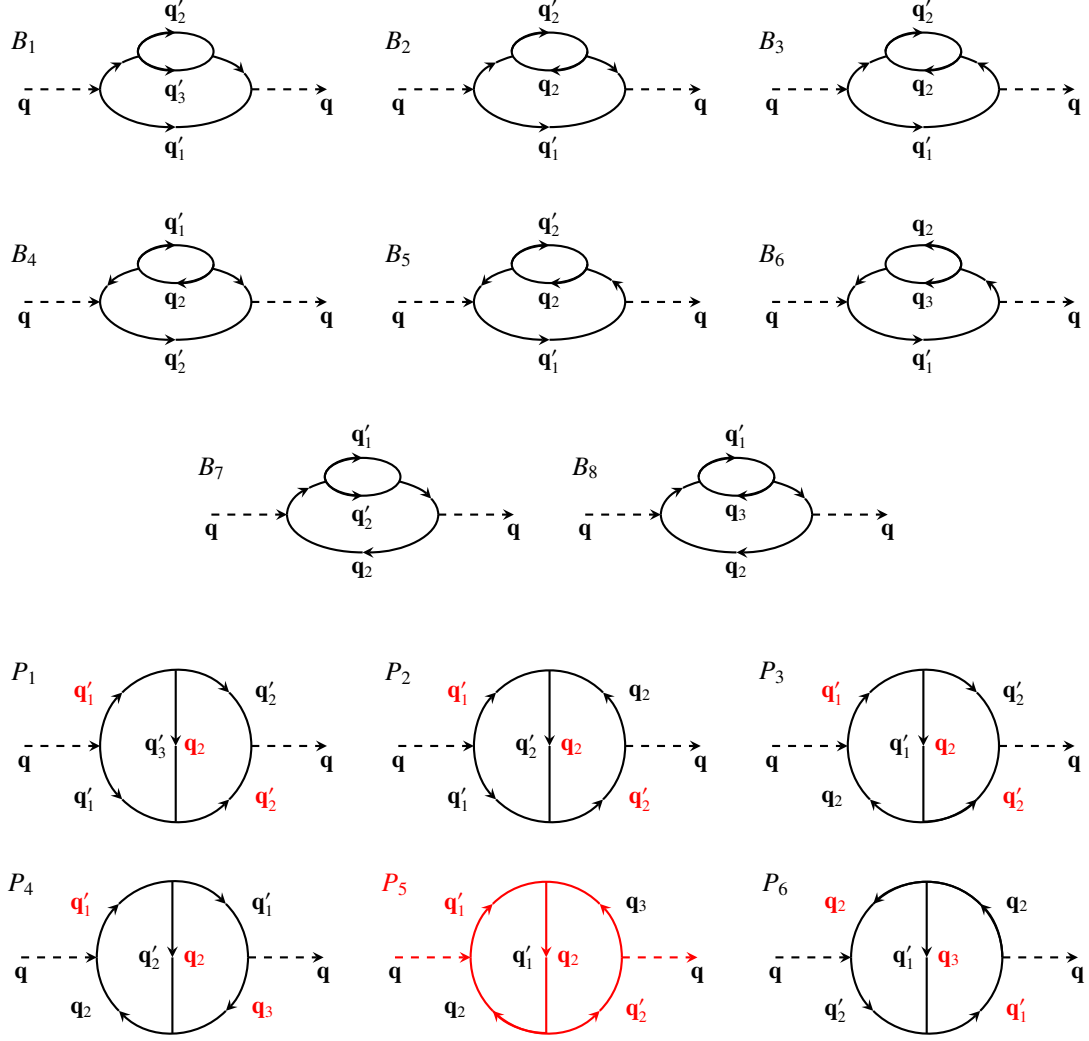


Figure 6: Contributions to self-energy $\Sigma(\mathbf{q}, z)$ at fourth order in $H_3^{(+)} + H_3^{(-)}$ are given by eight inner-loop diagrams (numbered B_1 to B_8) and six bridge diagrams (numbered P_1 to P_6). The wave vectors \mathbf{q}_i ($2 \leq i \leq n$) and \mathbf{q}'_j ($1 \leq j \leq n'$) near the inner lines are those of the incoming and outgoing phonons of the four-phonon $n \rightarrow n'$ collisional processes in the Landau-style physical interpretation of section 4.2 (for bridge diagrams: wave vectors of type I contributions in black, type II in red, in the sense of equation (63)); for the sake of simplicity, wave vectors of virtual phonons are not shown (they are deduced by conservation of momentum at each vertex). The contributions of the non-resonant processes of H_3 , subleading in the $\epsilon \rightarrow 0$ limit, are not shown. On the other hand, once this limit is taken, the diagram P_5 (more precisely, its type II contribution, hence the red color) diverges linearly for $\tilde{\zeta} \equiv (z - \epsilon_q)/k_B T \epsilon^2 = 0$, revealing a non-physical pole in Green's function, see section 4.3.

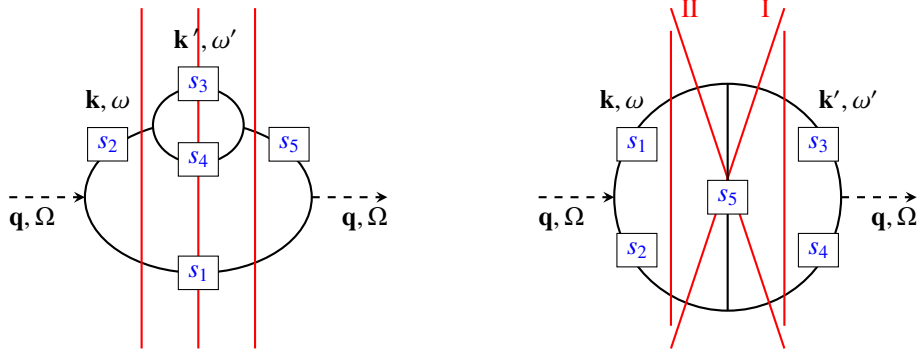


Figure 7: In the expansion of the self-energy $\Sigma(\mathbf{q}, z)$, generic forms of fourth-order diagrams in H_3 for inner-loop (left-hand side) or bridge diagrams (right-hand side). The boxes contain the possible $s_j = \pm 1$ orientations of the internal lines and indicate their numbering j . Given the conservation of the Matsubara energy-momentum at each vertex, there are only two independent internal wave vectors \mathbf{k}, \mathbf{k}' and Matsubara energies ω, ω' ; the others are given by equations (52) (inner loop) and (61) (bridge). The red lines are a graphical construction for finding the energy denominators in the simplified forms (54) and (63) of the double Matsubara sums, which apply to leading order in ϵ when all internal wave vectors make a small angle $O(\epsilon)$ with \mathbf{q} . In the simplified form (54), the quantity ζ_1 corresponds to the two outer red lines of the inner-loop diagram (indeed, $s_2 = s_5$ at the leading order in ϵ) and ζ_2 corresponds to the central red line. In the simplified form (63), the quantity ζ_1 corresponds to the left vertical red line of the bridge diagram, ζ_2 to the other vertical red line, ζ_3 to the oblique line numbered II and ζ_4 to the oblique line numbered I.

To go to the $\epsilon \rightarrow 0$ limit in (53), we directly set the angles to zero in each coupling amplitude \mathcal{A} (which brings out a factor $3(1 + \Lambda)$), then expand the energy denominators of (54) on the model of (14); for the “small-denominator” effect to take full action, the internal vectors \mathbf{k}_j must all make a small angle $O(\epsilon)$ with the incoming wave vector \mathbf{q} , which imposes³⁷

$$\text{sign}(q - s_2 k) = s_1 \quad ; \quad \text{sign}(s_2 k - s_3 k') = s_4 \quad ; \quad s_2 s_5 = 1 \quad (56)$$

The first two conditions in (56) restrict the range of variation of wave numbers k and k' . The last, which is independent of them, eliminates diagrams B_3 and B_4 , of subleading contributions. Remembering the definitions (11,18) of $\tilde{\zeta}$ and (9) of \bar{q} , we arrive in dimension $d = 2$ at the result (for $\text{Im } \tilde{\zeta} \neq 0$ but of arbitrary sign):

$$\tilde{\Sigma}_{B_i}^{(4,2)}(\bar{q}, \tilde{\zeta}) = \frac{\bar{q}}{1 + \delta_{s_3, s_4}} \left(\frac{9(1 + \Lambda)^2}{8\rho\xi^2} \right)^2 \int_{\mathcal{D}_1^B} \frac{\bar{k} d\bar{k}}{(2\pi)^2} \int_{\mathcal{D}_2^B(\bar{k})} \frac{\bar{k}' d\bar{k}'}{(2\pi)^2} \bar{k}^2 \bar{k}'^2 (\bar{q} - s_2 \bar{k})(s_2 \bar{k} - s_3 \bar{k}') (\bar{n}_{k'}^{\text{lin}} - \bar{n}_{k' - s_2 s_3 k}^{\text{lin}}) (\bar{n}_{s_2 k}^{\text{lin}} - \bar{n}_{s_2 k - q}^{\text{lin}}) I(\bar{k}, \bar{k}') \quad (57)$$

with the occupation numbers (21) extended to negative wavenumbers and the angular integral³⁸

$$I(\bar{k}, \bar{k}') = \int_{\mathbb{R}} d\tilde{\theta} \int_{\mathbb{R}} d\tilde{\phi} \frac{1}{[\tilde{\zeta} - (A_1^B + B_1^B \tilde{\theta}^2)]^2 [\tilde{\zeta} - (A_2^B + B_1^B \tilde{\theta}^2 + B_2^B \tilde{\phi}^2)]} \quad (58)$$

involving coefficients

$$A_1^B = \frac{3\gamma}{8} (\bar{k} - s_2 \bar{q}) \bar{k} \bar{q} \quad ; \quad A_2^B = \frac{3\gamma}{8} \bar{k} \bar{k}' (s_2 \bar{k}' - s_3 \bar{k}) + A_1^B \quad ; \quad B_1^B = \frac{-\bar{k} \bar{q} / 2}{\bar{k} - s_2 \bar{q}} \quad ; \quad B_2^B = \frac{-\bar{k} \bar{k}' / 2}{s_2 \bar{k}' - s_3 \bar{k}} \quad (59)$$

and integration domains \mathcal{D}_1^B over \bar{k} , then $\mathcal{D}_2^B(\bar{k})$ over \bar{k}' at fixed \bar{k} , satisfying conditions (56) and cut-off (26) $\bar{k}_j < \eta$, $1 \leq j \leq 5$. In the left-hand side of (57), the second integer in the exponent reminds us to which order in ϵ the function $\Sigma^{(4)}$ is calculated (here to second order), and the tilde over Σ means, as in (10), that the result has been divided by $k_B T \epsilon^2$. Finally, we check on a case-by-case basis that expression (57) has a finite limit when the cutoff $\eta \rightarrow +\infty$ (for the quantum field).³⁹

37. When $\mathbf{k}_2 = \mathbf{k}$ and $\mathbf{k}_3 = \mathbf{k}'$ form a zero angle with \mathbf{q} , the other wave vectors \mathbf{k}_j given by (52) must satisfy the condition $\mathbf{k}_j \cdot \mathbf{q} = k_j q$.

38. In the integral, before taking the limit $\epsilon \rightarrow 0$, we set $\tilde{\theta} = \theta/\epsilon$ and $\tilde{\phi} = (\theta - \theta')/\epsilon$, where θ is the angle between \mathbf{q} and \mathbf{k} , θ' the angle between \mathbf{q} and \mathbf{k}' .

39. For example, in the case of the diagram B_8 ($s_1 = s_4 = -1, s_2 = s_3 = s_5 = 1$), the domains $\mathcal{D}_1^B = [\bar{q}, \eta]$ and $\mathcal{D}_2^B(\bar{k}) = [\bar{k}, \eta]$ are unbounded

Calculating a generic bridge diagram. The beginning is very similar to the previous case. We number the internal lines as on the right-hand side of Figure 7, with the same sign convention, except for the vertical line (the ‘‘bridge’’), with sign $s_5 = 1$ when oriented downwards (which we have limited ourselves to in Figure 6 to avoid double counting). We keep as independent quadrivectors

$$(\mathbf{k}_1, \omega_1) = (\mathbf{k}, \omega) \quad ; \quad (\mathbf{k}_3, \omega_3) = (\mathbf{k}', \omega') \quad (60)$$

the others deduced by energy-momentum conservation, e.g. for wave vectors:

$$\mathbf{k}_2 = s_2(\mathbf{q} - s_1\mathbf{k}) \quad ; \quad \mathbf{k}_4 = s_4(\mathbf{q} - s_3\mathbf{k}') \quad ; \quad \mathbf{k}_5 = s_5(s_1\mathbf{k} - s_3\mathbf{k}') \quad (61)$$

The contribution of diagram P_i to the self-energy is then written [7]:

$$\Sigma_{P_i}^{(4)}(\mathbf{q}, z) = (-k_B T)^2 \int \frac{d^d k}{(2\pi)^d} \int \frac{d^d k'}{(2\pi)^d} \mathcal{A}(\mathbf{k}_1, \mathbf{k}_2; \mathbf{q}) \mathcal{A}(\mathbf{k}_3, \mathbf{k}_5; \mathbf{k}_1) \mathcal{A}(\mathbf{k}_2, \mathbf{k}_5; \mathbf{k}_4) \mathcal{A}(\mathbf{k}_3, \mathbf{k}_4; \mathbf{q}) \sum_{\omega, \omega' \in 2i\pi k_B T \mathbb{Z}} \frac{1}{\prod_{j=1}^5 (\omega_j - \varepsilon_{\mathbf{k}_j})} \quad (62)$$

No need here to divide by a symmetry factor. The explicit calculation of the Matsubara double sum is given in Appendix C, which also establishes its simplified expression in the limit of small angles $O(\epsilon)$ between the wave vectors:

$$\sum_{\omega, \omega' \in 2i\pi k_B T \mathbb{Z}} \frac{(k_B T)^2}{\prod_{j=1}^5 (\omega_j - \varepsilon_{\mathbf{k}_j})} \underset{\epsilon \rightarrow 0}{\text{diag. } P} -s_1 s_2 s_4 s_5 \frac{(\bar{n}_{-s_2 \varepsilon_2} - \bar{n}_{s_1 \varepsilon_1})(\bar{n}_{\varepsilon_3} - \bar{n}_{-s_3 s_5 \varepsilon_5})}{(\zeta - \zeta_1)(\zeta - \zeta_2)(\zeta - \zeta_4)} - s_1 s_2 s_4 s_5 \frac{(\bar{n}_{-s_3 s_5 \varepsilon_5} - \bar{n}_{-s_3 s_4 \varepsilon_4})(\bar{n}_{s_1 \varepsilon_1} - \bar{n}_{-s_2 \varepsilon_2})}{(\zeta - \zeta_1)(\zeta - \zeta_2)(\zeta - \zeta_3)} \quad (63)$$

with variable ζ and ζ_j all of order $k_B T \epsilon^2$,

$$\zeta_1 \equiv s_1 \varepsilon_{\mathbf{k}_1} + s_2 \varepsilon_{\mathbf{k}_2} - \varepsilon_{\mathbf{q}} \quad ; \quad \zeta_2 \equiv s_3 \varepsilon_{\mathbf{k}_3} + s_4 \varepsilon_{\mathbf{k}_4} - \varepsilon_{\mathbf{q}} \quad ; \quad \zeta_3 \equiv s_1 \varepsilon_{\mathbf{k}_1} + s_4 \varepsilon_{\mathbf{k}_4} - s_5 \varepsilon_{\mathbf{k}_5} - \varepsilon_{\mathbf{q}} \quad ; \quad \zeta_4 \equiv s_2 \varepsilon_{\mathbf{k}_2} + s_3 \varepsilon_{\mathbf{k}_3} + s_5 \varepsilon_{\mathbf{k}_5} - \varepsilon_{\mathbf{q}} \quad (64)$$

There are this time two contributions to the right-hand side, called type I and type II in this order. Quantities ζ_j are energy differences between intermediate and initial states, as in the inner-loop case, except that four straight lines must be introduced to identify them, see right-hand side of Figure 7: two vertical lines for ζ_1 and ζ_2 , two oblique lines for ζ_3 and ζ_4 . Indeed, from the point of view of the oblique line marked I on the figure, the internal line of the bridge is oriented from left to right if $s_5 = 1$, and ζ_4 must have a plus sign in front of $s_5 \varepsilon_{\mathbf{k}_5}$ in equation (64); for oblique line II, the opposite is true, hence the minus sign in front of $s_5 \varepsilon_{\mathbf{k}_5}$ in ζ_3 .

When $\epsilon \rightarrow 0$, the limit of small angles in the energy denominators and in the coupling amplitudes \mathcal{A} is taken as before, except that a distinction must be made between the two types. For type I contribution, we obtain (for $\text{Im } \tilde{\zeta} \neq 0$ but of arbitrary sign)

$$\tilde{\Sigma}_{P_i}^{(4,2)}(\bar{q}, \tilde{\zeta}) = \bar{q} \left(\frac{9(1 + \Lambda)^2}{8\rho\xi^2} \right)^2 \int_{\mathcal{D}_1^p} \frac{\bar{k} d\bar{k}}{(2\pi)^2} \int_{\mathcal{D}_2^p(\bar{k})} \frac{\bar{k}' d\bar{k}'}{(2\pi)^2} \bar{k} \bar{k}' (\bar{q} - s_1 \bar{k}) (\bar{q} - s_3 \bar{k}') (\bar{k} - s_1 s_3 \bar{k}') (\bar{n}_{\bar{k}'}^{\text{lin}} - \bar{n}_{\bar{k}' - s_1 s_3 \bar{k}}^{\text{lin}}) (\bar{n}_{s_1 \bar{k}}^{\text{lin}} - \bar{n}_{s_1 \bar{k} - \bar{q}}^{\text{lin}}) J(\bar{k}, \bar{k}') \quad (65)$$

with the angular integral

$$J(\bar{k}, \bar{k}') = \int_{\mathbb{R}} d\tilde{\theta} \int_{\mathbb{R}} d\tilde{\theta}' \frac{1}{[\tilde{\zeta} - (A_1^p + B_1^p \tilde{\theta}^2)][\tilde{\zeta} - (A_2^p + B_2^p \tilde{\theta}'^2)][\tilde{\zeta} - (A_4^p + B_1^p \tilde{\theta}^2 + B_4^p (\tilde{\theta} - \tilde{\theta}')^2)]} \quad (66)$$

For type II contribution, we obtain (again for $\text{Im } \tilde{\zeta} \neq 0$ but of arbitrary sign)

$$\tilde{\Sigma}_{P_i}^{(4,2)}(\bar{q}, \tilde{\zeta}) = \bar{q} \left(\frac{9(1 + \Lambda)^2}{8\rho\xi^2} \right)^2 \int_{\mathcal{D}_1^p} \frac{\bar{k} d\bar{k}}{(2\pi)^2} \int_{\mathcal{D}_2^p(\bar{k})} \frac{\bar{k}' d\bar{k}'}{(2\pi)^2} \bar{k} \bar{k}' (\bar{q} - s_1 \bar{k}) (\bar{q} - s_3 \bar{k}') (\bar{k} - s_1 s_3 \bar{k}') (\bar{n}_{\bar{k}' - s_3 \bar{q}}^{\text{lin}} - \bar{n}_{\bar{k}' - s_1 s_3 \bar{k}}^{\text{lin}}) (\bar{n}_{s_1 \bar{k}}^{\text{lin}} - \bar{n}_{s_1 \bar{k} - \bar{q}}^{\text{lin}}) K(\bar{k}, \bar{k}') \quad (67)$$

when $\eta \rightarrow +\infty$ but the bosonic amplification factors $(\bar{n}_{\bar{k}'}^{\text{lin}} - \bar{n}_{\bar{k}' - \bar{k}}^{\text{lin}})(\bar{n}_{\bar{k}}^{\text{lin}} - \bar{n}_{\bar{k} - \bar{q}}^{\text{lin}}) = O[\exp(-\bar{k} - \bar{k}')] are rapidly decreasing in the two decoupled integration variables ($\bar{k}, \bar{k}' = \bar{k}' - \bar{k}$) and suppress any power-law divergence that might arise from the other factors ; in the case of B_7 ($s_1 = -1, s_2 = s_3 = s_4 = s_5 = 1$), $\mathcal{D}_1^p = [\bar{q}, \eta]$ and $\mathcal{D}_2^p(\bar{k}) = [0, \bar{k}]$ remain unbounded and the bosonic factors $(1 + \bar{n}_{\bar{k}'}^{\text{lin}} + \bar{n}_{\bar{k} - \bar{k}'}^{\text{lin}})(\bar{n}_{\bar{k}}^{\text{lin}} - \bar{n}_{\bar{k} - \bar{q}}^{\text{lin}}) = O(\exp(-\bar{k}))$ are now rapidly decreasing only in variable \bar{k} but, since $\bar{k}' < \bar{k}$, the integral over \bar{k}' at fixed \bar{k} is at most $O(\bar{k}^\alpha)$, $\alpha > 0$, and the integral over \bar{k} converges if $\eta \rightarrow +\infty$.$

with the angular integral

$$K(\bar{k}, \bar{k}') = \int_{\mathbb{R}} d\bar{\theta} \int_{\mathbb{R}} d\bar{\theta}' \frac{1}{[\tilde{\zeta} - (A_1^P + B_1^P \bar{\theta}^2)][\tilde{\zeta} - (A_2^P + B_2^P \bar{\theta}'^2)][\tilde{\zeta} - (A_3^P + B_2^P \bar{\theta}'^2 + B_3^P (\bar{\theta} - \bar{\theta}')^2)]} \quad (68)$$

Irrespective of type, the coefficients are

$$A_1^P = \frac{3\gamma}{8}(\bar{k} - s_1 \bar{q})\bar{k}\bar{q} \quad ; \quad A_2^P = \frac{3\gamma}{8}(\bar{k}' - s_3 \bar{q})\bar{k}'\bar{q} \quad ; \quad A_4^P = A_1^P + \frac{3\gamma}{8}\bar{k}\bar{k}'(s_1 \bar{k}' - s_3 \bar{k}) \quad ; \quad A_3^P = A_1^P + A_2^P - A_4^P \quad (69)$$

$$B_1^P = \frac{-\bar{k}\bar{q}/2}{\bar{k} - s_1 \bar{q}} \quad ; \quad B_2^P = \frac{-\bar{k}'\bar{q}/2}{\bar{k}' - s_3 \bar{q}} \quad ; \quad B_4^P = \frac{-\bar{k}\bar{k}'/2}{s_1 \bar{k}' - s_3 \bar{k}} \quad ; \quad B_3^P = -B_4^P \quad (70)$$

The integration domains \mathcal{D}_1^P and $\mathcal{D}_2^P(\bar{k})$ are also independent of type; they take into account the cut-off (26) on all internal wave vectors \mathbf{k}_j , $1 \leq j \leq 5$, as well as conditions

$$\text{sign}(q - s_1 k) = s_2 \quad ; \quad \text{sign}(q - s_3 k') = s_4 \quad ; \quad \text{sign}(s_1 k - s_3 k') = s_5 \quad (71)$$

ensuring that \mathbf{k}_2 , \mathbf{k}_4 and \mathbf{k}_5 are collinear with and in the same direction as \mathbf{q} as soon as \mathbf{k} and \mathbf{k}' are. For all s_j orientations taken from Figure 6, conditions (71) are compatible, so none of the P_i diagrams is subleading in ϵ . Finally, we verify the existence of a finite limit in (65,67) when cutoff $\eta \rightarrow +\infty$ (for the quantum field).

4.2. Calculation using Landau approach

The calculation of $\Sigma^{(4)}$ as in reference [7], although systematic and rigorous, does not explicitly say which collisional processes between phonons lie behind each diagram in Figure 6. Here we develop a more heuristic method, inspired by reference [1] and valid to the leading order in ϵ , which answers the question, gives the result in compact form (rather than spread into a dozen or so integral contributions) and makes it easy to show that the contribution of H_4 is subleading in the $\epsilon \rightarrow 0$ limit.

Reference [1] explains, for Hamiltonian (1), how to calculate by an extended Fermi golden rule the damping rate of phonon mode \mathbf{q} due to $n \rightarrow n'$ collisions, n being the number of incoming \mathbf{q}_i phonons (they include one and only one phonon of wave-vector \mathbf{q}) and n' the number of outgoing \mathbf{q}'_j phonons (they do not include any phonon of wave-vector \mathbf{q}). The ordinary cases of Beliaev and Landau processes correspond to $(n, n') = (1, 2)$ and $(n, n') = (2, 1)$, they have $n + n' = 3$ phonons; here, it will be about four-phonon processes, like $(n, n') = (2, 2)$. We start by writing kinetic equations for the phonon occupation numbers, provisionally assumed to be out of equilibrium, counting positively the direct process $n \rightarrow n'$ (which tends to empty mode \mathbf{q}) and negatively the inverse process $n' \rightarrow n$ (which tends to fill it):

$$\begin{aligned} \frac{d}{dt} n_{\mathbf{q}} = & -\frac{1}{(n-1)!} \int \left(\prod_{i=2}^n \frac{d^d q_i}{(2\pi)^d} \right) \frac{1}{n'} \int \left(\prod_{j=1}^{n'} \frac{d^d q'_j}{(2\pi)^d} \right) \frac{2\pi}{\hbar} \mathcal{A}_{i \rightarrow f}^2 \delta(E_i - E_f) (2\pi)^d \delta \left(\sum_{i=1}^n \mathbf{q}_i - \sum_{j=1}^{n'} \mathbf{q}'_j \right) \\ & \times \left[\prod_{i=1}^n n_{\mathbf{q}_i} \prod_{j=1}^{n'} (1 + n_{\mathbf{q}'_j}) - \prod_{i=1}^n (1 + n_{\mathbf{q}_i}) \prod_{j=1}^{n'} n_{\mathbf{q}'_j} \right] \quad (72) \end{aligned}$$

We have taken the thermodynamic limit, and divided by symmetry numbers taking into account the invariance of the process by permutation of the $n-1$ last incoming wave vectors (we agree that $\mathbf{q}_1 = \mathbf{q}$) and by permutation of the n' outgoing wave vectors. We recognize in (72) the Dirac distribution of energy conservation, the factor $2\pi/\hbar$ and the square of a transition amplitude $\mathcal{A}_{i \rightarrow f}$ between initial state $|i\rangle = |(\mathbf{q}_i)_{1 \leq i \leq n}\rangle$ and final state $|f\rangle = |(\mathbf{q}'_j)_{1 \leq j \leq n'}\rangle$ typical of the golden rule, as well as a Dirac distribution of momentum conservation and the bosonic amplification factors. The principle of microreversibility was used to factorize the squared amplitude of the direct process.

We then take the excitation procedure (4), where all phonon modes are at thermal equilibrium except \mathbf{q} , hence the substitution $n_{\mathbf{k}} \rightarrow \bar{n}_{\mathbf{k}}$, $\mathbf{k} \neq \mathbf{q}$, and linearize (72) around $n_{\mathbf{q}} = \bar{n}_{\mathbf{q}}$ for weak excitation, which gives the back-to-

equilibrium equation $(d/dt)(n_{\mathbf{q}} - \bar{n}_{\mathbf{q}})|_{t=0^+} = -\Gamma_{\mathbf{q}}^{n \rightarrow n'}(n_{\mathbf{q}} - \bar{n}_{\mathbf{q}})$ with rate

$$\Gamma_{\mathbf{q}}^{n \rightarrow n'} = \frac{1}{(n-1)!} \int \left(\prod_{i=2}^n \frac{d^d q_i}{(2\pi)^d} \right) \frac{1}{n!} \left(\int \prod_{j=1}^{n'} \frac{d^d q'_j}{(2\pi)^d} \right) \frac{2\pi}{\hbar} \mathcal{A}_{i \rightarrow f}^2 \delta(E_i - E_f) (2\pi)^d \delta \left(\sum_{i=1}^n \mathbf{q}_i - \sum_{j=1}^{n'} \mathbf{q}'_j \right) \\ \times \left[\prod_{i=2}^n \bar{n}_{\mathbf{q}_i} \prod_{j=1}^{n'} (1 + \bar{n}_{\mathbf{q}'_j}) - \prod_{i=2}^n (1 + \bar{n}_{\mathbf{q}_i}) \prod_{j=1}^{n'} \bar{n}_{\mathbf{q}'_j} \right] \quad (73)$$

where, unlike equation (72), all products on the incoming wave vectors exclude mode \mathbf{q} and therefore start at $i = 2$. The difference with the golden rule lies in the calculation of amplitude $\mathcal{A}_{i \rightarrow f}$. Usually, we simply have $\mathcal{A}_{i \rightarrow f} = \langle f | \mathcal{H}_3 | i \rangle$. Reference [1] deals precisely with the useful case of four-phonon collisions, where $\mathcal{A}_{i \rightarrow f}$ is obtained by treating $H_3 = \mathcal{H}_3/L^{d/2}$ at second order and $H_4 = \mathcal{H}_4/L^d$ at first order of perturbation theory:

$$\mathcal{A}_{i \rightarrow f} = \langle f | \mathcal{H}_4 | i \rangle + \sum_{|\lambda\rangle} \frac{\langle f | \mathcal{H}_3 | \lambda \rangle \langle \lambda | \mathcal{H}_3 | i \rangle}{E_i - E_\lambda} \quad (74)$$

and the sum is taken over all possible intermediate phonon Fock states $|\lambda\rangle$. A simple power counting as in section 1 shows that \mathcal{H}_4 's contribution to (74) is subleading in the small-angle limit $\epsilon \rightarrow 0$;⁴⁰ so we omit it in the following. In the energy denominator, we have chosen the reference energy E_i of the initial state rather than E_f of the final state, because we are talking about a $i \rightarrow f$ transition, as recalled by the choice of f in bra and i in ket in the matrix element in the numerator, which is not a serious physical reason. Fortunately, this doesn't matter, since the amplitude is used in (72) on the energy shell ($E_i = E_f$): the result is invariant by exchanging the roles of i and f in any term of the sum in the right-hand side of (74):

$$\frac{\langle f | \mathcal{H}_3 | \lambda \rangle \langle \lambda | \mathcal{H}_3 | i \rangle}{E_i - E_\lambda} (\text{direct direction}) \longleftrightarrow \frac{\langle i | \mathcal{H}_3 | \lambda \rangle \langle \lambda | \mathcal{H}_3 | f \rangle}{E_f - E_\lambda} (\text{inverse direction}) \quad (75)$$

The total damping rate is obtained by summing $\Gamma_{\mathbf{q}}^{n \rightarrow n'}$ over the collisional processes $n \rightarrow n'$ relevant to the order under consideration. From the following obvious rules, (i) the diagram giving the transition amplitude $\mathcal{A}_{i \rightarrow f}$ is connected, i.e. there is no possible decoupling of the $n \rightarrow n'$ process into two independent collisional processes, (ii) any intermediate state (between successive actions of \mathcal{H}_3) must differ from the initial and final states, we find at order four in $H_3^{(+)} + H_3^{(-)}$ as the only possibilities the processes $1 \rightarrow 3$, $2 \rightarrow 2$ and $3 \rightarrow 1$:⁴¹

$$\Gamma_{\mathbf{q}}^{(4)} = \Gamma_{\mathbf{q}}^{1 \rightarrow 3} + \Gamma_{\mathbf{q}}^{2 \rightarrow 2} + \Gamma_{\mathbf{q}}^{3 \rightarrow 1} \quad (76)$$

Heuristically, we generalize this formalism to the calculation of the fourth-order contribution in $H_3^{(+)} + H_3^{(-)}$ to the self-energy of mode \mathbf{q} . As with the damping rate, we assume that it is the sum of the contributions of the above-mentioned $n \rightarrow n'$ collisional processes:

$$\Sigma^{(4)}(\mathbf{q}, z) = \Sigma_{1 \rightarrow 3}(\mathbf{q}, z) + \Sigma_{2 \rightarrow 2}(\mathbf{q}, z) + \Sigma_{3 \rightarrow 1}(\mathbf{q}, z) \quad (77)$$

Knowing that the energy-conserving Dirac distribution in (73) ultimately comes from the identity

$$\lim_{\delta \rightarrow 0^+} \text{Im} \frac{1}{E_i + i\delta - E_f} = -\pi \delta(E_i - E_f) \quad , \quad (78)$$

that the displaced variable $\zeta = z - \epsilon_{\mathbf{q}}$ plays the role of $i\delta$ in the pole approximation (8) and a self-energy differs from

40. In view of equations (25,27), the contribution of \mathcal{H}_4 to (74) is of order $(mc^2/\rho)\epsilon^2$; in view of equations (14,15), that of \mathcal{H}_3 is of order $(mc^2/\rho)\epsilon^0$.

41. In reference [1], unlike in our case, the acoustic branch has a concave start ($\gamma < 0$ in equation (3)): only process $2 \rightarrow 2$ preserves momentum-energy and gives a non-zero contribution to (76); however, it was miscalculated, and the error has been corrected in reference [5].

a rate by a factor of $-i\hbar/2$, we arrive without hesitation at the form

$$\Sigma_{n \rightarrow n'}^{(4)}(\mathbf{q}, z) = \frac{1}{(n-1)!} \int \left(\prod_{i=2}^n \frac{d^d q_i}{(2\pi)^d} \right) \frac{1}{n!} \int \left(\prod_{j=1}^{n'} \frac{d^d q'_j}{(2\pi)^d} \right) \frac{\mathcal{A}_{i \rightarrow f}^2(\mathbf{q}, z)}{\zeta + E_i - E_f} (2\pi)^d \delta \left(\sum_{i=1}^n \mathbf{q}_i - \sum_{j=1}^{n'} \mathbf{q}'_j \right) \times \left[\prod_{i=2}^n \bar{n}_{\mathbf{q}_i} \prod_{j=1}^{n'} (1 + \bar{n}_{\mathbf{q}'_j}) - \prod_{i=2}^n (1 + \bar{n}_{\mathbf{q}_i}) \prod_{j=1}^{n'} \bar{n}_{\mathbf{q}'_j} \right] \quad (79)$$

The only pitfall lies in the construction of the ζ dependence of the $\mathcal{A}_{i \rightarrow f}$ transition amplitude. The choice of E_i or E_f as reference energy is no longer irrelevant. Choosing E_i as in the left-hand side of (75) means taking the point of view of a $i \rightarrow f$ transition, i.e. travelling through time in the ordinary direction; the correct integration path is precisely C_+ , the one spanned by variable ζ in (6); E_i must therefore be replaced by $\zeta + E_i$ in the energy denominator internal to $\mathcal{A}_{i \rightarrow f}$. On the other hand, choosing E_f as in the right-hand side of (75) means taking the opposite point of view of a $f \rightarrow i$ transition, i.e. going backward in time; the correct integration path for the Green's function is then C_- [13], which runs in the lower half-plane parallel to the real axis from $-\infty$ to $+\infty$ and is spanned by variable $-\zeta$ in (6); E_f must therefore be replaced by $-\zeta + E_f$ in the energy denominator internal to $\mathcal{A}_{i \rightarrow f}$.

To decide according to the intermediate state $|\lambda\rangle$, we need to rely on the following property. By construction, function $\Sigma^{(4)}(\mathbf{q}, z)$ depends on the mode through its wave vector \mathbf{q} but not its energy $\varepsilon_{\mathbf{q}}$ (when using the original complex energy z as a variable), and therefore cannot have an energy denominator containing $\varepsilon_{\mathbf{q}}$. The opposite is true when using the displaced variable ζ . This means that, if in the direct direction of the transition amplitude, the action on $|i\rangle$ of operator $\mathcal{H}_3^{(\pm)}$ does not cause the phonon of wave vector \mathbf{q} to disappear, its energy $\varepsilon_{\mathbf{q}}$ appears in E_λ and therefore disappears in $\zeta + E_i - E_\lambda$, and reverse direction of the transition amplitude must be used, this rule being applied intermediate state by intermediate state. Hence our final prescription on the transition amplitude to be included in (79):⁴²

$$\mathcal{A}_{i \rightarrow f}(\mathbf{q}, z) = \sum_{|\lambda\rangle / \mathbf{q} \notin |\lambda\rangle} \frac{\langle f | \mathcal{H}_3^{(\pm)} | \lambda \rangle \langle \lambda | \mathcal{H}_3^{(\pm)} | i \rangle}{\zeta + E_i - E_\lambda} + \sum_{|\lambda\rangle / \mathbf{q} \in |\lambda\rangle} \frac{\langle i | \mathcal{H}_3^{(\pm)} | \lambda \rangle \langle \lambda | \mathcal{H}_3^{(\pm)} | f \rangle}{-\zeta + E_f - E_\lambda} \quad (80)$$

From expression (80) we derive the transition amplitude for process $1 \rightarrow 3$ (knowing that $\mathbf{q}'_1 + \mathbf{q}'_2 + \mathbf{q}'_3 = \mathbf{q}$):

$$\mathcal{A}_{\mathbf{q} \rightarrow \mathbf{q}'_1, \mathbf{q}'_2, \mathbf{q}'_3}(\mathbf{q}, \zeta) = \frac{\mathcal{A}(\mathbf{q}'_1, \mathbf{q}'_2; \mathbf{q}'_1 + \mathbf{q}'_2) \mathcal{A}(\mathbf{q}'_1 + \mathbf{q}'_2, \mathbf{q}'_3; \mathbf{q})}{\zeta + \varepsilon_{\mathbf{q}} - (\varepsilon_{\mathbf{q}'_1 + \mathbf{q}'_2} + \varepsilon_{\mathbf{q}'_3})} + \frac{\mathcal{A}(\mathbf{q}'_2, \mathbf{q}'_3; \mathbf{q}'_2 + \mathbf{q}'_3) \mathcal{A}(\mathbf{q}'_2 + \mathbf{q}'_3, \mathbf{q}'_1; \mathbf{q})}{\zeta + \varepsilon_{\mathbf{q}} - (\varepsilon_{\mathbf{q}'_2 + \mathbf{q}'_3} + \varepsilon_{\mathbf{q}'_1})} + \frac{\mathcal{A}(\mathbf{q}'_1, \mathbf{q}'_3; \mathbf{q}'_1 + \mathbf{q}'_3) \mathcal{A}(\mathbf{q}'_1 + \mathbf{q}'_3, \mathbf{q}'_2; \mathbf{q})}{\zeta + \varepsilon_{\mathbf{q}} - (\varepsilon_{\mathbf{q}'_1 + \mathbf{q}'_3} + \varepsilon_{\mathbf{q}'_2})} \quad (81)$$

42. In reality, the collisional processes $n \rightarrow n'$ with n incoming phonons \mathbf{q}_i and n' outgoing phonons \mathbf{q}'_j occur in a thermal bath, and the modes of the virtual phonons \mathbf{k} (neither incoming nor outgoing) are not initially empty. The corresponding bosonic amplification factors $(n_{\mathbf{k}} + 1)^{1/2}$ and $n_{\mathbf{k}}^{1/2}$ would therefore have to be taken into account in the expression (80) of the transition amplitude, and the contribution of the new allowed processes, in which a virtual phonon \mathbf{k} is annihilated before being recreated (which is forbidden in vacuum), would have to be included. However, these two modifications exactly cancel each other and the expression (80) remains unchanged. Let's check this on a single term of the first sum in (80). To this aim, let's describe in more detail the corresponding transition $|i\rangle \rightarrow |\lambda\rangle \rightarrow |f\rangle$ by noting $|i\rangle = |i_1\rangle \otimes |i_2\rangle \otimes |n_{\mathbf{k}} : \mathbf{k}\rangle$ and $|f\rangle = |f_1\rangle \otimes |f_2\rangle \otimes |n_{\mathbf{k}} : \mathbf{k}\rangle$, where $|i_1\rangle$ ($|i_2\rangle$) are the incoming phonons annihilated by the first (second) action of \mathcal{H}_3 , $|f_1\rangle$ ($|f_2\rangle$) are the outgoing phonons created by the first (second) action of \mathcal{H}_3 and $|n_{\mathbf{k}} : \mathbf{k}\rangle$ the Fock state with $n_{\mathbf{k}}$ quanta in the virtual phonon mode, so the intermediate state is written $|\lambda\rangle = |f_1\rangle \otimes |i_2\rangle \otimes |n_{\mathbf{k}} + 1 : \mathbf{k}\rangle$ (we don't take into account the other modes, spectators, nor the thermal occupation of incoming and outgoing modes, since their bosonic factors are included in (72,79)). In this example, $\mathbf{q} \notin |\lambda\rangle$ hence $\mathbf{q} \in |i_1\rangle$. The components of \mathcal{H}_3 ensuring the transitions $|i\rangle \rightarrow |\lambda\rangle$ and $|\lambda\rangle \rightarrow |f\rangle$ are written respectively $W_1 = \mathcal{A}_1 \hat{b}_{\mathbf{k}}^\dagger (\prod_{\mathbf{q}'_j \in f_1} \hat{b}_{\mathbf{q}'_j}^\dagger) (\prod_{\mathbf{q}_i \in i_1} \hat{b}_{\mathbf{q}_i})$ and $W_2 = \mathcal{A}_2 (\prod_{\mathbf{q}'_j \in f_2} \hat{b}_{\mathbf{q}'_j}^\dagger) (\prod_{\mathbf{q}_i \in i_2} \hat{b}_{\mathbf{q}_i}) \hat{b}_{\mathbf{k}}$. In the presence of the thermal bath, (i) the numerator $\langle f | \mathcal{H}_3^{(\pm)} | \lambda \rangle \langle \lambda | \mathcal{H}_3^{(\pm)} | i \rangle = \langle f | W_2 | \lambda \rangle \langle \lambda | W_1 | i \rangle$ becomes $\mathcal{A}_1 \mathcal{A}_2 (1 + n_{\mathbf{k}})$, (ii) the new associated process, corresponding to the inverse order of action of W_1 and W_2 , has numerator $\langle f | W_1 | \lambda' \rangle \langle \lambda' | W_2 | i \rangle = \mathcal{A}_1 \mathcal{A}_2 n_{\mathbf{k}}$, (iii) the new intermediate state $|\lambda'\rangle = |i_1\rangle \otimes |f_2\rangle \otimes |n_{\mathbf{k}} - 1 : \mathbf{k}\rangle$ contains the phonon \mathbf{q} so its energy denominator must be taken from the second sum of (80), and happens to be the exact opposite of the denominator of the former process, the calculation giving $-\zeta + E_f - E_{\lambda'} = -(\zeta + E_i - E_\lambda)$. Ultimately, the linear contributions in $n_{\mathbf{k}}$ of the two processes exactly cancel each other in the transition amplitude $\mathcal{A}_{i \rightarrow f}(\mathbf{q}, z)$, which allows us to forget the thermal background as is done in (80). Similar reasoning, but limited to $2 \rightarrow 2$ processes on the energy shell, can already be found in reference [5].

then for process $2 \rightarrow 2$ (knowing that $\mathbf{q}'_1 + \mathbf{q}'_2 = \mathbf{q} + \mathbf{q}_2$):

$$\begin{aligned} \mathcal{A}_{\mathbf{q}, \mathbf{q}_2 \rightarrow \mathbf{q}'_1, \mathbf{q}'_2}(\mathbf{q}, \zeta) &= \frac{\mathcal{A}(\mathbf{q}'_1, \mathbf{q}'_2; \mathbf{q}'_1 + \mathbf{q}'_2) \mathcal{A}(\mathbf{q}, \mathbf{q}_2; \mathbf{q} + \mathbf{q}_2)}{\zeta + \epsilon_{\mathbf{q}} + \epsilon_{\mathbf{q}_2} - \epsilon_{\mathbf{q} + \mathbf{q}_2}} - \frac{\mathcal{A}(\mathbf{q}'_1 - \mathbf{q}, \mathbf{q}'_2; \mathbf{q}_2) \mathcal{A}(\mathbf{q}'_1 - \mathbf{q}, \mathbf{q}; \mathbf{q}'_1)}{\zeta + \epsilon_{\mathbf{q}} + \epsilon_{\mathbf{q}'_1 - \mathbf{q}} - \epsilon_{\mathbf{q}'_1}} \\ &+ \frac{\mathcal{A}(\mathbf{q}'_2 - \mathbf{q}_2, \mathbf{q}_2; \mathbf{q}'_2) \mathcal{A}(\mathbf{q}'_2 - \mathbf{q}_2, \mathbf{q}'_1; \mathbf{q})}{\zeta + \epsilon_{\mathbf{q}} - (\epsilon_{\mathbf{q}'_1} + \epsilon_{\mathbf{q}'_2 - \mathbf{q}_2})} + \frac{\mathcal{A}(\mathbf{q} - \mathbf{q}'_2, \mathbf{q}_2; \mathbf{q}'_1) \mathcal{A}(\mathbf{q} - \mathbf{q}'_2, \mathbf{q}'_2; \mathbf{q})}{\zeta + \epsilon_{\mathbf{q}} - (\epsilon_{\mathbf{q}'_2} + \epsilon_{\mathbf{q} - \mathbf{q}'_2})} - \frac{\mathcal{A}(\mathbf{q}'_2 - \mathbf{q}, \mathbf{q}'_1; \mathbf{q}_2) \mathcal{A}(\mathbf{q}'_2 - \mathbf{q}, \mathbf{q}; \mathbf{q}'_2)}{\zeta + \epsilon_{\mathbf{q}} + \epsilon_{\mathbf{q}'_2 - \mathbf{q}} - \epsilon_{\mathbf{q}'_2}} \end{aligned} \quad (82)$$

and finally for process $3 \rightarrow 1$ (knowing that $\mathbf{q}'_1 = \mathbf{q} + \mathbf{q}_2 + \mathbf{q}_3$):

$$\begin{aligned} \mathcal{A}_{\mathbf{q}, \mathbf{q}_2, \mathbf{q}_3 \rightarrow \mathbf{q}'_1}(\mathbf{q}, \zeta) &= -\frac{\mathcal{A}(\mathbf{q}_2, \mathbf{q}_3; \mathbf{q}_2 + \mathbf{q}_3) \mathcal{A}(\mathbf{q}_2 + \mathbf{q}_3, \mathbf{q}; \mathbf{q}'_1)}{\zeta + \epsilon_{\mathbf{q}} + \epsilon_{\mathbf{q}_2 + \mathbf{q}_3} - \epsilon_{\mathbf{q}'_1}} + \frac{\mathcal{A}(\mathbf{q} + \mathbf{q}_2, \mathbf{q}_3; \mathbf{q}'_1) \mathcal{A}(\mathbf{q}, \mathbf{q}_2; \mathbf{q} + \mathbf{q}_2)}{\zeta + \epsilon_{\mathbf{q}} + \epsilon_{\mathbf{q}_2} - \epsilon_{\mathbf{q} + \mathbf{q}_2}} \\ &+ \frac{\mathcal{A}(\mathbf{q} + \mathbf{q}_3, \mathbf{q}_2; \mathbf{q}'_1) \mathcal{A}(\mathbf{q}, \mathbf{q}_3; \mathbf{q} + \mathbf{q}_3)}{\zeta + \epsilon_{\mathbf{q}} + \epsilon_{\mathbf{q}_3} - \epsilon_{\mathbf{q} + \mathbf{q}_3}} \end{aligned} \quad (83)$$

In these equations (81,82,83), the three contributions where we had to choose the opposite direction in (75), i.e. take E_f rather than E_i as the reference energy, are easy to spot as they start with a minus sign.

Our prescription (79,80) gives simple but generally different results from the exact fourth-order diagrammatic theory, given the expressions for Matsubara double sums in Appendix C. Remarkably, however, once these sums have been replaced by their simplified expressions (54,63), which is legitimate at small angles, it is in perfect agreement with the value of $\Sigma^{(4)}$ predicted by the diagrams in Figure 6; this can be verified with the aid of the correspondence table 1, obtained from the coupling amplitudes in (53,62) and the energy denominators in (54,63), and which makes it possible to associate with each internal line on this figure an incoming \mathbf{q}_i , outgoing \mathbf{q}'_j or virtual (linear combination of the previous ones) phonon of a $n \rightarrow n'$ process, thus giving a clear physical meaning to the corresponding diagram.⁴³ Ultimately, the prescription (79,80) leads in $d = 2$ to a rigorously equivalent but much more compact expression of $\Sigma^{(4)}$ at leading order in ϵ :

$$\tilde{\Sigma}_{\bar{q}}^{(4,2)}(\tilde{\zeta}) = \frac{1}{3} \iint_{\mathbb{T}_{\bar{q}}} \frac{\bar{q}'_1 d\bar{q}'_1}{(2\pi)^2} \frac{\bar{q}'_2 d\bar{q}'_2}{(2\pi)^2} \Phi(\bar{q}'_1, \bar{q}'_2) + \iint_{\mathbb{R}^{+2} \setminus \mathbb{T}_{\bar{q}}} \frac{\bar{q}'_1 d\bar{q}'_1}{(2\pi)^2} \frac{\bar{q}'_2 d\bar{q}'_2}{(2\pi)^2} \Phi(\bar{q}'_1, \bar{q}'_2) + \iint_{\mathbb{R}^{+2}} \frac{\bar{q}_2 d\bar{q}_2}{(2\pi)^2} \frac{\bar{q}_3 d\bar{q}_3}{(2\pi)^2} \Phi(-\bar{q}_2, -\bar{q}_3) \quad (84)$$

where we have kept the order of processes $1 \rightarrow 3$, $2 \rightarrow 2$ and $3 \rightarrow 1$, $\mathbb{T}_{\bar{q}}$ is the triangle $\{(\bar{q}'_1, \bar{q}'_2) \in \mathbb{R}^{+2} \mid \bar{q}'_1 + \bar{q}'_2 \leq \bar{q}\}$ and, as before, the tilde on $\Sigma_{\bar{q}}$ indicates a division by $k_B T \epsilon^2$. One and the same function is involved in the integrand

43. The verification is facilitated by the following result: according to our Landau prescription, each diagrammatic contribution to the Matsubara sums (54,63) is given by $\sigma / \prod_j (\zeta - \zeta_j)$ with $\sigma = s(f_1 f_2 - f_3 f_4)$, where (i) the global sign s is the product of the orientations s_i of the virtual phonon lines (indeed, if a virtual phonon goes back in time, its energy appears with a plus sign in the denominator in the corresponding $(\zeta - \zeta_j)$ factor, so it contributes through the second sum of (80) and a global minus sign must be included), (ii) each f_k is the product of the bosonic amplification factors of the lines connected to the vertex k (the line i contributes to f_k by a factor \bar{n}_{ϵ_i} if it goes towards the vertex, or by a factor $1 + \bar{n}_{\epsilon_i}$ if it goes away from it, which is written $s_i(1 + \bar{n}_{s_i \epsilon_i})$ if the line is to the right of the vertex and $s_i \bar{n}_{s_i \epsilon_i}$ if it is to the left), excluding, however, external lines and virtual phonon lines, whose occupation numbers do not appear in the prescription (79,80). Diagram vertices are numbered from left to right; in the case of bridge diagrams, the degeneracy of internal vertex numbering is lifted by rotating the vertical phonon line by a small angle to the left (type I, effective orientation s_5) or to the right (type II, effective orientation $-s_5$). One thus finds, all signs factorized, $\sigma_B = s_1 s_2 s_3 s_4 s_5 [(1 + \bar{n}_{s_1 \epsilon_1})(1 + \bar{n}_{s_3 \epsilon_3})(1 + \bar{n}_{s_4 \epsilon_4}) - \bar{n}_{s_1 \epsilon_1} \bar{n}_{s_3 \epsilon_3} \bar{n}_{s_4 \epsilon_4}]$ for inner-loop diagrams ($s = s_2 s_5$), $\sigma_{PI} = s_1 s_2 s_3 s_4 s_5 [(1 + \bar{n}_{s_2 \epsilon_2})(1 + \bar{n}_{s_3 \epsilon_3})(1 + \bar{n}_{s_5 \epsilon_5}) - \bar{n}_{s_2 \epsilon_2} \bar{n}_{s_3 \epsilon_3} \bar{n}_{s_5 \epsilon_5}]$ and $\sigma_{PII} = s_1 s_2 s_3 s_4 (-s_5) [(1 + \bar{n}_{s_1 \epsilon_1})(1 + \bar{n}_{s_4 \epsilon_4})(1 + \bar{n}_{-s_5 \epsilon_5}) - \bar{n}_{s_1 \epsilon_1} \bar{n}_{s_4 \epsilon_4} \bar{n}_{-s_5 \epsilon_5}]$ for bridge diagrams ($s = s_1 s_4$ for type I, $s = s_2 s_3$ for type II). We then find exactly the simplified forms (54,63) if we use energy conservation at the second vertex, respectively $s_2 \epsilon_2 = s_3 \epsilon_3 + s_4 \epsilon_4$, $s_1 \epsilon_1 = s_3 \epsilon_3 + s_5 \epsilon_5$ and $s_2 \epsilon_2 = s_4 \epsilon_4 + (-s_5) \epsilon_5$, through the identity $\bar{n}_{a+b} = \bar{n}_a \bar{n}_b / (1 + \bar{n}_a + \bar{n}_b)$, and the equality $s_2 = s_5$ in the inner-loop diagrams.

| | | | | | |
|-------|---|---------|---|------------|---|
| B_1 | all the squares of 1 \rightarrow 3 | P_1^I | all crossed terms of 1 \rightarrow 3 | P_1^{II} | 3 rd term \times 4 th term of 2 \rightarrow 2 |
| B_2 | squares of 3 rd and 4 th terms of 2 \rightarrow 2 | P_2^I | 1 st term \times 3 rd term of 2 \rightarrow 2 | P_2^{II} | 3 rd term \times 5 th term of 2 \rightarrow 2 |
| B_3 | 2 nd term \times 3 rd term of 2 \rightarrow 2 | P_3^I | 1 st term \times 4 th term of 2 \rightarrow 2 | P_3^{II} | 2 nd term \times 4 th term of 2 \rightarrow 2 |
| B_4 | 4 th term \times 5 th term of 2 \rightarrow 2 | P_4^I | 1 st term \times 2 nd term of 2 \rightarrow 2 | P_4^{II} | 1 st term \times 3 rd term of 3 \rightarrow 1 |
| B_5 | squares of 2 nd and 5 th terms of 2 \rightarrow 2 | P_5^I | 2 nd term \times 3 rd term of 3 \rightarrow 1 | P_5^{II} | 2 nd term \times 5 th term of 2 \rightarrow 2 |
| B_6 | square of 1 st term of 3 \rightarrow 1 | P_6^I | 1 st term \times 5 th term of 2 \rightarrow 2 | P_6^{II} | 1 st term \times 2 nd term of 3 \rightarrow 1 |
| B_7 | square of 1 st term of 2 \rightarrow 2 | | | | |
| B_8 | squares of 2 nd and 3 rd terms of 3 \rightarrow 1 | | | | |

Table 1: In the calculation of the self-energy at fourth-order in H_3 , correspondence between the Feynman diagrams in Figure 6 and the square or crossed terms (double products) of the quantities $\mathcal{A}_{i \rightarrow f}^2(\mathbf{q}, z)$ involved in Landau prescription (79); the various terms of the $\mathcal{A}_{i \rightarrow f}(\mathbf{q}, z)$ transition amplitudes referred to are those of equations (81, 82, 83) written in that order. For bridge diagrams, it was necessary to distinguish between type I and type II, as in (63). The correspondence holds after integration on the wave vectors as in (79), which makes, for example, the squares of each of the terms of (81), which differ by a permutation of \mathbf{q}'_j , or the double products of 2nd and 4th terms and 5th and 3rd terms of (82), which are mapped one onto the other by exchange of \mathbf{q}'_1 and \mathbf{q}'_2 , give the same contribution.

of the $n \rightarrow n'$ contributions, only the integration domain changes with the process under consideration:⁴⁴

$$\Phi(\bar{q}'_1, \bar{q}'_2) = \frac{1}{2} \bar{q} \left(\frac{9(1 + \Lambda)^2}{8\rho\xi^2} \right)^2 \bar{q}'_1 \bar{q}'_2 (\bar{q}'_1 + \bar{q}'_2 - \bar{q}) [(1 + \bar{n}_{q'_1}^{\text{lin}} + \bar{n}_{q'_2}^{\text{lin}}) \bar{n}_{q'_1 + q'_2 - q}^{\text{lin}} - \bar{n}_{q'_1}^{\text{lin}} \bar{n}_{q'_2}^{\text{lin}}] \times \int_{\mathbb{R}} d\tilde{\theta}_1 \int_{\mathbb{R}} d\tilde{\theta}_2 \left\{ \frac{\bar{q}'_1 + \bar{q}'_2}{\tilde{\zeta} + \bar{q}(\bar{q}'_1 + \bar{q}'_2)(\bar{q}'_1 + \bar{q}'_2 - \bar{q}) \left[\frac{(\bar{q}'_1 \bar{\theta}_1 + \bar{q}'_2 \bar{\theta}_2)^2}{2(\bar{q}'_1 + \bar{q}'_2 - \bar{q})^2 (\bar{q}'_1 + \bar{q}'_2)^2} - \frac{3\gamma}{8} \right]} + \frac{\bar{q} - \bar{q}'_1}{\tilde{\zeta} + \bar{q}\bar{q}'_1(\bar{q} - \bar{q}'_1) \left[-\frac{\bar{\theta}_1^2}{2(\bar{q}'_1 - \bar{q})^2} + \frac{3\gamma}{8} \right]} + \frac{\bar{q} - \bar{q}'_2}{\tilde{\zeta} + \bar{q}\bar{q}'_2(\bar{q} - \bar{q}'_2) \left[-\frac{\bar{\theta}_2^2}{2(\bar{q}'_2 - \bar{q})^2} + \frac{3\gamma}{8} \right]} \right\}^2 \quad (85)$$

$$\tilde{\zeta} - \frac{\bar{q}'_1(\bar{q}'_2 - \bar{q})\bar{\theta}_1^2 + \bar{q}'_2(\bar{q}'_1 - \bar{q})\bar{\theta}_2^2 - 2\bar{q}'_1\bar{q}'_2\bar{\theta}_1\bar{\theta}_2}{2(\bar{q}'_1 + \bar{q}'_2 - \bar{q})} + \frac{3\gamma}{8}(\bar{q}'_1 + \bar{q}'_2)(\bar{q}'_1 - \bar{q})(\bar{q}'_2 - \bar{q})$$

4.3. Failure of order four in the limit $\epsilon = k_B T / mc^2 \rightarrow 0$

An unexpected divergence. As a first simple application of the expansion of the self-energy to order four in H_3 , we had decided to calculate $\tilde{\Sigma}_{\bar{q}}^{(4,2)}(i0^+)$ numerically⁴⁵ to see if, through a better approximation of $\Sigma_{\mathbf{q}}(i0^+)$ in equation (8), this would bring the pole approximation closer to the numerical results by reducing the deviation in Figure 2d. To our surprise, we discovered that $\tilde{\Sigma}_{\bar{q}}^{(4,2)}(i\delta)$ diverges as $1/i\delta$ when $\delta \rightarrow 0^+$! We then confirmed this result analytically, showing that⁴⁶

$$\tilde{\Sigma}_{\bar{q}}^{(4,2)}(\tilde{\zeta}) \underset{\tilde{\zeta} \rightarrow 0}{\sim} \frac{-2}{3\pi^2 \gamma \tilde{\zeta}} \left(\frac{9(1 + \Lambda)^2}{8\rho\xi^2} \right)^2 \int_{\bar{q}}^{\eta} \bar{k} d\bar{k} \int_0^{\eta - \bar{k}} \bar{k}' d\bar{k}' (\bar{k} - \bar{q})(\bar{q} + \bar{k}') (\bar{n}_{k - q}^{\text{lin}} - \bar{n}_{\bar{k}}^{\text{lin}}) (\bar{n}_{k' + q}^{\text{lin}} - \bar{n}_{k' + k}^{\text{lin}}) \quad (86)$$

This divergence comes from the angular integral $K(\bar{k}, \bar{k}')$ (68) of bridge diagram P_5 . Let's analyze the behavior of (68) in the $\tilde{\zeta} \rightarrow 0$ limit for any orientation s_j of the internal lines. If it is divergent, it is necessarily dominated by a neighborhood of the cancellation locus of the integrand denominator in the $(\tilde{\theta}, \tilde{\theta}')$ plane for $\tilde{\zeta} = 0$. As the curvature parameter γ is > 0 , this locus is the union of the two vertical lines $\tilde{\theta} = \epsilon(-A_1^P/B_1^P)^{1/2}$ ($\epsilon = \pm 1$) where the first factor in the denominator vanishes, the two horizontal lines $\tilde{\theta}' = \epsilon'(-A_2^P/B_2^P)^{1/2}$ ($\epsilon' = \pm 1$) where the second factor vanishes, and the conic making the third factor vanish. The unfortunate thing is that the conic always passes through the intersection points $P_{\epsilon, \epsilon'} \equiv (\epsilon(-A_1^P/B_1^P)^{1/2}, \epsilon'(-A_2^P/B_2^P)^{1/2})$ of the horizontal and vertical lines, whatever the wave numbers \bar{k} , \bar{k}' and \bar{q} , on the sole condition that $\epsilon\epsilon' = s_2 s_4$. This follows from the identity on the coefficients (69, 70):

$$4A_1^P A_2^P B_1^P B_2^P (B_3^P)^2 = [A_2^P B_1^P (B_2^P + B_3^P) + A_1^P B_2^P B_3^P - A_3^P B_1^P B_2^P]^2 \quad (87)$$

44. As far as the bosonic factors are concerned, this is shown by making use of the relation $\bar{n}_{-k}^{\text{lin}} = -(1 + \bar{n}_k^{\text{lin}})$, $\forall k \in \mathbb{R}^*$.

45. The angular integrals are calculated analytically, only the integration over the wavenumbers is done by computer.

46. To facilitate the calculation of angular integrals, we have established (86) first in the case where $\tilde{\zeta} \rightarrow 0$ by positive imaginary parts, then extended to the case $\text{Im} \tilde{\zeta} < 0$ as in footnote 27.

Since the angular integral is two-dimensional, a possible divergent part $K_{\text{div}}(\bar{k}, \bar{k}')$ of $K(\bar{k}, \bar{k}')$ can only come from a small neighborhood of the triple intersection points P_{s_2, s_4} and $P_{-s_2, -s_4}$, where we replace each factor in the denominator by its linear approximation in $\tau = \tilde{\theta} - \varepsilon(-A_1^P/B_1^P)^{1/2}$ and $\tau' = \tilde{\theta}' - \varepsilon'(-A_2^P/B_2^P)^{1/2}$. This leaves

$$K_{\text{div}}(\bar{k}, \bar{k}') = \int_{\mathbb{R}^2} \frac{2d\tau d\tau'}{[\tilde{\zeta} - (\frac{3\gamma}{4})^{1/2} s_1 \bar{q} \bar{k} \tau][\tilde{\zeta} - (\frac{3\gamma}{4})^{1/2} s_3 \bar{q} \bar{k}' \tau']\{\tilde{\zeta} - (\frac{3\gamma}{4})^{1/2} s_3 \bar{k}' [s_1 \bar{k} \tau + (\bar{q} - s_1 \bar{k}) \tau']\}} = \frac{8\pi^2(1-s_2)(1-s_1 s_3)}{3\gamma \tilde{\zeta} \bar{q} \bar{k} \bar{k}' (s_1 \bar{k} - s_3 \bar{k}')} \quad (88)$$

where we have been able to extend the integral to the whole \mathbb{R}^2 since it converges to infinity, and have been able to restrict ourselves to the point P_{s_2, s_4} (at the cost of adding a global factor 2) by parity invariance $(\tilde{\theta}, \tilde{\theta}') \rightarrow (-\tilde{\theta}, -\tilde{\theta}')$. In the right-hand side of (88), we have explicitly calculated the integral over τ' and then over τ by the residue method (the integration path must be closed by a semicircle at infinity in the upper or lower half-plane containing the minimum number of poles in view of constraints (71)). The divergent part is therefore non-zero only if $s_2 = s_1 s_3 = -1$, i.e. if the lower left branch of the bridge loop is oriented to the left and the two upper branches have opposite orientations, which selects as announced diagram P_5 in Figure 6. Inserting the corresponding value of $K_{\text{div}}(\bar{k}, \bar{k}')$ into (67) yields equation (86). The same technique applied to type I contribution of bridge diagrams leads in (66) to a divergent part of the form^{47 48}

$$J_{\text{div}}(\bar{k}, \bar{k}') = \int_{\mathbb{R}^2} \frac{2d\tau d\tau'}{[\tilde{\zeta} - (\frac{3\gamma}{4})^{1/2} s_1 \bar{q} \bar{k} \tau][\tilde{\zeta} - (\frac{3\gamma}{4})^{1/2} s_3 \bar{q} \bar{k}' \tau']\{\tilde{\zeta} - (\frac{3\gamma}{4})^{1/2} s_1 \bar{k} [(\bar{q} - s_3 \bar{k}') \tau + s_3 \bar{k}' \tau']\}} = \frac{8\pi^2(1-s_1)(1-s_2 s_4)}{3\gamma \tilde{\zeta} \bar{q} \bar{k} \bar{k}' (s_1 \bar{k} - s_3 \bar{k}')} \quad (89)$$

and concludes that there is no divergence (to have $J_{\text{div}} \neq 0$, the upper left branch of the bridge loop would have to be oriented to the left, and the two lower branches would have to be of opposite orientations, which does not occur in Figure 6).

Physical implications. From the expansion of the self-energy to order four in H_3 , and still to leading order (two) in ε , we form a new approximation to the Green's function,

$$\tilde{\mathcal{G}}_{\bar{q}}^{(\leq 4, 2)}(\tilde{\zeta}) = \frac{1}{\tilde{\zeta} - \tilde{\Sigma}_{\bar{q}}^{(2, 2)}(\tilde{\zeta}) - \tilde{\Sigma}_{\bar{q}}^{(4, 2)}(\tilde{\zeta})} \quad (90)$$

One might think that it is more accurate and performs better than the one in section 3. Unfortunately, because of the divergence (86), this is not the case: in the weakly interacting regime, which is the most favorable, it has a pole $\tilde{\zeta}_{\bar{q}}^{n\phi}$ in the upper half-plane (and its complex conjugate in the lower half-plane), in the absence, it should be pointed out, of any analytic continuation, hence the exponent $n\phi$ ("non physical"). This violates the fundamental analyticity property of the Green's function on $\mathbb{C} \setminus \mathbb{R}$ [7], and leads, for example, to a signal diverging exponentially in time in (6) if path C_+ passes above $\tilde{\zeta}_{\bar{q}}^{n\phi}$, or not starting at one if it passes below. To show the existence of this pole, let's reduce the implicit equation

$$\tilde{\zeta}_{\bar{q}}^{n\phi} = \tilde{\Sigma}_{\bar{q}}^{(2, 2)}(\tilde{\zeta}_{\bar{q}}^{n\phi}) + \tilde{\Sigma}_{\bar{q}}^{(4, 2)}(\tilde{\zeta}_{\bar{q}}^{n\phi}) \quad (91)$$

to its leading order, assuming that $\tilde{\zeta}_{\bar{q}}^{n\phi}$ tends to zero as $(\rho\xi^2)^{-1}$ (by positive imaginary parts). Since $\tilde{\Sigma}_{\bar{q}}^{(2, 2)}(\tilde{\zeta})$ is already of order one in $(\rho\xi^2)^{-1}$, and is a derivable function of $\tilde{\zeta}$ at $i0^+$ (see Appendix A), we can replace it by its value at this point. In the case of $\tilde{\Sigma}_{\bar{q}}^{(4, 2)}(\tilde{\zeta})$, we keep its divergent part (86), as the second-order prefactor $(\rho\xi^2)^{-2}$ it contains is promoted to first order by division by $\tilde{\zeta}$, but we neglect its regular part, of second-order near $i0^+$. By making the universalizing change of variables (41, 42, 43) as in section 3, we are left with

$$\tilde{\zeta}_{\bar{q}}^{n\phi} = \tilde{\Sigma}_{\bar{q}}^{(2, 2)}(i0^+) - \frac{(2/\bar{q}^2) \int_{\bar{q}}^{\eta} \bar{k} d\bar{k} \int_0^{\eta-\bar{k}} \bar{k}' d\bar{k}' (\bar{k} - \bar{q})(\bar{k}' + \bar{q})(\bar{n}_{k-\bar{q}}^{\text{lin}} - \bar{n}_k^{\text{lin}})(\bar{n}_{k'+\bar{q}}^{\text{lin}} - \bar{n}_{k'+k}^{\text{lin}})}{\tilde{\zeta}_{\bar{q}}^{n\phi}} \quad (92)$$

47. In fact, the coefficients also satisfy the relationship obtained by exchanging indices 1 and 2 and replacing index 3 by index 4 in (87).

48. In the case of inner-loop diagrams, the existence of a triple nodal point is less surprising since the denominator of (58) comprises a squared trinomial. In fact, there are four of them, playing equivalent roles. For the sign choices $\varepsilon = s_1 s_2$ and $\varepsilon' = s_2 s_3 s_4$, the coefficients of τ and τ' in the linearized forms are all negative; setting them to -1 and taking $\tilde{\zeta} = i\delta$ to simplify, we get $\int_{[-1, 1]^2} 4d\tau d\tau' / [(i\delta - \tau)^2 (i\delta - \tau - \tau')]$, which is $O(1)$ when $\delta \rightarrow 0^+$.

where the first term in the right-hand side is given in (114). Since the integral in the numerator is > 0 , equation (92) on $\zeta_q^{n\phi}$ has a pure imaginary solution in the upper half-plane.⁴⁹ For the sake of completeness, let's point out that $\check{\Sigma}_q^{(4,2)}(\check{\zeta})$ has another linear divergence on the real axis, at $\check{\zeta}_0 = -3\gamma\bar{q}^3/32$,⁵⁰ as shown by Appendix D, which is less damaging as it does not imply the existence of a non-physical pole of the Green's function in the weakly interacting limit (it suffices to have $|\check{\Sigma}_q^{(2,2)}(i0^+)| \lll |\text{Re } \check{\zeta}_0|$ for this divergence to have little effect on signal damping in its half-width).

Applicability of order four. Does the appearance of a non-physical pole force us to question the validity of the diagrammatic expansion and, by extension, that of the many-body Green's function method? No. The theory was intended to be used in the $(\rho\xi^2)^{-1} \rightarrow 0$ weakly interacting limit at fixed reduced temperature $\epsilon = k_B T/mc^2$. However, we took the limit $\epsilon \rightarrow 0$ with a fixed order of expansion in $(\rho\xi^2)^{-1}$, which fails in dimension $d = 2$. Let's show that everything is fine, i.e. the non-physical pole disappears, when $\rho\xi^2\epsilon^2$ is large enough (at fixed \bar{q}).

To this end, let's see how the local analysis leading to (88) is modified when ϵ is small but not infinitesimal, by restricting ourselves directly to diagram P_5 , i.e. taking $s_1 = s_4 = s_5 = 1$, $s_2 = s_3 = -1$. If $\check{\zeta} = 0$, type II energy denominator in (63), which is also that of (88), is written $(-\zeta_1)(-\zeta_2)(-\zeta_3)$, where the energy defects ζ_i are those in equation (64). The first factor $-\zeta_1 = -(\epsilon_{\mathbf{k}} - \epsilon_{\mathbf{k}-\mathbf{q}} - \epsilon_{\mathbf{q}})$ is a function of the single angle $\theta = \epsilon\tilde{\theta}$ between \mathbf{q} and \mathbf{k} , and continues to vanish on two vertical lines in the plane $(\tilde{\theta}, \tilde{\theta}')$, at slightly modified abscissas, which negligibly changes (by a factor $1 + O(\epsilon^2)$) the coefficient of τ in (88); the second factor $-\zeta_2 = -(-\epsilon_{\mathbf{k}'} + \epsilon_{\mathbf{q}+\mathbf{k}'} - \epsilon_{\mathbf{q}})$ is a function of the single angle $\theta' = \epsilon\tilde{\theta}'$ between \mathbf{q} and \mathbf{k}' , and continues to vanish on two horizontal lines, slightly displaced, with the same negligible consequences on the coefficient of τ' in (88). On the other hand, the cancellation locus of the third factor, namely $-\zeta_3 = -(\epsilon_{\mathbf{k}} + \epsilon_{\mathbf{q}+\mathbf{k}'} - \epsilon_{\mathbf{k}+\mathbf{k}'} - \epsilon_{\mathbf{q}})$, is no longer exactly a conic in the $(\tilde{\theta}, \tilde{\theta}')$ plane and now passes slightly to the side of the intersection points $P_{-1,1}$ and $P_{1,-1}$ of the horizontal and vertical lines: this changes very slightly the coefficients of the linear combination of τ and τ' in (88), but above all adds, next to $\check{\zeta}$, the now non-zero value of $-\check{\zeta}_3$ in $P_{-1,1}$:

$$(-\check{\zeta}_3)_{P_{-1,1}} \underset{\epsilon \rightarrow 0}{\sim} -\frac{27}{64}\gamma^2\epsilon^2\bar{k}\bar{k}'(\bar{k}-\bar{q})(\bar{k}+\bar{k}')(\bar{k}'+\bar{q}) \quad (93)$$

We recalculate the right-hand side of (88) accordingly:

$$K_{\text{div}}^{P_5}(\bar{k}, \bar{k}') = -\frac{32\pi^2}{3\gamma\bar{q}\bar{k}\bar{k}'(\bar{k}+\bar{k}')\check{\zeta} - \frac{27}{64}\gamma^2\epsilon^2\bar{q}\bar{k}\bar{k}'(\bar{k}-\bar{q})(\bar{k}'+\bar{q})} \quad (94)$$

The new equation on the non-physical pole

$$\zeta_q^{n\phi} = \check{\Sigma}_q^{(2,2)}(i0^+) - \frac{2}{\bar{q}^2} \int_{\bar{q}}^{\eta} \bar{k} d\bar{k} \int_0^{\eta-\bar{k}} \bar{k}' d\bar{k}' \frac{(\bar{k}-\bar{q})(\bar{k}'+\bar{q})(\bar{n}_{k-q}^{\text{lin}} - \bar{n}_k^{\text{lin}})(\bar{n}_{k'+q}^{\text{lin}} - \bar{n}_{k'+k}^{\text{lin}})}{\zeta_q^{n\phi} - \frac{9}{8}\gamma u \epsilon^2 \bar{k}\bar{k}'(\bar{k}-\bar{q})(\bar{k}'+\bar{q})} \quad (95)$$

ceases to have a solution in the upper half-plane when $\gamma u \epsilon^2 > h(\bar{q})$, where u is the universal parameter (41) and $h(\bar{q})$ is a function exclusively of \bar{q} (and of the cut-off η if it is not sent to infinity in quantum theory), as can be seen by formally taking the limit $\gamma u \epsilon^2 \rightarrow +\infty$ in (95). For the classical field, we find numerically that $h(\bar{q})$ is a decreasing function of \bar{q} ; the problem of applicability of fourth-order theory for small values of ϵ therefore remains in the limit $\bar{q} \rightarrow 0$.⁵¹ To see this more simply, we can evaluate $\check{\Sigma}_q^{(4)}(i0^+)$ (fourth-order in H_3 contribution considered at all orders

49. Let us set $\zeta_q^{n\phi} = iy$. Then (92) is written as $y = -2B + A/y$ where the coefficients A and B are real > 0 . The resulting second-degree equation on y has one (and only one) positive root, $y_0 = A/[(A+B^2)^{1/2} + B]$. When $\bar{q} \rightarrow 0$, B has a finite, non-zero limit in view of (114), then A diverges as $1/\bar{q}$, so that $\zeta_q^{n\phi}$ diverges as $\bar{q}^{-1/2}$ and $\check{\zeta}_q^{n\phi}$ tends to zero as $\bar{q}^{1/2}$. Thus, condition $\text{Im } \zeta_q^{n\phi} \lll |\check{\Sigma}_q^{(2,2)}(i0^+)| = O(\bar{q})$, which makes the non-physical pole without effect on the signal in its time half-width, cannot be satisfied at wavenumber $\bar{q} \lesssim 1$. It can be satisfied at large wavenumber $\bar{q} \gg 1$, where $B \approx \bar{q}^2$ in view of (114) and $A \sim 2 \exp(-\bar{q})$.

50. Note that $\check{\zeta}_0$ is also the branch point of $\check{\Sigma}_q^{(2,2)}(\check{\zeta})$, see section 3.1 and footnote 31.

51. For the classical field ($\eta = 1$), we have the equivalent $h(\bar{q}) \sim \frac{8}{9}(\pi^2/2\bar{q})^{4/3}$ when $\bar{q} \rightarrow 0$ (in practice $\bar{q}^{1/3} \ll 1$). This is obtained by writing the right-hand side of (95) to leading order in \bar{q} (in particular, we replace \bar{q} by zero in the first integration bound and in the denominator of the integrand, and replace the numerator by its linear approximation in \bar{q}), then showing that the double integral is dominated by a neighborhood of $(\bar{k}, \bar{k}') = (0, 0)$ of radius $h(\bar{q})^{-1/4} \ll 1$ when $\bar{q} \rightarrow 0$, which allows us to replace the upper integration bounds by $+\infty$. The result is an analytically calculable double integral and the equation $\zeta_q^{n\phi} = -i + (1+i)\pi^2/[2\bar{q}(\frac{9}{8}\gamma u \epsilon^2)^{3/4}(\zeta_q^{n\phi})^{1/4}]$. It remains to express the fact that the non-physical pole has a zero imaginary part when it disappears.

in ϵ) in the limit $\epsilon \rightarrow 0$. All we need to do is replace $\zeta_{\bar{q}}^{n\phi}$ by $i0^+$ in the double integral in the right-hand side of (95), which we can then calculate explicitly for the quantum field (cutoff $\eta \rightarrow +\infty$):

$$\check{\Sigma}_{\bar{q}}^{(4)}(i0^+) \underset{\epsilon \rightarrow 0}{\sim} \frac{16g_2(e^{-\bar{q}})}{9\gamma u \epsilon^2 \bar{q}^2} \quad \text{hence} \quad \Sigma_{\bar{q}}^{(4)}(i0^+) \underset{\epsilon \rightarrow 0}{\sim} k_B T \left[\frac{(1+\Lambda)^2}{\gamma^{3/2} \rho \xi^2} \right]^2 \frac{2g_2(e^{-\bar{q}})}{\pi^2 \bar{q}} \quad (96)$$

At low temperature $\epsilon \ll 1$, the fourth order in H_3 (96) is therefore a small correction to the second order (114) only if $\gamma u \epsilon^2$ is much larger than a certain function of \bar{q} , namely $1/\bar{q}^2$ at low \bar{q} .⁵²

Conclusion. At a fixed reduced wave number \bar{q} of the phonon mode whose damping is being studied, the condition for the applicability of diagrammatic theory at order four in H_3 is not only that the universal parameter u is large enough (the expected weakly interacting regime) but also that the product $\gamma u \epsilon^2$ is large enough. The perturbative approach therefore presents a fundamental incompatibility with the limit studied in this article, the low-temperature $\epsilon \rightarrow 0$ limit with fixed interaction strength. In particular, for the numerical simulations in Figure 2, where $\bar{q} = 1/4$ and $\gamma = 1$, we find, by following with Newton's method the root of equation (95), written for the classical field, until it disappears, that we should have $u \epsilon^2 > 10.6$ or $\rho \xi^2 > 23.4$ for $\epsilon = 1/2$ and $\rho \xi^2 > 52.6$ for $\epsilon = 1/3$. However, $\rho \xi^2$ is at most 10 in Figure 2; the fourth-order theory developed in this section is therefore inapplicable.

5. Nonperturbative theories in H_3

As we saw in section 4, the theory at fourth order in H_3 is not usable in dimension $d = 2$ in the low-temperature limit $\epsilon = k_B T / mc^2 \rightarrow 0$. To account for the discrepancy between the theory at second order in H_3 and simulations on the decay time at $1/e$ of the phonon mode \mathbf{q} and on the real part of the associated signal (6) in the weakly interacting regime $(\rho \xi^2)^{-1} \ll 1$, see figures 1d and 2d, we propose here a non-perturbative theory guided by physical considerations. In brief, we omit the finite part and we regularize the divergent part of the fourth-order self-energy by giving a finite lifetime to the so-called virtual (or intermediate) phonons of four-phonon collisional processes; this brings out a contribution that turns out to be second-order in H_3 and thus corrects the eigenenergy expression to the leading order in the interaction strength. We present an atomic physics-type regularization in section 5.1 (virtual phonons \mathbf{K} acquire a complex energy $\epsilon_{\mathbf{K}} \rightarrow \epsilon_{\mathbf{K}} + \Sigma_{\mathbf{K}}^{(2,2)}(i0^+) = \epsilon_{\mathbf{K}} - (i\hbar/2)\Gamma_{\mathbf{K}}$) and a condensed matter-type regularization in section 5.2 (the frequency dependence of the self-energy $\Sigma_{\mathbf{K}}^{(2,2)}(\zeta)$ is retained in the complex energy of virtual phonons). Finally, in section 5.3, we give the new form of the theory in the $(\rho \xi^2)^{-1} \rightarrow 0$ limit, common to both regularizations and successfully replacing Fermi's golden rule.

5.1. Atomic physics-type regularization

We learn from section 4.3 that the addition of an infinitesimal complex part $i0^+$ to $\zeta = z - \epsilon_{\mathbf{q}}$, very common in the Green's function method, is not sufficient to give a finite value to $\check{\Sigma}_{\mathbf{q}}^{(4,2)}(\zeta = 0)$. Collisions between phonons, which render them unstable, naturally provide a non-infinitesimal imaginary contribution next to ζ in the energy denominators. Following the prescription of atomic physics, we therefore give virtual phonons a complex energy

$$\epsilon_{\mathbf{K}} \rightarrow \epsilon_{\mathbf{K}} + \Sigma_{\mathbf{K}}^{(2,2)}(i0^\pm) = \epsilon_{\mathbf{K}} \mp \frac{i\hbar}{2} \Gamma_{\mathbf{K}} \quad (97)$$

where $\Gamma_{\mathbf{K}}$ is the phonon- \mathbf{K} damping rate of Fermi's golden rule to order two in ϵ , see equation (23). Virtual phonons, by definition neither incoming nor outgoing in Landau's formulation of section 4.2, are those whose wave vectors are not shown in the diagrams of Figure 6. The sign to be taken in (97) in front of $\Gamma_{\mathbf{K}}$ or in the argument of $\Sigma_{\mathbf{K}}$ is the upper one if the phonon goes forward in time (internal line oriented to the right) or the lower one if the phonon goes backward in time (internal line oriented to the left).⁵³ On the other hand, we don't give a complex energy to incoming or outgoing phonons as this would question energy conservation in the gas during collisional processes. Consequently, there is no need to modify $\Sigma_{\mathbf{q}}(\zeta)$ to order two in H_3 , which has no virtual phonons.

52. The result (96) does not contradict equation (86) because the order of the limits $\bar{q} \rightarrow 0$ and $\epsilon \rightarrow 0$ is not the same.

53. In Landau's formulation, we choose $-i(\hbar/2)\Gamma_{\mathbf{K}}$ in the first sum of equation (80) and its opposite in the second sum, for the reasons explained below (79) (in the second sum, the transition amplitudes are reversed in time), which leads to the same result as in the diagrammatic formulation.

We apply procedure (97) to the divergent part of $\tilde{\Sigma}_{\bar{q}}^{(4,2)}$, which comes from the type II contribution of diagram P_5 , and omit all other contributions to $\tilde{\Sigma}_{\bar{q}}^{(4,2)}$, which turn out to be $O((\rho\xi^2)^{-2})$ and subleading when $(\rho\xi^2)^{-1} \rightarrow 0$.⁵⁴ As shown in Figure 6, the virtual phonons are then $\mathbf{k}_2 = \mathbf{k} - \mathbf{q}$ and $\mathbf{k}_3 = \mathbf{k}'$ in the notations of Figure 7. Both go backward in time ($s_2 = s_3 = -1$), so the quantities ζ_1 and ζ_2 in (63), that are written $\zeta_1 = \varepsilon_{\mathbf{k}} - \varepsilon_{\mathbf{k}-\mathbf{q}} - \varepsilon_{\mathbf{q}}$ and $\zeta_2 = -\varepsilon_{\mathbf{k}'} + \varepsilon_{\mathbf{k}'+\mathbf{q}} - \varepsilon_{\mathbf{q}}$, and the coefficients A_1^P and A_2^P in (68) are changed as follows,

$$\zeta_1 \rightarrow \zeta_1 - i\frac{\hbar}{2}\Gamma_{\mathbf{k}-\mathbf{q}} \quad ; \quad \zeta_2 \rightarrow \zeta_2 - i\frac{\hbar}{2}\Gamma_{\mathbf{k}'} \quad ; \quad A_1^P \rightarrow A_1^P - \frac{i}{2}\tilde{\Gamma}_{\bar{k}-\bar{q}} \quad ; \quad A_2^P \rightarrow A_2^P - \frac{i}{2}\tilde{\Gamma}_{\bar{k}'} \quad (98)$$

the order of the factors in the denominator of (68) respecting that of (63); here $\tilde{\Gamma}_{\bar{k}} = \hbar\Gamma_{\mathbf{K}}/k_B T \varepsilon^2$ in the spirit of equation (11). On the other hand, the quantity ζ_3 does not involve any virtual phonon and remains unchanged. The previously diverging part of the angular integral (88) becomes for $\text{Im } \tilde{\zeta} > 0$:⁵⁵

$$K_{\text{div. reg.}}^{P_{II}^5}(\bar{k}, \bar{k}') = -\frac{32\pi^2}{3\gamma\bar{q}\bar{k}\bar{k}'} \frac{1}{\tilde{\zeta}(\bar{k} + \bar{k}') + \frac{i}{2}\bar{k}'\tilde{\Gamma}_{\bar{k}-\bar{q}} + \frac{i}{2}(\bar{k} - \bar{q})\tilde{\Gamma}_{\bar{k}'}} \quad (99)$$

After replacing $K(\bar{k}, \bar{k}')$ by (99) in (67) and adding the contribution of second order in H_3 , we end up with the non-perturbative prescription for the self-energy correcting the result of section 3:

$$\tilde{\Sigma}_{\text{corr}}^{(2,2)}(\bar{q}, \tilde{\zeta}) = \tilde{\Sigma}_{\bar{q}}^{(2,2)}(\tilde{\zeta}) + \tilde{\Sigma}_{\text{div. reg.}}^{(4,2)}(\bar{q}, \tilde{\zeta}) \quad (100)$$

where the first contribution is that of equation (40) and the second, a regularization of the divergent part of $\tilde{\Sigma}_{\bar{q}}^{(4,2)}(\tilde{\zeta})$, is written, again for $\text{Im } \tilde{\zeta} > 0$:

$$\tilde{\Sigma}_{\text{div. reg.}}^{(4,2)}(\bar{q}, \tilde{\zeta}) = -\frac{2}{3\pi^2\gamma} \left(\frac{9(1 + \Lambda)^2}{8\rho\xi^2} \right)^2 \int_{\bar{q}}^{\eta} d\bar{k} \int_0^{\eta-\bar{k}} d\bar{k}' \frac{\bar{k}\bar{k}'(\bar{k} - \bar{q})(\bar{k}' + \bar{q})(\bar{k} + \bar{k}')}{\tilde{\zeta}(\bar{k} + \bar{k}') + \frac{i}{2}\bar{k}'\tilde{\Gamma}_{\bar{k}-\bar{q}} + \frac{i}{2}(\bar{k} - \bar{q})\tilde{\Gamma}_{\bar{k}'}} (\bar{n}_{\bar{k}'+\bar{q}}^{\text{lin}} - \bar{n}_{\bar{k}'+\bar{k}}^{\text{lin}})(\bar{n}_{\bar{k}-\bar{q}}^{\text{lin}} - \bar{n}_{\bar{k}}^{\text{lin}}) \quad (101)$$

By inserting function (100) into equation (12) (with $\nu = \sigma$ in dimension $d = 2$) in its classical field version, we obtain a much better agreement with numerical simulations for the weakest interaction strength, see the orange solid line in Figure 8a and the black solid line in Figure 8b, to be compared respectively with the black solid line in Figure 8a and the black dashed line in Figure 8b corresponding to the uncorrected second order in H_3 .

5.2. Condensed matter regularization

It is well known in condensed matter physics that the complex energy of a quasiparticle in an interacting system depends on the frequency at which it is observed, i.e. the frequency at which the response functions are measured. This is the essence of Σ in (6). In (97), therefore, we need to replace the fixed complex energy $\mp(i\hbar/2)\Gamma_{\mathbf{K}}$ of the virtual phonon \mathbf{K} with a function of the integration variable ζ :

$$\varepsilon_{\mathbf{k}} \rightarrow \varepsilon_{\mathbf{K}} + \Sigma_{\mathbf{K}}^{(2)}(\pm(\zeta + \Delta E) - \varepsilon_{\mathbf{K}}) \quad (102)$$

where we need to take the sign $+$ if the phonon \mathbf{K} goes forward in time, and the sign $-$ if it goes backward. The quantity ΔE is obtained by reinterpreting the energy denominator in which phonon \mathbf{K} participates in $\Sigma^{(4)}$ as that of the free propagator of this phonon with complex energy $z_{\mathbf{K}} = \zeta + \Delta E$. So, if phonon \mathbf{K} goes forward in time (sign $s_{\mathbf{K}} = +1$ before $\varepsilon_{\mathbf{K}}$ in (64)), it will contribute to $\Sigma^{(4)}$ in simplified forms (54,63) through factor $1/(\zeta + \Delta E - \varepsilon_{\mathbf{K}})$, which is precisely its unperturbed propagator at complex energy $z_{\mathbf{K}}$ and therefore at complex energy redefined as in

54. In the absence of divergence at $\zeta = 0$, adding an imaginary part to $\varepsilon_{\mathbf{K}}$ does not change the leading order of the diagram, which remains fourth-order in H_3 .

55. We continue to linearize around the same triple intersection point of the cancellation loci, grouping the complex corrections with variable $\tilde{\zeta}$, so that in the integral in (88), we replace $\tilde{\zeta}$ by $\tilde{\zeta} + (i/2)\tilde{\Gamma}_{\bar{k}-\bar{q}}$ in the first factor and by $\tilde{\zeta} + (i/2)\tilde{\Gamma}_{\bar{k}'}$ in the second factor in the denominator.

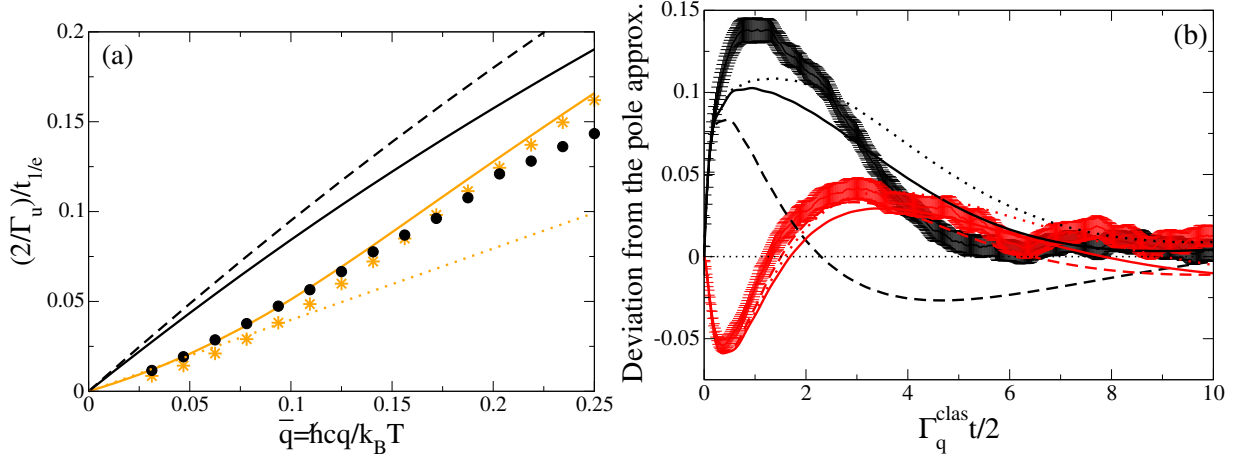


Figure 8: (a) Inverse of the decay time at 1/e of the modulus of signal $s(t)$ (6) as a function of the wavenumber q of the modes along Ox , for the parameters of Figure 1d, in particular $(\rho\xi^2)^{-1} = 0.1$ (this is the weakest interaction strength in Figure 1). Black discs: numerical experiment with $\epsilon = 1/2$. Black dashed line: Fermi's golden rule (34) for the classical phonon-field and in the $\epsilon \rightarrow 0$ limit. Black solid line: many-body Green's function method with the $\tilde{\Sigma}_{\bar{q}}^{(2,2)}(\tilde{\zeta})$ (40) self-energy (leading order in H_3 and ϵ). Orange solid line: idem with the $\tilde{\Sigma}_{\text{corr}}^{(2,2)}(\bar{q}, \tilde{\zeta}) = \tilde{\Sigma}_{\bar{q}}^{(2,2)}(\tilde{\zeta}) + \tilde{\Sigma}_{\text{div. reg.}}^{(4,2)}(\bar{q}, \tilde{\zeta})$ self-energy of equation (100) (we keep only the fourth-order divergent part in H_3 and regularize it according to the atomic physics prescription by giving by hand Fermi's golden rule complex energy to the virtual phonons). Orange stars: idem with the $\tilde{\Sigma}_{\text{div. reg.}}^{(4,2)}(\bar{q}, \tilde{\zeta})$ component of the self-energy (106) obtained by a condensed matter physics-type regularization (virtual phonons \mathbf{K} are given a complex energy $\Sigma_{\mathbf{K}}^{(2,2)}(\zeta_{\mathbf{K}})$ depending on frequency i.e. on variable ζ in (6)). Orange dotted line: tangent at the origin (109) for the $(\rho\xi^2)^{-1} \rightarrow 0$ limit of regularized theories. All self-energies are written in their classical field versions to allow comparison with numerics. The Γ_u rate used as a unit is that of equation (34) giving Γ_q^{clas} . (b) Signal deviation from the pole approximation $s(t) - s_{\text{pole}}(t)$ for parameters in Figure 2d, in particular $\bar{q} = 1/4$ and $(\rho\xi^2)^{-1} = 0.1$. Curves with error bars: numerical experiment. Dashed line: Green's function method with self-energy $\tilde{\Sigma}_{\bar{q}}^{(2,2)}(\tilde{\zeta})$. Solid line: idem taking the self-energy $\tilde{\Sigma}_{\text{corr}}^{(2,2)}(\bar{q}, \tilde{\zeta})$ from equation (100). Dotted line: idem using expression (106) for the $\tilde{\Sigma}_{\text{div. reg.}}^{(4,2)}(\bar{q}, \tilde{\zeta})$ component of self-energy $\tilde{\Sigma}_{\bar{q}}^{(2,2)}(\tilde{\zeta})$. The real part of the signal is in black, the imaginary part in red.

(7) $\zeta_{\mathbf{K}} = z_{\mathbf{K}} - \epsilon_{\mathbf{K}}$. We therefore propose to replace it by the Green's function (6) of phonon \mathbf{K} written as in (7), with $\Sigma_{\mathbf{K}}$ calculated to order two in H_3 :

$$\frac{1}{\zeta + \Delta E - \epsilon_{\mathbf{K}}} \rightarrow \frac{1}{\zeta + \Delta E - \epsilon_{\mathbf{K}} - \Sigma_{\mathbf{K}}^{(2)}(\zeta + \Delta E - \epsilon_{\mathbf{K}})} \quad (103)$$

which explains the substitution (102). If the virtual phonon goes backward in time (sign $s_{\mathbf{K}} = -1$), we reduce to the previous case through the chain of transformations

$$\frac{1}{\zeta + \Delta E + \epsilon_{\mathbf{K}}} = -\frac{1}{-(\zeta + \Delta E) - \epsilon_{\mathbf{K}}} \rightarrow -\frac{1}{-(\zeta + \Delta E) - \epsilon_{\mathbf{K}} - \Sigma_{\mathbf{K}}^{(2)}(-(\zeta + \Delta E) - \epsilon_{\mathbf{K}})} = \frac{1}{\zeta + \Delta E + \epsilon_{\mathbf{K}} + \Sigma_{\mathbf{K}}^{(2)}(-(\zeta + \Delta E) - \epsilon_{\mathbf{K}})} \quad (104)$$

again in accordance with (102). In practice, as in section 5.1, we keep only the divergent part of $\tilde{\Sigma}_{\bar{q}}^{(4,2)}$ (coming from the type II contribution of diagram P_5), in which the virtual phonons both go backward in time and are of wave vector $\mathbf{K} = \mathbf{k} - \mathbf{q}$ (with $\Delta E = \epsilon_{\mathbf{q}} - \epsilon_{\mathbf{k}}$ so that $\zeta - \zeta_1 = \zeta + \Delta E + \epsilon_{\mathbf{k}-\mathbf{q}}$) or $\mathbf{K} = \mathbf{k}'$ (with $\Delta E = \epsilon_{\mathbf{q}} - \epsilon_{\mathbf{k}'+\mathbf{q}}$ so that $\zeta - \zeta_2 = \zeta + \Delta E + \epsilon_{\mathbf{k}'}$). After regularization, the divergent part (88) of the angular integral becomes

$$K_{\text{div. reg.}}^{P_5^{\text{II}}}(\bar{k}, \bar{k}') = \int_{\mathbb{R}^2} \frac{2d\tau d\tau'}{[\tilde{\zeta} - \alpha\tau + \tilde{\Sigma}_{\bar{k}-\bar{q}}^{(2,2)}(-\tilde{\zeta} + \alpha\tau)][\tilde{\zeta} - \alpha'\tau' + \tilde{\Sigma}_{\bar{k}'}^{(2,2)}(-\tilde{\zeta} + \alpha'\tau')](\tilde{\zeta} - \beta\tau - \beta'\tau')} \quad (105)$$

where the coefficients are those of τ and τ' in the integral in (88): $\alpha = (3\gamma/4)^{1/2}\bar{q}\bar{k}$, $\alpha' = -(3\gamma/4)^{1/2}\bar{q}\bar{k}'$, $\beta = -(3\gamma/4)^{1/2}\bar{k}\bar{k}'$, $\beta' = (3\gamma/4)^{1/2}(\bar{k} - \bar{q})\bar{k}'$. As functions $\tilde{\Sigma}^{(2,2)}$ in the denominator of (105) have branch cuts in the complex plane, see section 3.2, Cauchy's theorem no longer allows us to calculate the double integral and we can

only integrate once, for example over τ' , restricting ourselves as usual to $\text{Im } \tilde{\zeta} > 0$.⁵⁶ By inserting the corresponding contribution to $K(\bar{k}, \bar{k}')$ in (67), we end up with the corrected self-energy of the same form as (100), now with

$$\begin{aligned} \tilde{\Sigma}_{\text{div. reg.}}^{(4,2)}(\bar{q}, \tilde{\zeta}) &= \bar{q} \left(\frac{9(1 + \Lambda)^2}{8\rho\xi^2} \right)^2 \\ &\times \int_{\bar{q}}^{\eta} \frac{\bar{k}d\bar{k}}{(2\pi)^2} \int_0^{\eta-\bar{k}} \frac{\bar{k}'d\bar{k}'}{(2\pi)^2} \int_{-\infty}^{+\infty} d\tau \frac{(-4i\pi/\beta')\bar{k}\bar{k}'(\bar{k}-\bar{q})(\bar{k}'+\bar{q})(\bar{k}+\bar{k}')(\bar{n}_{k'+q}^{\text{lin}} - \bar{n}_{k'+k}^{\text{lin}})(\bar{n}_{k-q}^{\text{lin}} - \bar{n}_k^{\text{lin}})}{\left[\tilde{\zeta} - \alpha\tau + \tilde{\Sigma}_{\bar{k}-\bar{q}}^{(2,2)}(-\tilde{\zeta} + \alpha\tau) \right] \left[-\frac{\beta}{\beta'}(\tilde{\zeta} - \alpha'\tau) + \tilde{\Sigma}_{\bar{k}'}^{(2,2)}\left(\frac{\beta}{\beta'}(\tilde{\zeta} - \alpha'\tau)\right) \right]} \end{aligned} \quad (106)$$

knowing that $\alpha' - \beta' = \beta$. The results of this approach are shown as orange stars in Fig. 8a and as red and black dotted lines in Fig. 8b.⁵⁷ The two regularization procedures, atomic physics or condensed matter, ultimately give results close to each other and close to the simulations, which reassures us as to their validity.

5.3. Regularized theory in the weakly interacting limit

Here we calculate the limit of regularized theories when $(\rho\xi^2)^{-1} \rightarrow 0$. To do this, we scale variable $\tilde{\zeta}$ and functions $\tilde{\Sigma}$ to their characteristic values $\propto (\rho\xi^2)^{-1}$ by means of changes of variables (42) and (43), marked with a Czech accent (a factor \bar{q} has been taken out in view of taking the $\bar{q} \rightarrow 0$ limit, and all parameters are collected together in the quantity $u \propto \rho\xi^2$ of equation (41)), then we take the $u \rightarrow +\infty$ limit at fixed $\tilde{\zeta}$ in equations (100) and (101). Contrary to what happened at uncorrected second order in H_3 (43), there remains a dependency in $\tilde{\zeta}$:⁵⁸

$$\tilde{\Sigma}_{\text{corr}}^{(2,2)}(\bar{q}, \tilde{\zeta}) \xrightarrow[u \rightarrow +\infty]{\text{Im } \tilde{\zeta} > 0} \tilde{\Sigma}_{\text{corr}\infty}^{(2,2)}(\bar{q}, \tilde{\zeta}) \equiv -\frac{i}{2}\check{\Gamma}_{\bar{q}} - \frac{2}{\bar{q}} \int_{\bar{q}}^{\eta} d\bar{k} \int_0^{\eta-\bar{k}} d\bar{k}' \frac{\bar{k}\bar{k}'(\bar{k}-\bar{q})(\bar{k}'+\bar{q})(\bar{k}+\bar{k}')(\bar{n}_{k'+q}^{\text{lin}} - \bar{n}_{k'+k}^{\text{lin}})(\bar{n}_{k-q}^{\text{lin}} - \bar{n}_k^{\text{lin}})}{\check{\zeta}\bar{q}(\bar{k}+\bar{k}') + \frac{1}{2}\bar{k}'(\bar{k}-\bar{q})(\check{\Gamma}_{\bar{k}-\bar{q}} + \check{\Gamma}_{\bar{k}'})} \quad (107)$$

Here, $\check{\Gamma}_{\bar{k}} = 2i\check{\Sigma}_{\bar{k}}^{(2,2)}(i0^+)$ is the golden rule damping rate at leading order in ϵ and scaled as in (42), $\check{\Gamma}_{\bar{k}} = 8u\Gamma_{\mathbf{K}}/(3\gamma\epsilon^2\hbar cK)$; we have $\check{\Gamma}_{\bar{k}} = \check{\Gamma}_{\bar{k}}^{\text{clas}} = 2\eta - \bar{K}$ given (34) in the case of the classical field and $\check{\Gamma}_{\bar{k}} = 4\zeta(2) + \bar{K}^2/6$ given (23) or (114) in the case of the infinite cut-off quantum field. Starting from the regularized form (106), we obtain exactly the same expression as (107).⁵⁹ Remarkably, signal (6) associated with the self-energy (107) takes real values at all times.⁶⁰ When $(\rho\xi^2)^{-1} \rightarrow 0$, therefore, there is persistent disagreement with Fermi's golden rule on the real part of the signal, as predicted in Figure 8b, but not on the imaginary part, of zero limit in both theories. Figure 9 shows, as a function of the reduced wavenumber \bar{q} , the decay time at 1/e of the phonon mode \mathbf{q} deduced from (107) for quantum field theory (cutoff $\eta \rightarrow +\infty$). This is our prediction to leading order in temperature and interaction strength for a two-dimensional superfluid, which replaces and corrects that of Fermi's golden rule shown as a dashed line in Fig. 9. Three simple

56. The denominator of the integrand in (105) has a branch cut with respect to variable τ only in the strict upper half-plane because $\text{Im}(\tilde{\zeta}/\alpha) > 0$, and with respect to variable τ' only in the strict lower half-plane because $\text{Im}(\tilde{\zeta}/\alpha') < 0$. We can therefore integrate on τ' by the residue theorem, closing the integration path with a large semicircle at infinity in the upper half-plane; this path necessarily surrounds the pole $\tau'_0 = (\tilde{\zeta} - \beta\tau)/\beta'$ arising from the third factor in the denominator of (105) because $\text{Im } \tau'_0 > 0$. The integrand of the result in (106) this time has a branch cut with respect to variable τ both in the upper half-plane ($\text{Im}(\tilde{\zeta}/\alpha) > 0$) and in the lower half-plane ($\text{Im}(\tilde{\zeta}/\alpha') < 0$), which prevents the integration path from being closed only at infinity.

57. Getting them is rather cumbersome, since each evaluation of functions $\tilde{\Sigma}_{\bar{k}}^{(2,2)}$ requires numerical integration over a wavenumber, as in (40). We have discretized the reduced wavenumbers with a step of 1/64 (results in the figure), but we have verified that a step of 1/96 leads to very similar results.

58. In two steps, we show that the Green's function associated with self-energy (107) has, as it should, no pole in the upper complex half-plane. First, we establish the upper bound $\text{Im } \tilde{\Sigma}_{\text{corr}\infty}^{(2,2)}(\bar{q}, \tilde{\zeta}) \leq \text{Im } \tilde{\Sigma}_{\text{corr}\infty}^{(2,2)}(\bar{q}, 0) \forall \tilde{\zeta} \in \mathbb{C}, \text{Im } \tilde{\zeta} \geq 0$; to this end, we write the denominator of the integrand in (107) in the form $x + iy$, with $x \in \mathbb{R}$ and $y \in \mathbb{R}^+$, then use the chain $\text{Im}[-1/(x + iy)] = y/(x^2 + y^2) \leq 1/y \leq 2/[\bar{k}'(\bar{k} - \bar{q})(\check{\Gamma}_{\bar{k}-\bar{q}} + \check{\Gamma}_{\bar{k}'})]$. In a second step, we check that $\text{Im } \tilde{\Sigma}_{\text{corr}\infty}^{(2,2)}(\bar{q}, 0) < 0 \forall \bar{q} > 0$. It follows that equation $\tilde{\zeta} = \tilde{\Sigma}_{\text{corr}\infty}^{(2,2)}(\bar{q}, \tilde{\zeta})$ cannot have a solution $\tilde{\zeta}$ with a positive imaginary part without leading to the contradiction $\text{Im } \tilde{\zeta} < 0$.

59. Variable changes $\tilde{\zeta} = (3\gamma\bar{q}/8u)\check{\zeta}$ and $\tau = (3\gamma\bar{q}/8u)\check{\tau}$ are carried out simultaneously, and the limit $u \rightarrow +\infty$ is taken under the integral sign at fixed $\check{\tau}$. Then the branch cuts of functions $\tilde{\Sigma}_{\bar{k}}^{(2,2)}$ are rejected at infinity, these functions are replaced by constants, e.g. $\lim_{u \rightarrow +\infty} (8u/3\gamma\bar{q})\tilde{\Sigma}_{\bar{k}-\bar{q}}^{(2,2)}((3\gamma\bar{q}/8u)(\alpha\check{\tau} - \tilde{\zeta})) = [(\bar{k} - \bar{q})/\bar{q}]\tilde{\Sigma}_{\bar{k}-\bar{q}}^{(2,2)}(i0^-) = [(\bar{k} - \bar{q})/\bar{q}](i/2)\check{\Gamma}_{\bar{k}-\bar{q}}$, and the integral over $\check{\tau}$ can be calculated by Cauchy's formula. We find (107).

60. This results from the property $\check{\Sigma}(\check{\zeta})^* = -\check{\Sigma}(-\check{\zeta}^*)$, $\forall \check{\zeta} \in \mathbb{C} \setminus i\mathbb{R}^-$, satisfied by function $\tilde{\Sigma}_{\text{corr}\infty}^{(2,2)}(\bar{q}, \tilde{\zeta})$ (if we extend the expression in the right-hand side as it is to the case $\text{Im } \tilde{\zeta} < 0$).

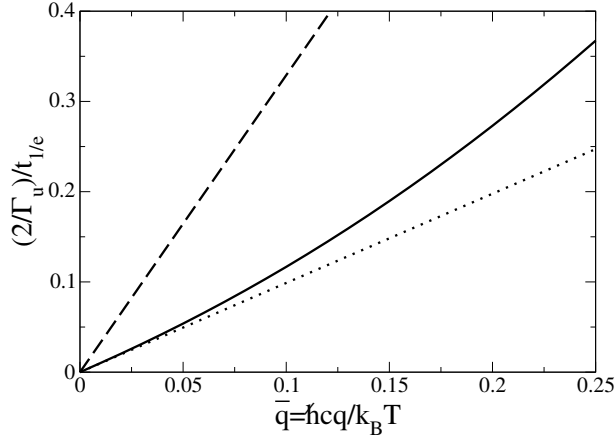


Figure 9: In the low-temperature limit $\epsilon = k_B T / mc^2 \rightarrow 0$ then weakly interacting limit $(\rho \xi^2)^{-1} \rightarrow 0$ for the quantum field of infinite cut-off η , inverse of the decay time at $1/e$ of signal (6) for the phonon mode \mathbf{q} in a two-dimensional superfluid, as a function of the reduced wavenumber \bar{q} . Solid line: prediction from non-perturbative theories in section 5, corresponding to the corrected self-energy (107) in section 5.3. Dotted line: slope at origin (109). Dashed line: golden rule (23). The rate Γ_u serving as unit is given by (34).

analytical predictions can be drawn from equation (107). Firstly, in the $\bar{q} \rightarrow 0$ limit, the $\check{\zeta}$ dependence disappears in the right-hand side of (107) and signal (6) becomes purely exponential, $s(t) = \exp(-A\check{t})$ with

$$A = \frac{1}{2}\check{\Gamma}_0 + 4 \int_0^\eta d\bar{k} \int_0^{\eta-\bar{k}} d\bar{k}' \frac{\bar{k}\bar{k}'(\bar{k} + \bar{k}')(\bar{n}_{\bar{k}'}^{\text{lin}} - \bar{n}_{\bar{k}'+\bar{k}}^{\text{lin}}) \frac{d}{d\bar{k}} \bar{n}_{\bar{k}}^{\text{lin}}}{\check{\Gamma}_{\bar{k}} + \check{\Gamma}_{\bar{k}'}} = \begin{cases} [1 - 4(4 \ln \frac{4}{3} - 1)]\eta \approx 0.4 \eta & \text{(classical field)} \\ 0.988618\dots & \text{(quantum field)} \end{cases} \quad (108)$$

If we leave the rescaled time \check{t} (42), which brings out the quantity Γ_u already introduced in (34) since $\check{t} = \bar{q}\Gamma_u t/2$, we find that this corresponds to a corrected damping rate tending towards zero linearly in \bar{q} :

$$\Gamma_q^{\text{corr } \infty} \underset{\bar{q} \rightarrow 0}{\sim} A\Gamma_u \bar{q} = A \frac{9k_B T \epsilon^2 (1 + \Lambda)^2}{4\pi \hbar (3\gamma)^{1/2} \rho \xi^2} \bar{q} \sim \begin{cases} \frac{A}{\eta} \Gamma_q^{\text{clas}} \approx 0.4 \Gamma_q^{\text{clas}} & \text{(classical field)} \\ \frac{A}{2\zeta(2)} \Gamma_q \approx 0.3 \Gamma_q & \text{(quantum field)} \end{cases} \quad (109)$$

shown as a dotted line in Figure 9 for the quantum field and in Figure 8a for the classical field. Here, Γ_q^{clas} and Γ_q are the damping rates of the golden rule for the classical field (34) and for the quantum field (23). This shows that the slope at the origin of the corrected rate is considerably smaller than that of the golden rule. Then, in the $\bar{q} \rightarrow +\infty$ limit, of course for the infinite cut-off quantum field, the integral in the right-hand side of (107) tends uniformly towards zero in the upper half-plane and the signal decay becomes purely exponential, with a rate equivalent to that of the golden rule:⁶¹

$$\Gamma_q^{\text{corr } \infty} \underset{\bar{q} \rightarrow +\infty}{\sim} \Gamma_q \underset{\bar{q} \rightarrow +\infty}{\sim} \frac{3k_B T \epsilon^2 (1 + \Lambda)^2}{16\pi (3\gamma)^{1/2} \rho \xi^2} \bar{q}^3 \quad (110)$$

Finally, in the limit of long times $\check{t} \rightarrow +\infty$ at fixed \bar{q} , the signal decay is not exponential but power-law up to a logarithm, taking the same form for the classical and quantum fields, as shown in Appendix E:

$$s_{\text{corr } \infty}^{(2,2)}(t) \underset{\check{t} \rightarrow +\infty}{\sim} \frac{\bar{q}^4 (d\bar{n}_q^{\text{lin}}/d\bar{q}) \ln(\check{t}^2)}{[\check{\Gamma}_0 \check{\Sigma}_{\text{corr } \infty}^{(2,2)}(\bar{q}, 0) \check{t}]^2} \quad (111)$$

For $\bar{q} = 1/4$, we find numerically from the self-energy (107) that the asymptotic behavior (111) is not reached before a reduced time $\Gamma_q t/2 = 100$, for both the quantum and classical fields, which goes far beyond our simulations in Fig. 8b and prevents us from testing it.

61. This result is also that of zero temperature, which explains why the right-hand side of (110) is in fact independent of temperature when we return to the non-scaled wave number q . As it results from the effective Hamiltonian of quantum hydrodynamics, it is then only valid at the leading order in $q\xi$, i.e. in the linear part of the acoustic branch.

6. Conclusion

In this work, we have considered the phonon gas of a two-dimensional superfluid described by quantum hydrodynamics, an effective low-energy theory, with cubic and quartic coupling between phonons for an acoustic branch $\varepsilon_{\mathbf{q}}$ which is a convex function of wavenumber q . Two important parameters characterize the system: the reduced temperature $\epsilon = k_B T / mc^2$ and the interaction strength $(\rho \xi^2)^{-1}$ between superfluid particles, where c is the speed of sound and ρ the density of the superfluid in the ground state, m the mass of a particle and $\xi = \hbar / mc$ the relaxation length. In this system, we have studied the damping of the phonon mode \mathbf{q} excited by a Bragg pulse in the linear response and collisionless regime, limiting ourselves to the leading order in ϵ as going beyond this would make no sense with our model Hamiltonian.

A first unexpected result is that in dimension two, taking the low-temperature limit, $\epsilon \rightarrow 0$ at fixed $(\rho \xi^2)^{-1}$, is not enough to bring the phonon gas into the weak-coupling regime. This defeats the pole approximation, Fermi's golden rule and the assumption of exponential decay. Indeed, as we show by a scaling-law reasoning, the self-energy $\Sigma(\mathbf{q}, z)$ has a typical value and a scale of variation in energy in the vicinity of $z = \varepsilon_{\mathbf{q}}$ both of order $k_B T \epsilon^2$, whereas it would be necessary to have a typical value much lower than the scale of variation to be able to apply the golden rule (as is the case in dimension three where the scale of variation remains $k_B T \epsilon^2$ but the typical value is lowered to $k_B T \epsilon^4$ due to a reduction of the density of final states at low energy). This first theoretical result is confirmed by classical field simulations.

A second unexpected result of the two-dimensional case is that, even in the weakly interacting limit $(\rho \xi^2)^{-1} \rightarrow 0$ in the superfluid, a perturbative calculation does not give access to the self-energy to the leading order in ϵ . Thus, the calculation of $\Sigma(\mathbf{q}, z)$ at second order in the cubic phonon coupling does not reproduce the damping of mode \mathbf{q} observed numerically, and the fourth-order calculation exhibits (after taking the $\epsilon \rightarrow 0$ limit at fixed $\bar{q} = \hbar c q / k_B T$ and $(\rho \xi^2)^{-1}$) an unphysical divergence in $z = \varepsilon_{\mathbf{q}}$ that renders it useless.

To break this deadlock, guided by physical intuition, we give a finite lifetime to the virtual phonons (those present only in the intermediate state of four-phonon collisional processes). This removes the divergence of the fourth-order contribution by transforming it into a formally second-order contribution, which corrects the second-order calculation. The regularized theory is found to be in good agreement with simulations in the weakly interacting regime. It makes it possible to take the $(\rho \xi^2)^{-1} \rightarrow 0$ limit in the expression of $\Sigma(\mathbf{q}, z)$ to the leading order in ϵ and to propose a phonon damping law replacing that of the golden rule. The new law is non-exponential, except in the $\bar{q} \rightarrow 0$ limit where it is characterized by the rate (109), linear in wavenumber like the golden rule but with a coefficient about three times smaller, and in the $\bar{q} \rightarrow +\infty$ limit where its rate (110) reproduces that of the golden rule.

Acknowledgements : Alan Serafin received funding from the European Horizon 2020 research and innovation project macQsimal number 820393. This article is part of a special issue dedicated to the CNRS Gold Medal awarded to Jean Dalibard in December 2021. The authors congratulate Jean on his award and thank him for his brilliant lectures at the Collège de France and for all the enriching discussions they had with him on cold atomic gases (Y.C. in particular recalls with emotion his teaching on Fermi's golden rule at the ENS "DEA de physique quantique" in 1987-1988).

Appendix A. Analytic continuation of $\check{\Sigma}_{\bar{q}}^{(2,2)}(\check{\zeta})$ to the lower half-plane and validity conditions of the golden rule

To analytically continue from the upper complex half-plane to the lower half-plane expression (43) of the self-energy $\check{\Sigma}_{\bar{q}}^{(2,2)}(\check{\zeta})$, we proceed in two steps: (i) we reduce (43) to a single integral, that of an analytic function of a well-chosen variable x over an interval of \mathbb{R} , and (ii) to extend this integral to $\text{Im } \check{\zeta} < 0$, we deform the integration path on x in the complex plane and rotate the branch cuts of the corresponding analytic function. In application, we give conditions for the validity of Fermi's golden rule, which are necessary but not sufficient.

Reduce to a single integral. In Landau's contribution to (43), i.e. in the second integral, we perform the change of variable $x = \bar{k}(\bar{k} + \bar{q})$ or $\bar{k} = (x + \bar{q}^2/4)^{1/2} - \bar{q}/2$, where $x \in \mathbb{R}^+$. In Beliaev's contribution, the integrand is invariant by changing \bar{k} to $\bar{q} - \bar{k}$, which allows us to restrict the integration on \bar{k} to the interval $[0, \bar{q}/2]$ at the cost of multiplying by a factor 2; we then perform the now injective change of variable $x = \bar{k}(\bar{k} - \bar{q})$ to $\bar{k} = \bar{q}/2 - (\bar{q}^2/4 + x)^{1/2}$, where $x \in [-\bar{q}^2/4, 0]$; we use the identity $\bar{n}_k^{\text{lin}} = -(1 + \bar{n}_{-\bar{k}}^{\text{lin}})$ to give the bosonic amplification factor the same structure of difference of occupation numbers as in Landau. In both cases, we arrive at the same integrand, except that Beliaev

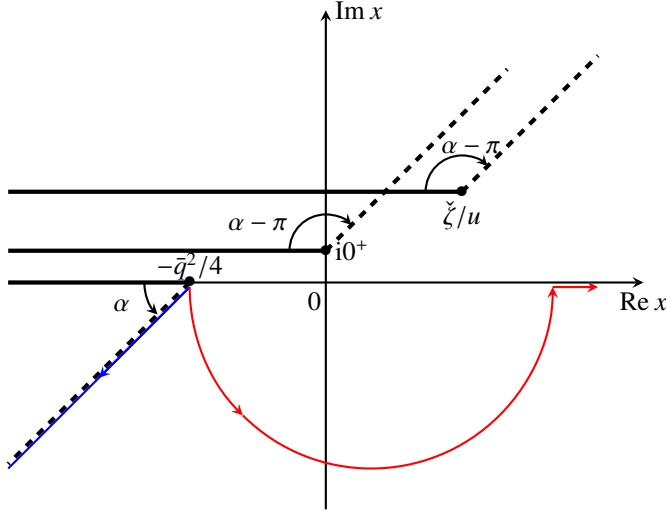


Figure 10: Graphical illustration of the method for analytically continuing $\Sigma_{\bar{q}}^{(2,2)}(\zeta)$ from the upper half-plane $\text{Im } \zeta > 0$ to the lower half-plane $\text{Im } \zeta < 0$ using integral form (112). Red curve: first deformation of the integration path on variable x in the complex plane. Black half-lines: singularity lines of the integrand of (112) considered as a function of x , in thick solid line for their original position, in thick dashed line after rotation by an angle α or $\alpha - \pi$ as shown ($\alpha = \pi/4$ on the figure). Black discs: branch points x_0 of the corresponding $(x - x_0)^{1/2}$ square root functions. Blue half-line: final integration path on x , leading to the result sought (45).

shows a global factor $(-x)^{1/2}/(\zeta/u - x)^{1/2}$ where Landau contains a factor $x^{1/2}/(x - \zeta/u)^{1/2}$; however, we can give them the common expression $(x - i0^+)^{1/2}/(x - \zeta/u)^{1/2}$ by means of the relations $(-x)^{1/2} = i(x - i0^+)^{1/2}\forall x < 0$, $x^{1/2} = (x - i0^+)^{1/2}\forall x > 0$, $(\zeta/u - x)^{1/2} = i(x - \zeta/u)^{1/2}\forall x \in \mathbb{R}$ knowing that $\text{Im}(\zeta/u) > 0$. We arrive at the single integral we're looking for:

$$\Sigma_{\bar{q}}^{(2,2)}(\zeta) = \frac{1}{2i\bar{q}} \int_{-\bar{q}^2/4}^{+\infty} dx \frac{x \sqrt{x - i0^+}}{\sqrt{x - \zeta/u} \sqrt{x + \bar{q}^2/4}} \left[\frac{1}{e^{\sqrt{x + \bar{q}^2/4 - \bar{q}^2/2}} - 1} - \frac{1}{e^{\sqrt{x + \bar{q}^2/4 + \bar{q}^2/2}} - 1} \right] \quad (112)$$

Extending it analytically. Integrand of (112) is an analytic function of x in the complex plane, except for the three singularity lines resulting from the branch cuts of the three square roots involved: $i0^+ + \mathbb{R}^-$ in the numerator, $\zeta/u + \mathbb{R}^-$ and $-\bar{q}^2/4 + \mathbb{R}^-$ in the denominator, shown in black in Figure 10.⁶² This allows the integration path to be deformed at will, provided it doesn't cross any singularity of the integrand, see the red line in Figure 10. You'd think this would be enough to make the integrand analytic in ζ/u in the region between the red line and the real axis; but it's not, because when ζ/u enters this region, the (horizontal) branch cut attached to it necessarily crosses the red line. So we have to do better, by also deforming the branch cuts of the integrand; the simplest way to do this is to introduce the new $z_\theta^{1/2} \equiv \exp(i\theta/2)[\exp(-i\theta)z]^{1/2}$ square-root determinations, parameterized by the angle $\theta \in]-\pi, \pi[$ by which the original branch cut was rotated (the \mathbb{R}^- half-line being sent to $\exp(i\theta)\mathbb{R}^-$). As long as the branch cuts, in their rotating motion, do not sweep the integration path in red, the integrand does not change on this path and the value of the integrand is preserved. We decide to rotate the $(x + \bar{q}^2/4)^{1/2}$ branch cut by an arbitrary angle $\alpha \in]0, \pi/2[$, and the other two by an angle $\alpha - \pi \in]-\pi, -\pi/2[$ so that they are parallel but in the opposite direction to the first one, see the dashed lines in Figure 10. Finally, we take as our final integration path the blue half-line in Figure 10, which follows the new branch cut of $(x + \bar{q}^2/4)^{1/2}$ ⁶³ from below and which we parameterize as follows, $x = \exp(i\alpha)(-v - i0^+) - \bar{q}^2/4$, $v \in \mathbb{R}^+$. Then

$$(x + \bar{q}^2/4)_\alpha^{1/2} = -ie^{i\alpha/2} \sqrt{v} ; (x - \zeta/u)_{\alpha-\pi}^{1/2} = -ie^{i\alpha/2} [v + e^{-i\alpha}(\bar{q}^2/4 + \zeta/u)]^{1/2} ; (x - i0^+)_{\alpha-\pi}^{1/2} = -ie^{i\alpha/2} (v + e^{-i\alpha} \bar{q}^2/4)^{1/2} \quad (113)$$

62. The integrand also has poles $x_n = 2in\pi(\bar{q} + 2in\pi)$, $n \in \mathbb{Z}^*$, coming from the Bose occupation numbers ($x = 0$ is not a pole because of the factor x in the numerator). Future continuous deformations of the integration path in (112), shown in red and then blue in Fig. 10, do not pass over any of these poles under the following conditions, which are assumed to be verified in the following (they ensure that the most dangerous pole $x_{n=-1}$ remains to the left of the blue half-line at an angle α): (i) $-\bar{q}^2/4 > \text{Re } x_{-1} = -(2\pi)^2$ i.e. $\bar{q} < 4\pi$, (ii) $\tan \alpha > 2\pi\bar{q}/[(2\pi)^2 - \bar{q}^2/4]$.

63. We could close the integration path with a circular arc of radius $R \rightarrow +\infty$, of contribution $\rightarrow 0$ since the integrand there is exponentially small in \sqrt{R} .

where all $i0^+$ could be omitted without difficulty in the right-hand sides. The complex number $\check{\zeta}/u$ can now be made to descend continuously into the lower half-plane, remaining constantly to the right or left of the blue half-line without the latter being crossed by the branch cut attached to $\check{\zeta}/u$: we have indeed continued $\check{\Sigma}_{\check{q}}^{(2,2)}(\check{\zeta})$ analytically to $\text{Im } \check{\zeta} < 0$. It remains to set $v = \bar{k}^2$, $\bar{k} \in \mathbb{R}^+$, to arrive at the announced result (45) with $\phi = \alpha - \pi \in] - \pi, -\pi/2[$.

Application. Now that we know from equation (112) that $\check{\Sigma}_{\check{q}}^{(2,2)}(\check{\zeta})$ has no branch point at $\check{\zeta} = 0$, we can calculate its value and derivative at $\check{\zeta} = i0^+$. For its value, the simplest way is to make $\check{\zeta}$ tend towards zero by positive imaginary parts under the integral sign in form (43); we integrate over \bar{k} after expanding the occupation numbers in integer series of variable $\exp(-\bar{k})$, which brings up Bose functions $g_\alpha(z)$ evaluated at $z = 1$ or at $z = \exp(-\bar{q})$ (in the latter case, they cancel out in the final result). For the derivative, the simplest way is to use the analytic continuation (45), whose integrand shows no singularity on the integration path for $\check{\zeta} = 0$; we can then differentiate with respect to $\check{\zeta}$ and take the limit $\check{\zeta} \rightarrow 0$ under the integral sign.⁶⁴ We finally obtain

$$\check{\Sigma}_{\check{q}}^{(2,2)}(\check{\zeta} = i0^+) = \frac{1}{i} \left(\frac{\bar{q}^2}{12} + 2\zeta(2) \right) \quad ; \quad \frac{d}{d\check{\zeta}} \check{\Sigma}_{\check{q}}^{(2,2)}(\check{\zeta} = i0^+) = \frac{1}{u\bar{q}} \left(\frac{\pi}{2} + \frac{i\bar{q}}{4} \right) \quad (114)$$

The value of the function is simply a rewriting of result (23) under the effect of the change of variables in (42,43). Its derivative is involved in a well-known validity condition of the golden rule [13], $|\text{Im}(d/d\check{\zeta})\Sigma_{\mathbf{q}}(\zeta = i0^+)| \ll 1$, which is written here as $1/(4u) \ll 1$ and imposes, unsurprisingly, $u \gg 1$. A more precise condition requires that the residue Z of the Green's function, which appears as a factor of the exponential $\exp(-\check{\zeta}\check{q}\check{t})$ in the exact expression (115) of the signal $s^{(2,2)}(t)$, be very close to the value one taken in the golden rule, which adds the constraint $|\text{Re}(d/d\check{\zeta})\Sigma_{\mathbf{q}}(\zeta = i0^+)| \ll 1$, here $\bar{q} \gg \pi/(2u)$. As shown in Figure 1d, in which $u \simeq 18.14$, these conditions are not sufficient. Sections 4.3 and 5 help to understand why (in essence, a singularity appears at $\zeta = i0^+$ in $\Sigma_{\mathbf{q}}^{(4)}(\zeta)$, the fourth-order contribution in H_3 , making the present second-order calculation irrelevant in the limit $\epsilon \rightarrow 0$).

Appendix B. First deviation of the signal from the golden-rule exponential for the theory at second order in H_3

Here we establish result (47) of section 3.2, valid in the weakly interacting limit $u \rightarrow +\infty$ at fixed \check{t} and $Q = u^{1/2}\bar{q}$ as in (46), by starting from the writing (44) of the signal. To this end, guided by Fig. 4b, we first apply the residue theorem to the contour formed by the union of the path C_+ , the portions of the circle at infinity and the contour around the branch cut $-Q^2/4 - e^{i(\phi+\pi)}\mathbb{R}^+$: the integral of $\exp(-i\check{\zeta}\check{t})\check{\mathcal{G}}_{\check{q}}^{(2,2)}(\check{\zeta})$ on this contour is $2i\pi$ times the residue in $\check{\zeta} = \check{\zeta}_{\check{q}}$, the pole of the Green's function analytically continued to the lower half-plane by means of (45). The signal (44) can therefore be written exactly as the sum of the contributions of the pole $\check{\zeta}_{\check{q}}$ and the contour:

$$s^{(2,2)}(t) = \frac{\exp(-i\check{\zeta}_{\check{q}}\check{t})}{1 - \frac{d}{d\check{\zeta}} \check{\Sigma}_{\check{q}\downarrow}^{(2,2)}(\check{\zeta}_{\check{q}})} + e^{iQ^2\check{t}/4} \int_0^{e^{i(\phi+\pi)}(+\infty)} \frac{dz}{2i\pi} \frac{(\check{\Sigma}_- - \check{\Sigma}_+) \exp(iz\check{t})}{(-Q^2/4 - z - \check{\Sigma}_-)(-Q^2/4 - z - \check{\Sigma}_+)} \quad (115)$$

where the complex variable z goes in a straight line from 0 to $\exp[i(\phi + \pi)](+\infty)$ and we note $\check{\Sigma}_{\pm} \equiv \check{\Sigma}_{\check{q}\downarrow}^{(2,2)}(-Q^2/4 - z + e^{i(\phi+\pi)}i0^{\pm})$ the values of the analytic continuation (45) of the self-energy immediately to the left (sign +) or right (sign -) of the branch cut. We then make use of the fundamental property⁶⁵

$$\check{\Sigma}_{\check{q}\downarrow}^{(2,2)}(\check{\zeta}) - \check{\Sigma}_{\check{q}\downarrow}^{(2,2)}(0) \stackrel{Q \text{ fixed}}{u \rightarrow +\infty} \frac{e^{i\phi/2}}{iu^{1/2}} \int_0^{+\infty} dK \left\{ \frac{(K^2 - e^{-i\phi}Q^2/4)^{1/2}}{[K^2 - e^{-i\phi}(\check{\zeta} + Q^2/4)]^{1/2}} - 1 \right\} + O(1/u) \quad (116)$$

64. If we stick to form (43), we can't take the derivative under the integral sign without making a non-absolutely convergent integral appear. We can proceed in a hybrid way after choosing an infinitesimal infrared cut κ over \bar{k} : in form (43), limited to $\bar{k} > \kappa$ in each contribution, we differentiate under the integral sign and then let $\check{\zeta}$ tend towards 0; in form (112), limited to $-\kappa\bar{q} < x < \kappa\bar{q}$, we keep the exact expression of the factor $(x - i0^+)^{1/2}/(x - \check{\zeta}/u)^{1/2}$ but expand the rest of the integrand in powers of x (zero order is in fact sufficient), and we analytically calculate the resulting integral for $\check{\zeta} = s + i0^+$, where s is a real number (if necessary in terms of hypergeometric functions) then we calculate its derivative with respect to s at $s = 0$. The final result is the same.

65. The leading term is obtained by writing the difference in the left-hand side of (116) as a single integral over \bar{k} by means of (45), multiplying by $u^{1/2}$, then making the change of variable $\bar{k} = K/u^{1/2}$ before taking the limit $u \rightarrow +\infty$ under the integral sign.

In the contribution of the contour to (115), at the leading order in $u^{-1/2}$, we can thus replace in the denominator $\check{\Sigma}_\pm$ by $\check{\Sigma}_{\bar{q}\downarrow}^{(2,2)}(0) \rightarrow -2i\zeta(2) = -i\pi^2/3$ according to (114), and in the numerator the difference $\check{\Sigma}_- - \check{\Sigma}_+$ by its asymptotic equivalent, which is written

$$\check{\Sigma}_- - \check{\Sigma}_+ \underset{u \rightarrow +\infty}{\overset{Q \text{ fixed}}{\sim}} \frac{e^{i\phi/2}}{iu^{1/2}} \int_0^{+\infty} dK (K^2 - e^{-i\phi} Q^2/4)^{1/2} \left[\frac{1}{(K^2 - x + i0^-)^{1/2}} - \frac{1}{(K^2 - x + i0^+)^{1/2}} \right] \quad (117)$$

knowing that $z = e^{i(\phi+\pi)}x$, $x > 0$. The integrand in (117) is non-zero only for $K < x^{1/2}$, which prompts us to put $K = x^{1/2} \sin \alpha$, $\alpha \in [0, \pi/2]$, especially as this makes the square roots in the denominator disappear: we find $S_{\text{contour}}(\check{\gamma})$ in (48). In the implicit equation defining the pole, rewritten by setting aside its zero-order approximation, $\check{\zeta}_{\bar{q}} - \check{\Sigma}_{\bar{q}\downarrow}^{(2,2)}(0) = \check{\Sigma}_{\bar{q}\downarrow}^{(2,2)}(\check{\zeta}_{\bar{q}}) - \check{\Sigma}_{\bar{q}\downarrow}^{(2,2)}(0)$, it suffices for the right-hand side to use (116) with $\check{\zeta} = -i\pi^2/3$; the convenient choice $\phi = (-\pi)^+$ (on which the result does not depend) yields $\delta\check{\zeta}_{\bar{q}}$ in (49). Finally, to obtain the first deviation from one of the residue, simply differentiate (116) with respect to $\check{\zeta}$ (under the integral sign in the right-hand side), replace $\check{\zeta}$ by $-i\pi^2/3$ and then take $\phi = (-\pi)^+$: one finds $\delta\check{Z}$ in (49).

Appendix C. Double Matsubara sums in the theory at fourth order in H_3

Here we explicitly calculate the Matsubara sums contributing to (53,62) in section 4.1 and show how to obtain their simplified forms (54,63) in the small-angle limit. The calculation relies on the generalization of relation (37) to any number J of factors in the summand, which is demonstrated as in footnote 25:

$$\sum_{n \in \mathbb{Z}} \frac{1}{\prod_{j=1}^J (2i\pi n - \bar{\varepsilon}_j)} = \sum_{j=1}^J \frac{-\bar{n}_{\varepsilon_j}}{\prod_{\substack{k=1 \\ k \neq j}}^J (\bar{\varepsilon}_j - \bar{\varepsilon}_k)} \quad \forall J \geq 2 \quad (118)$$

Internal-loop diagrams. Let's write the sum appearing in (53) after outputting a factor $(k_B T)^5$ in the denominator (we have set $\varepsilon_{\mathbf{k}_j} = k_B T \bar{\varepsilon}_j$) and expressing the Matsubara energies in terms of the independent variables $\omega = 2i\pi k_B T n$ and $\omega' = 2i\pi k_B T n'$ as in equations (51,52), for a complex energy z temporarily equal to $\Omega = k_B T \bar{\Omega} \in 2i\pi k_B T \mathbb{Z}$:

$$S_{B_i}(z) = (k_B T)^{-5} \sum_{n, n' \in \mathbb{Z}} \frac{1}{s_1(\bar{\Omega} - 2i\pi s_2 n) - \bar{\varepsilon}_1} \frac{1}{2i\pi n - \bar{\varepsilon}_2} \frac{1}{2i\pi n' - \bar{\varepsilon}_3} \frac{1}{2i\pi s_4(s_2 n - s_3 n') - \bar{\varepsilon}_4} \frac{1}{2i\pi s_2 s_5 n - \bar{\varepsilon}_5} \quad (119)$$

Using (37), let's calculate the sum over n' of the product of the two factors that depend on n' , then let's make variable $\bar{\Omega}$ disappear from the occupation numbers as in the first equality of (38). After the clever change of variable $n \rightarrow s_2 n$, which doesn't affect the summation domain since $s_2 = \pm 1$, we're left with

$$S_{B_i}(z) = (k_B T)^{-5} \sum_{n \in \mathbb{Z}} \frac{s_1 s_2 s_4 s_5 (\bar{n}_{\varepsilon_3} - \bar{n}_{-s_3 s_4 \varepsilon_4})}{[2i\pi n - (\bar{\Omega} - s_1 \bar{\varepsilon}_1)](2i\pi n - s_2 \bar{\varepsilon}_2)(2i\pi n - s_5 \bar{\varepsilon}_5)[2i\pi n - (s_3 \bar{\varepsilon}_3 + s_4 \bar{\varepsilon}_4)]} \quad (120)$$

We've taken out all the necessary factors to put the result into a simple form, as in the left-hand side of relation (118), which makes this relation easy to use:

$$S_{B_i}(z) = -(k_B T)^{-2} s_1 s_2 s_4 s_5 (\bar{n}_{\varepsilon_3} - \bar{n}_{-s_3 s_4 \varepsilon_4}) \left\{ \frac{1}{z - z_2} \left[\frac{\bar{n}_{-s_1 \varepsilon_1}}{(z - z_1)(z - z_3)} - \frac{\bar{n}_{s_3 \varepsilon_3 + s_4 \varepsilon_4}}{(z_2 - z_1)(z_2 - z_3)} \right] + \frac{1}{z_1 - z_3} \left[\frac{\bar{n}_{s_2 \varepsilon_2}}{(z_1 - z)(z_1 - z_2)} - \frac{\bar{n}_{s_5 \varepsilon_5}}{(z_3 - z)(z_3 - z_2)} \right] \right\} \quad (121)$$

At this point, we have analytically continued the result for variable z over $\mathbb{C} \setminus \mathbb{R}$ and introduced the energies of the three intermediate states (marked by the red vertical lines on the left-hand side of Figure 7) counted algebraically, $z_1 = s_1 \varepsilon_1 + s_2 \varepsilon_2$, $z_2 = s_1 \varepsilon_1 + s_3 \varepsilon_3 + s_4 \varepsilon_4$ and $z_3 = s_1 \varepsilon_1 + s_5 \varepsilon_5$. In the case of $s_2 = s_5$, we also have $\varepsilon_2 = \varepsilon_5$ and $z_1 = z_3$,

since \mathbf{k}_2 is then equal to \mathbf{k}_5 ; this reveals a division by zero in the second contribution of (121) between curly braces, which we therefore extend by continuity with L'Hospital's rule. After some skilful rearrangement, we arrive at:⁶⁶

$$S_{B_i}^{s_2=s_5}(z) = -(k_B T)^{-2} s_1 s_4 (\bar{n}_{\varepsilon_3} - \bar{n}_{-s_3 s_4 \varepsilon_4}) \left[\frac{\bar{n}_{-s_1 \varepsilon_1} - \bar{n}_{s_2 \varepsilon_2}}{(z - z_1)^2 (z - z_2)} + \frac{\bar{n}_{s_2 \varepsilon_2} - \bar{n}_{s_3 \varepsilon_3 + s_4 \varepsilon_4}}{(z_2 - z_1)^2 (z - z_2)} + \frac{\bar{n}_{s_2 \varepsilon_2} (1 + \bar{n}_{s_2 \varepsilon_2})}{k_B T (z_2 - z_1) (z_1 - z)} \right] \quad (122)$$

Note that the global factor $(k_B T)^{-2}$ in (121,122) simplifies with the factor $(-k_B T)^2$ in (53). Finally, consider the small-angle limit $\epsilon \rightarrow 0$ in (122), in which z , z_1 and z_2 are written as $\varepsilon_q + O(k_B T \epsilon^2)$. Between the square brackets, the second contribution is subleading because $s_3 \varepsilon_3 + s_4 \varepsilon_4 = s_2 \varepsilon_2 + z_2 - z_1 = s_2 \varepsilon_2 + O(k_B T \epsilon^2)$, so its numerator tends to zero; the third is also subleading because its denominator is of order $(k_B T)^3 \epsilon^4$ instead of $(k_B T)^3 \epsilon^6$ like the others. We find (54).

Bridge diagrams. We proceed as before, with the same notations. The double sum in (62) is written

$$S_{P_i}(z) = (k_B T)^{-5} \sum_{n, n' \in \mathbb{Z}} \frac{1}{2i\pi n - \bar{\varepsilon}_1} \frac{1}{s_2(\bar{\Omega} - 2i\pi s_1 n) - \bar{\varepsilon}_2} \frac{1}{2i\pi n' - \bar{\varepsilon}_3} \frac{1}{s_4(\bar{\Omega} - 2i\pi s_3 n') - \bar{\varepsilon}_4} \frac{1}{2i\pi s_5(s_1 n - s_3 n') - \bar{\varepsilon}_5} \quad (123)$$

Using relation (118) with $J = 3$, we calculate the sum over n' , perform a partial fraction decomposition of the result for variable $2i\pi n$ and then make the change of variable $n \rightarrow s_1 n$, so that

$$S_{P_i}(z) = \frac{(k_B T)^{-5} s_1 s_2 s_4 s_5}{\bar{\Omega} - s_3 \bar{\varepsilon}_3 - s_4 \bar{\varepsilon}_4} \sum_{n \in \mathbb{Z}} \frac{1}{(2i\pi n - s_1 \bar{\varepsilon}_1)[2i\pi n - (\bar{\Omega} - s_2 \bar{\varepsilon}_2)]} \left[\frac{\bar{n}_{\varepsilon_3} - \bar{n}_{-s_3 s_5 \varepsilon_5}}{2i\pi n - (s_3 \varepsilon_3 + s_5 \varepsilon_5)} + \frac{\bar{n}_{-s_3 s_5 \varepsilon_5} - \bar{n}_{-s_3 s_4 \varepsilon_4}}{2i\pi n - (\bar{\Omega} + s_5 \varepsilon_5 - s_4 \varepsilon_4)} \right] \quad (124)$$

We use (118) again and then analytically continue over z to $\mathbb{C} \setminus \mathbb{R}$; there are two terms between the square brackets in (124), so two contributions, type I and type II in that order:

$$S_{P_i^I}(z) = \frac{(k_B T)^{-2} s_1 s_2 s_4 s_5 (\bar{n}_{\varepsilon_3} - \bar{n}_{-s_3 s_5 \varepsilon_5})}{z_2 - z} \left[\frac{\bar{n}_{s_1 \varepsilon_1}}{(z_1 - z)(z_1 - z_4)} + \frac{\bar{n}_{-s_2 \varepsilon_2}}{(z - z_1)(z - z_4)} + \frac{\bar{n}_{s_3 \varepsilon_3 + s_5 \varepsilon_5}}{(z_4 - z_1)(z_4 - z)} \right] \quad (125)$$

$$S_{P_i^{II}}(z) = \frac{(k_B T)^{-2} s_1 s_2 s_4 s_5 (\bar{n}_{-s_3 s_5 \varepsilon_5} - \bar{n}_{-s_3 s_4 \varepsilon_4})}{z_2 - z} \left[\frac{\bar{n}_{s_1 \varepsilon_1}}{(z_1 - z)(z_3 - z)} + \frac{\bar{n}_{-s_2 \varepsilon_2}}{(z - z_1)(z_3 - z_1)} + \frac{\bar{n}_{s_5 \varepsilon_5 - s_4 \varepsilon_4}}{(z - z_3)(z_1 - z_3)} \right] \quad (126)$$

with the algebraic energies of the intermediate states marked by the red lines on the right-hand side of Figure 7, $z_1 = s_1 \varepsilon_1 + s_2 \varepsilon_2$ and $z_2 = s_3 \varepsilon_3 + s_4 \varepsilon_4$ common to both types, $z_4 = s_2 \varepsilon_2 + s_3 \varepsilon_3 + s_5 \varepsilon_5$ for type I and finally $z_3 = s_1 \varepsilon_1 + s_4 \varepsilon_4 - s_5 \varepsilon_5$ for type II. These variables are not independent since $z_1 + z_2 = z_3 + z_4$. It remains to take the limit of small angles $\epsilon \rightarrow 0$, in which $z = \varepsilon_q + O(k_B T \epsilon^2)$ and $z_j = \varepsilon_q + O(k_B T \epsilon^2)$, $1 \leq j \leq 4$. Then $s_3 \varepsilon_3 + s_5 \varepsilon_5 = s_1 \varepsilon_1 + O(k_B T \epsilon^2)$ and we can, at leading order, replace $\bar{n}_{s_3 \varepsilon_3 + s_5 \varepsilon_5}$ by $\bar{n}_{s_1 \varepsilon_1}$ in (125); grouping by occupation number and simplifying, we find the first contribution to the right-hand side of (63). Similarly, we replace $\bar{n}_{s_5 \varepsilon_5 - s_4 \varepsilon_4}$ by $\bar{n}_{-s_2 \varepsilon_2}$ at leading order in (126), which reproduces the second contribution to (63).

Appendix D. A linear divergence of $\tilde{\Sigma}_{\bar{q}}^{(4,2)}(\tilde{\zeta})$ away from the origin

As we show in this appendix, the $\tilde{\Sigma}_{\bar{q}}^{(4,2)}(\tilde{\zeta})$ component of the self-energy at fourth-order in H_3 and second-order in ϵ , obtained by summing all the contributions (57), (65), (67) of the fourth-order diagrams in section 4.1, diverges linearly when $\tilde{\zeta} \rightarrow \tilde{\zeta}_0 \equiv -3\gamma\bar{q}^3/32$ (here by positive imaginary parts):

$$\tilde{\Sigma}_{\bar{q}}^{(4,2)}(\tilde{\zeta}) \underset{\tilde{\zeta} \rightarrow \tilde{\zeta}_0}{\text{Im } \tilde{\zeta} > 0} \frac{\bar{q}^3 (\bar{n}_{\bar{q}/2}^{\text{lin}} + 1/2)}{24i\pi^2 \gamma (\tilde{\zeta} - \tilde{\zeta}_0)} \left(\frac{9(1 + \Lambda)^2}{8\rho\xi^2} \right)^2 \left[\int_0^{\bar{q}/2} d\bar{k}' \bar{k}' (\bar{k}' - \bar{q}/2) (\bar{n}_{\bar{k}'}^{\text{lin}} - \bar{n}_{\bar{k}' - \bar{q}/2}^{\text{lin}}) + 2 \int_{\bar{q}/2}^{\eta} d\bar{k}' \bar{k}' (\bar{k}' - \bar{q}/2) (\bar{n}_{\bar{k}'}^{\text{lin}} - \bar{n}_{\bar{k}' - \bar{q}/2}^{\text{lin}}) \right] \quad (127)$$

This results from two phenomena. (i) At a fixed reduced wavenumber \bar{k} , the angular integral (58) in inner-loop diagrams diverges at $\tilde{\zeta} = A_1^B$ with exponent 3/2 because, for this value of $\tilde{\zeta}$, the denominator of the integrand has $\tilde{\theta} = 0$

66. In particular, we use the identity $(z_1 - z_2)^{-2}(z - z_2)^{-1} + (z_1 - z_2)^{-2}(z_1 - z)^{-1} + (z_1 - z)^{-2}(z_1 - z_2)^{-1} = (z - z_1)^{-2}(z - z_2)^{-1}$.

as quadruple root. To see this quantitatively, we can use the identity $\int_{\mathbb{R}} d\tilde{\theta}/(z-\tilde{\theta}^2)^2 = -i\pi \operatorname{sign}(\operatorname{Im} z)/(2z^{3/2})$, $\forall z \in \mathbb{C} \setminus \mathbb{R}$, with $z = (\tilde{\zeta} - A_1^B)/B_1^B$. (ii) This $(\tilde{\zeta} - A_1^B)^{-3/2}$ divergence occurs at a position A_1^B depending on \bar{k} , as shown in equation (59), so it is generally washed out by integration over \bar{k} at fixed $\tilde{\zeta}$ in (57), unless $\tilde{\zeta}$ coincides with a parabolic extremum of $A_1^B(\bar{k})$ on the integration domain \mathcal{D}_1^B . To see this, let's choose an arbitrary reduced wavenumber \bar{k}_0 in \mathcal{D}_1^B , let's set $\tilde{\zeta} = w + A_1^B(\bar{k}_0)$ and take the limit $w \rightarrow 0$ by positive imaginary parts in (57): the result can only diverge if the value of the integral

$$\sigma_{\bar{k}_0}(w) = \int_{\bar{k}_0-\varepsilon}^{\bar{k}_0+\varepsilon} \frac{d\bar{k}}{[w + A_1^B(\bar{k}_0) - A_1^B(\bar{k})]^{3/2}} \quad (128)$$

diverges in this limit, where $\varepsilon > 0$ is fixed. Since we can take ε to be as small as we like without changing the conclusion, we can replace $A_1^B(\bar{k}) - A_1^B(\bar{k}_0)$ in (128) by its Taylor expansion in \bar{k}_0 to the non-zero leading order. If $(dA_1^B/d\bar{k})(\bar{k} = \bar{k}_0) \neq 0$, an expansion to order one is sufficient, and there is no divergence because $\int_{\mathbb{R}} d\kappa/(w - \kappa)^{3/2} = 0$.⁶⁷ Otherwise, expansion to second order is required, and there is linear divergence $[\tilde{\zeta} - A_1^B(\bar{k}_0)]^{-1}$ as predicted by (127) because

$$\int_{\mathbb{R}} \frac{d\kappa}{(w - \kappa^2)^{3/2}} = \frac{2}{iw} \quad \text{and} \quad \int_{\mathbb{R}} \frac{d\kappa}{(w + \kappa^2)^{3/2}} = \frac{2}{w} \quad \forall w \in \mathbb{C}, \operatorname{Im} w > 0 \quad (129)$$

Let's go into more detail on the example of diagram B_1 in Figure 6, in which the signs s_i of the internal line orientations are all 1, the integration domain on \bar{k} is $\mathcal{D}_1^B = [0, \bar{q}]$ and that on \bar{k}' at fixed \bar{k} is $\mathcal{D}_2^B(\bar{k}) = [0, \bar{k}]$. Note that $A_1^B(\bar{k})$ reaches its minimum at $\bar{k}_0 = \bar{q}/2$, in the interior of \mathcal{D}_1^B and therefore with zero derivative, and that this minimum is precisely $\tilde{\zeta}_0 = -3\gamma\bar{q}^3/32$, as in (127). To obtain an equivalent of $\tilde{\Sigma}_{B_1}^{(4,2)}(\bar{q}, \tilde{\zeta})$ when $\tilde{\zeta} \rightarrow \tilde{\zeta}_0$, we can treat $\tilde{\theta}^2$, $(\bar{k} - \bar{q}/2)^2$ and $w = \tilde{\zeta} - \tilde{\zeta}_0$ as infinitesimals of the same order. So, in the angular integral (58), we can replace $\tilde{\zeta}$ by $\tilde{\zeta}_0 + i0^+$ and $\tilde{\theta}^2$ by 0 in the second factor in the denominator, and everywhere replace \bar{k} by $\bar{k}_0 = \bar{q}/2$ except in coefficient $A_1^B(\bar{k})$, which is written as $A_1^B(\bar{k}) = \tilde{\zeta}_0 + (3\gamma\bar{q}/8)(\bar{k} - \bar{q}/2)^2$. After calculating the integral over ϕ and then over $\tilde{\theta}$ using the residue theorem, it remains

$$I(\bar{k}, \bar{k}') \sim \frac{-8\pi^2}{(6\gamma\bar{q}^3)^{1/2}\bar{k}'} \frac{1}{[w - (3\gamma/8)\bar{q}(\bar{k} - \bar{q}/2)^2]^{3/2}} \quad (130)$$

which can be inserted in the integrand of (57), replacing \bar{k} by $\bar{k}_0 = \bar{q}/2$ in all other factors and in the upper bound of integration over \bar{k}' . We then change the order of integration. In the now internal integral over \bar{k} at fixed \bar{k}' , it only remains

$$\int_0^{\bar{q}} \frac{d\bar{k}}{[w - (3\gamma/8)\bar{q}(\bar{k} - \bar{q}/2)^2]^{3/2}} \sim \left(\frac{8}{3\gamma\bar{q}}\right)^{1/2} \int_{-\infty}^{+\infty} \frac{d\kappa}{(w - \kappa^2)^{3/2}} = \left(\frac{8}{3\gamma\bar{q}}\right)^{1/2} \frac{2}{iw} \quad (131)$$

where we have made the change of variable $\bar{k} = \bar{q}/2 + [8/(3\gamma\bar{q})]^{1/2}\kappa$, extended the integration bounds over κ to $\pm\infty$ without changing the leading behavior and used equation (129). We finally obtain the divergent part of diagram B_1 :

$$\tilde{\Sigma}_{B_1}^{(4,2)}(\bar{q}, \tilde{\zeta}) \underset{\tilde{\zeta} \rightarrow \tilde{\zeta}_0}{\operatorname{Im} \tilde{\zeta} > 0} \frac{\bar{q}^3(\bar{n}_{\bar{q}/2}^{\operatorname{lin}} + 1/2)}{24i\pi^2\gamma(\tilde{\zeta} - \tilde{\zeta}_0)} \left(\frac{9(1 + \Lambda)^2}{8\rho\xi^2}\right)^2 \int_0^{\bar{q}/2} d\bar{k}' \bar{k}' (\bar{k}' - \bar{q}/2)(\bar{n}_{\bar{k}'}^{\operatorname{lin}} - \bar{n}_{\bar{k}' - \bar{q}/2}^{\operatorname{lin}}) \quad (132)$$

Diagram B_2 is treated in the same way and gives a similar divergent contribution (with a two times larger prefactor and the integral over \bar{k}' from $\bar{q}/2$ to η). Diagrams B_3 and B_4 are subleading in ε because $s_5 \neq s_2$ and must be omitted here. Diagrams B_5 and B_6 lead to a strictly increasing coefficient $A_1^B(\bar{k}) = (3\gamma/8)\bar{q}\bar{k}(\bar{k} + \bar{q})$ on the integration interval $\bar{k} \in [0, \eta - \bar{q}]$ and therefore cannot contribute to the linear divergence (127). Diagrams B_7 and B_8 have the same problem, with $A_1^B(\bar{k}) = (3\gamma/8)\bar{q}\bar{k}(\bar{k} - \bar{q})$ and $\mathcal{D}_1^B = [\bar{q}, \eta] > \bar{q}/2$. It remains to combine the contributions of B_1 and B_2 to obtain (127), whose expression between square brackets in the quantum field case tends towards $-\bar{q}(16\pi^2 + \bar{q}^2)/48$ when $\eta \rightarrow +\infty$.

Finally, let's explain why bridge diagrams do not contribute to the linear divergence (127) on the example of diagram P_1 (all $s_i = 1$, $\mathcal{D}_1^P = [0, \bar{q}]$ and $\mathcal{D}_2^P(\bar{k}) = [0, \bar{k}]$, type II). As noted in section 4.3, the angular integral (68) diverges linearly at some $\tilde{\zeta} = X_0(\bar{k}, \bar{k}')$ if the cancellation loci of the three factors in the denominator of (68) intersect at

67. If \bar{k}_0 lies on the edge of \mathcal{D}_1^B , the neighborhood of \bar{k}_0 reduces to $[\bar{k}_0, \bar{k}_0 + \varepsilon]$ or $[\bar{k}_0 - \varepsilon, \bar{k}_0]$ and there is square-root divergence because $\int_0^{+\infty} d\kappa/(w - \kappa)^{3/2} = -2/w^{1/2}$. This divergence is subleading and ignored here.

the same point in the $(\tilde{\theta}, \tilde{\theta}')$ plane. The triple intersection condition in the general case $X_0 \neq 0$ is obtained by replacing all coefficients A_i^P by $A_i^P - X_0$ in (87); the resulting second-degree equation on X_0 has the obvious zero solution, to which section 4.3 was implicitly restricted, and a second real root, $X_0(\bar{k}, \bar{k}') = -3\gamma\bar{k}(\bar{k} - \bar{q})\bar{k}'(\bar{k}' - \bar{q})/(2\bar{q})$; the latter leads to a triple intersection in the plane $(\tilde{\theta}, \tilde{\theta}')$, at points with coordinates $\pm[\sqrt{3\gamma}/(2\bar{q})][(\bar{q} - \bar{k})(\bar{q} - 2\bar{k}'), -(\bar{q} - 2\bar{k})(\bar{q} - \bar{k}')$, if we add constraints $\bar{k} > \bar{q}/2$ and $\bar{k}' < \bar{q}/2$ to have the right signs in the coefficients of the small deviations (τ, τ') at these points (otherwise, as in (88), there is no divergence). Then, proceeding as in (88), we obtain the divergent part of the angular integral (for $\tilde{\zeta} \rightarrow X_0$ by positive imaginary parts),

$$K_{\text{div}}(\bar{k}, \bar{k}') = \frac{-32\pi^2}{3\gamma\bar{q}\bar{k}\bar{k}'(\bar{k} - \bar{k}')[\tilde{\zeta} - X_0(\bar{k}, \bar{k}')]}$$
 (133)

to be integrated on $(\bar{k}, \bar{k}') \in [\bar{q}/2, \bar{q}] \times [0, \bar{q}/2]$ after multiplication by the same function of (\bar{k}, \bar{k}') as in (67). Now $X_0(\bar{k}, \bar{k}')$ has a parabolic minimum, located at $(\bar{k}, \bar{k}') = (\bar{q}/2, \bar{q}/2)$ and precisely equal to $\tilde{\zeta}_0$! The singularity (133) will therefore survive the wave number integration if $\tilde{\zeta} \rightarrow \tilde{\zeta}_0$ as in (127). Let's then perform the change of variables $(\bar{k} = \kappa + \bar{q}/2, \bar{k}' = -\kappa' + \bar{q}/2)$ and treat $w = \tilde{\zeta} - \tilde{\zeta}_0$, κ^2 and κ'^2 as infinitesimals of the same order. By writing the function multiplying $[\tilde{\zeta} - X_0(\bar{k}, \bar{k}')]^{-1}$ to the leading order in κ and κ' and replacing the pole $X_0(\bar{k}, \bar{k}')$ by its quadratic approximation in κ and κ' near the minimum, we obtain the equivalent

$$\tilde{\Sigma}_{P_1^{\text{th}}}^{(4,2)}(\bar{q}, \tilde{\zeta}) \underset{w \rightarrow 0}{\overset{\text{Im } w > 0}{\sim}} (\bar{q}/2)^4 \left(\frac{9(1 + \Lambda)^2}{8\rho\xi^2} \right)^2 (2\bar{n}_{\bar{q}/2}^{\text{lin}} + 1) \frac{(-32\pi^2)}{3\gamma(2\pi)^4} \int_0^{\bar{q}/2} d\kappa \int_0^{\bar{q}/2} d\kappa' \frac{1}{\kappa + \kappa'} \frac{1}{w - (3\gamma\bar{q}/8)(\kappa^2 + \kappa'^2)}$$
 (134)

We can extend the integration bounds $\bar{q}/2$ to $+\infty$ without losing equivalence. The double integral is then easily calculated in polar coordinates (K, α) , where $K = (\kappa^2 + \kappa'^2)^{1/2}$ spans \mathbb{R}^+ and α spans $[0, \pi/2]$. We finally find a square-root divergence, $\propto (\tilde{\zeta} - \tilde{\zeta}_0)^{-1/2}$, subleading in (127).

Appendix E. The long-time behavior of the signal in the $(\rho\xi^2)^{-1} \rightarrow 0$ limit of non-perturbative theories

Here we obtain the asymptotic behavior (111) of the signal associated with the self-energy $\check{\Sigma}_{\text{corr}\infty}^{(2,2)}(\bar{q}, \check{\zeta})$ of equation (107). To this end, we apply the technique of Appendix B by folding back the integration path C_+ in (6) onto the branch cut of $\check{\Sigma}_{\text{corr}\infty}^{(2,2)}(\bar{q}, \check{\zeta})$ located on $i\mathbb{R}^-$ and described parametrically by $\zeta = -i\check{y}$, $\check{y} \geq 0$ (this branch cut is the set of values of $\check{\zeta}$ cancelling the denominator of the integrand in (107)). Transposing equation (115) to the present case, we obtain

$$s_{\text{corr}\infty}^{(2,2)}(t) \underset{\check{y} \rightarrow +\infty}{\sim} \int_0^{+\infty} \frac{d\check{y}}{2\pi} \frac{\delta\sigma_{\bar{q}}(\check{y}) \exp(-\check{y}\check{t})}{\left[\check{\Sigma}_{\text{corr}\infty}^{(2,2)}(\bar{q}, 0) \right]^2} \quad \text{where} \quad \delta\sigma_{\bar{q}}(\check{y}) = \check{\Sigma}_{\text{corr}\infty}^{(2,2)}(\bar{q}, 0^+ - i\check{y}) - \check{\Sigma}_{\text{corr}\infty}^{(2,2)}(\bar{q}, 0^- - i\check{y})$$
 (135)

is the discontinuity of the self-energy across its branch cut at distance \check{y} from the origin. The identity in the sense of distributions $1/(\check{y} + i0^+) = \text{v.p.}(1/\check{y}) - i\pi\delta(\check{y})$ leads to

$$\delta\sigma_{\bar{q}}(\check{y}) = -\frac{4\pi}{\bar{q}^2} \int_{\bar{q}}^{\eta} d\bar{k} \int_0^{\eta - \bar{k}} d\bar{k}' \bar{k}\bar{k}'(\bar{k} - \bar{q})(\bar{k}' + \bar{q})(\bar{n}_{\bar{k}'+\bar{q}}^{\text{lin}} - \bar{n}_{\bar{k}'+\bar{k}}^{\text{lin}})(\bar{n}_{\bar{k}-\bar{q}}^{\text{lin}} - \bar{n}_{\bar{k}}^{\text{lin}}) \delta\left(\check{y} - \bar{k}'(\bar{k} - \bar{q}) \frac{\check{\Gamma}_{\bar{k}-\bar{q}} + \check{\Gamma}_{\bar{k}'}}{2\bar{q}(\bar{k} + \bar{k}')}\right)$$
 (136)

In the $\check{t} \rightarrow +\infty$ limit, the exponential function in (135) restricts the integral to arbitrarily small values of \check{y} and it suffices to know the leading behavior of $\delta\sigma_{\bar{q}}(\check{y})$ when $\check{y} \rightarrow 0^+$. Since the reduced rates $\check{\Gamma}_{\bar{k}}$ cannot tend to zero, the argument of the Dirac distribution in (136) can be zero in the limit $\check{y} \rightarrow 0$ only if \bar{k}' or $\bar{k} - \bar{q}$ is infinitesimal. For an arbitrary choice of a bound ε that is not infinitesimal but $\ll 1$, we can then restrict the integration domain on \bar{k} and \bar{k}' to the two parts, (i) $\bar{k} \in [\bar{q}, \bar{q} + \varepsilon]$, $\bar{k}' \in [0, \eta - \bar{k}]$ and (ii) $\bar{k} \in [\bar{q} + \varepsilon, \eta - \varepsilon]$, $\bar{k}' \in [0, \varepsilon]$.⁶⁸ In part (i) of the integration domain, we have $\bar{k} - \bar{q} \leq \varepsilon \ll 1$ so we can replace the various quantities depending on \bar{k} in (136) by their Taylor expansion at $\bar{k} = \bar{q}$ to leading order, e.g. $(\bar{k} - \bar{q})(\bar{n}_{\bar{k}-\bar{q}}^{\text{lin}} - \bar{n}_{\bar{k}}^{\text{lin}}) \simeq 1$, $\bar{n}_{\bar{k}'+\bar{q}}^{\text{lin}} - \bar{n}_{\bar{k}'+\bar{k}}^{\text{lin}} \simeq (\bar{k} - \bar{q})(-d/d\bar{k}')\bar{n}_{\bar{k}'+\bar{q}}^{\text{lin}}$ or $\check{\Gamma}_{\bar{k}-\bar{q}} \simeq \check{\Gamma}_0$ and

68. We note in part (ii) that, if $\bar{k} \leq \eta - \varepsilon$, we have $\varepsilon \leq \eta - \bar{k}$ so \bar{k}' , which must remain $\leq \eta - \bar{k}$, can indeed go as far as ε . We also check that “missing bit” $\bar{k} \in [\eta - \varepsilon, \eta]$, $\bar{k}' \in [0, \varepsilon]$ gives a negligible contribution $O(\check{y}\varepsilon)$ to $\delta\sigma_{\bar{q}}(\check{y})$.

the upper integration bound on \bar{k}' can be replaced by $\eta - \bar{q}$. The argument of the Dirac distribution in (136) becomes an affine function of $\bar{k} - \bar{q}$, making it easy to integrate over \bar{k} :

$$\delta\sigma_{\bar{q}}^{(i)}(\check{y}) \simeq -16\pi\bar{q}\check{y} \int_0^{\eta-\bar{q}} d\bar{k}' \frac{(\bar{k}' + \bar{q})^3}{(\check{\Gamma}_0 + \check{\Gamma}_{\bar{k}'})^2} \left(-\frac{d}{d\bar{k}'} \bar{n}_{\bar{k}'+q}^{\text{lin}} \right) Y \left(\varepsilon - \frac{2(\bar{k}' + \bar{q})\bar{q}\check{y}}{\bar{k}'(\check{\Gamma}_0 + \check{\Gamma}_{\bar{k}'})} \right) \simeq -16\pi\bar{q}\check{y} \int_{\bar{q}^2\check{y}/\varepsilon\check{\Gamma}_0}^{\eta-\bar{q}} \frac{d\bar{k}'}{\bar{k}'} \frac{(\bar{k}' + \bar{q})^3}{(\check{\Gamma}_0 + \check{\Gamma}_{\bar{k}'})^2} \left(-\frac{d}{d\bar{k}'} \bar{n}_{\bar{k}'+q}^{\text{lin}} \right) \quad (137)$$

The form of the second integral in (137) is based on the following reasoning: if $\check{y} \rightarrow 0$ at fixed ε , the argument of the Heaviside function Y in the first integral is positive, unless $\bar{k}' \rightarrow 0$; at the edge of the support of this function Y , we therefore have $\bar{k}' \ll 1$, which allows us to replace in its argument the second term by its leading-order approximation in \bar{k}' ; this brings up $Y(\varepsilon - \bar{q}^2\check{y}/\bar{k}'\check{\Gamma}_0)$, hence the lower bound announced in the integration over \bar{k}' . In part (ii) of the integration domain, we proceed in the same way: since $\bar{k}' \leq \varepsilon \ll 1$, we replace the various quantities in (136) by their leading order in \bar{k}' . As the argument of the Dirac distribution becomes an affine function of \bar{k}' , we integrate over this variable; the resulting function $Y(\varepsilon - \frac{2\bar{q}\bar{k}\check{y}}{(\bar{k}-\bar{q})(\check{\Gamma}_{\bar{k}-\bar{q}} + \check{\Gamma}_0)})$ is inoperative when $\check{y} \rightarrow 0$ because $\bar{k} - \bar{q}$ is here $\geq \varepsilon$, hence

$$\delta\sigma_{\bar{q}}^{(ii)}(\check{y}) \simeq -16\pi\bar{q}\check{y} \int_{\bar{q}+\varepsilon}^{\eta-\varepsilon} \frac{d\bar{k}}{\bar{k} - \bar{q}} \frac{\bar{k}^3}{(\check{\Gamma}_{\bar{k}-\bar{q}} + \check{\Gamma}_0)^2} (\bar{n}_q^{\text{lin}} - \bar{n}_k^{\text{lin}})(\bar{n}_{k-q}^{\text{lin}} - \bar{n}_k^{\text{lin}}) \quad (138)$$

It remains to take the limit $\varepsilon \rightarrow 0$ in results (137,138). To do this, we separate each integrand into its infrared divergent part $\propto 1/\bar{k}'$ or $\propto 1/(\bar{k} - \bar{q})$ and its regular part.⁶⁹ In the integral of the regular parts, we can make ε tend to zero within the integration bounds without damage. In the integral of divergent parts, doing the same gives rise to dangerous contributions $\pm \ln \varepsilon$, but which exactly cancel out in the sum of parts (i) and (ii). Finally,

$$\delta\sigma_{\bar{q}}(\check{y}) \underset{\check{y} \rightarrow 0^+}{=} \frac{4\pi\bar{q}^4}{\check{\Gamma}_0^2} \left(-\frac{d}{d\bar{q}} \bar{n}_q^{\text{lin}} \right) \check{y} \ln \check{y} + C_{\bar{q}}\check{y} + O(\check{y}^2 \ln \check{y}) \quad (139)$$

For the sake of brevity, we do not give the expression of the coefficient $C_{\bar{q}}$ of the linear part in (139), to which our method nevertheless gives access. The form of $O(\dots)$ in (139), on the other hand, has been obtained numerically. Insertion of the leading term $\propto \check{y} \ln \check{y}$ in (135) leads to the announced result (111).

References

- [1] L. Landau, I. Khalatnikov, “Teoriya vyazkosti Geliya-II”, Zh. Eksp. Teor. Fiz. **19**, 637 (1949).
- [2] D.T. Son, M. Wingate, “General coordinate invariance and conformal invariance in nonrelativistic physics: Unitary Fermi gas”, Ann. Physics **321**, 197 (2006).
- [3] S. Van Loon, C.A.R. Sá de Melo, “Effects of quantum fluctuations on the low-energy collective modes of two-dimensional superfluid Fermi gases from the BCS to the Bose Limit”, Phys. Rev. Lett. **131**, 113001 (2023).
- [4] I. Khalatnikov, *An Introduction to the Theory of Superfluidity* (CRC Press-Taylor & Francis, Boca Raton, 2018).
- [5] H. Kurkjian, Y. Castin, A. Sinatra, “Three-phonon and four-phonon interaction processes in a pair-condensed Fermi gas”, Annalen der Physik **529**, 1600352 (2017).
- [6] H.J. Maris, *Phonon-phonon interactions in liquid helium*, Rev. Mod. Phys. **49**, 341 (1977).
- [7] A.L. Fetter, J.D. Walecka, *Quantum Theory of Many-Particle Systems* (Dover, Mineola, 2003).
- [8] D.R. Meacher, D. Boiron, H. Metcalf, C. Salomon, G. Grynberg, “Method for velocimetry of cold atoms”, Phys. Rev. A **50**, R1992(R) (1994).
- [9] J. Stenger, S. Inouye, A.P. Chikkatur, D.M. Stamper-Kurn, D.E. Pritchard, W. Ketterle, “Bragg spectroscopy of a Bose-Einstein condensate”, Phys. Rev. Lett. **82**, 4569 (1999).
- [10] J. Steinhauer, R. Ozeri, N. Katz, N. Davidson, “Excitation spectrum of a Bose-Einstein condensate”, Phys. Rev. Lett. **88**, 120407 (2002).
- [11] G. Veeravalli, E. Kuhnle, P. Dyke, C.J. Vale, “Bragg spectroscopy of a strongly interacting Fermi gas”, Phys. Rev. Lett. **101**, 250403 (2008).
- [12] A. Sinatra, C. Lobo, Y. Castin, “The truncated Wigner method for Bose condensed gases: limits of validity and applications”, J. Phys. B **35**, 3599 (2002).
- [13] C. Cohen-Tannoudji, J. Dupont-Roc, G. Grynberg, *Processus d’interaction entre photons et atomes* (EDP Sciences/CNRS Éditions, Paris, 1988).
- [14] M.A. Escobedo, C. Manuel, “Effective field theory and dispersion law of the phonons of a nonrelativistic superfluid”, Phys. Rev. A **82**, 023614 (2010).
- [15] A. Andreev, I.M. Khalatnikov, “Sound in Liquid Helium II Near Absolute Zero”, Zh. Eksp. Teor. Fiz. **44**, 2058 (1963) [Sov. Phys. JETP **17**, 1384 (1963)].

69. To calculate the coefficient of the divergent part $1/(\bar{k} - \bar{q})$, we use the fact that $\lim_{\bar{k} \rightarrow \bar{q}} (\bar{n}_q^{\text{lin}} - \bar{n}_k^{\text{lin}})(\bar{n}_{k-q}^{\text{lin}} - \bar{n}_k^{\text{lin}}) = (-d/d\bar{q})\bar{n}_q^{\text{lin}}$.

- [16] Ming-Chiang Chung, A.B. Bhattacharjee, “Damping in 2D and 3D dilute Bose gases”, *New J. Phys.* **11**, 123012 (2009).
- [17] M. Bohlen, L. Sobirey, N. Luick, H. Biss, T. Enss, Th. Lompe, H. Moritz, “Sound Propagation and Quantum-Limited Damping in a Two-Dimensional Fermi Gas”, *Phys. Rev. Lett.* **124**, 240403 (2020).
- [18] P. Christodoulou, M. Galka, N. Dogra, R. Lopes, J. Schmitt, Z. Hadzibabic, “Observation of first and second sound in a BKT superfluid”, *Nature* **594**, 191 (2021).
- [19] J.L. Ville, R. Saint-Jalm, É. Le Cerf, M. Aidelsburger, S. Nascimbène, J. Dalibard, J. Beugnon, “Sound Propagation in a Uniform Superfluid Two-Dimensional Bose Gas”, *Phys. Rev. Lett.* **121**, 145301 (2018).
- [20] A. Cappellaro, F. Toigo, L. Salasnich, “Collisionless dynamics in two-dimensional bosonic gases”, *Phys. Rev. A* **98**, 043605 (2018).
- [21] Miki Ota, F. Larcher, F. Dalfovo, L. Pitaevskii, N.P. Proukakis, S. Stringari, “Collisionless Sound in a Uniform Two-Dimensional Bose Gas”, *Phys. Rev. Lett.* **121**, 145302 (2018).
- [22] V.L. Berezinskii, “Destruction of long-range order in one-dimensional and two-dimensional systems having a continuous symmetry group II. Quantum systems”, *Zh. Eksp. Teor. Fiz.* **61**, 1144 (1971) [*Sov. Phys. JETP* **34**, 610 (1972)].
- [23] D.R. Nelson, J.M. Kosterlitz, “Universal Jump in the Superfluid Density of Two-Dimensional Superfluids”, *Phys. Rev. Lett.* **39**, 1201 (1977).
- [24] R. Saint-Jalm, *Exploration de la physique à deux dimensions avec des gaz de Bose dans des potentiels à fond plat: ordre en phase et symétrie dynamique*, PhD thesis of École normale supérieure and PSL University (Paris, October 2019).
- [25] H. Kurkjian, Y. Castin, A. Sinatra, *Brouillage thermique d’un gaz cohérent de fermions*, *Comptes Rendus Physique* **17**, 789 (2016).
- [26] Y. Castin, R. Dum, “Bose-Einstein condensates with vortices in rotating traps”, *Eur. Phys. J. D* **7**, 399 (1999).
- [27] Z. Hadzibabic, J. Dalibard, “Two-dimensional Bose fluids: An atomic physics perspective”, *Rivista del Nuovo Cimento* **34**, 389 (2011).
- [28] V.N. Popov, *Functional Integrals in Quantum Field Theory and Statistical Physics* (Reidel, Dordrecht, 1983).
- [29] C. Mora, *Gaz de bosons et de fermions condensés : phases de Fulde-Ferrell-Larkin-Ovchinnikov et quasicondensats*, PhD thesis of Université Paris VI (Paris, March 2004).
- [30] C. Mora, Y. Castin, “Ground state energy of the two-dimensional weakly interacting Bose gas: First correction beyond Bogoliubov theory”, *Phys. Rev. Lett.* **102**, 180404 (2009).
- [31] D.S. Petrov, G.V. Shlyapnikov, “Interatomic collisions in a tightly confined Bose gas”, *Phys. Rev. A* **64**, 012706 (2001).
- [32] L. Pricoupenko, M. Olshanii, “Stability of two-dimensional Bose gases in the resonant regime”, *J. Phys. B* **40**, 2065 (2007).
- [33] L. Pricoupenko, “Isotropic contact forces in arbitrary representation: Heterogeneous few-body problems and low dimensions”, *Phys. Rev. A* **83**, 062711 (2011).
- [34] A. Serafin, *Deux études de propriétés collectives de systèmes quantiques*, PhD thesis of Sorbonne University (Paris, December 2022).
- [35] W.H. Press, S.A. Teukolsky, W.T. Vetterling, B.P. Flannery, *Numerical Recipes* (Cambridge University Press, Cambridge, 1988).
- [36] A. Sinatra, Y. Castin, E. Witkowska, “Nondiffusive phase spreading of a Bose-Einstein condensate at finite temperature”, *Phys. Rev. A* **75**, 033616 (2007).